Inertial Fusion Energy
Reactor Design Studies
Volume I

DOE/ER-54101
MDC 92E0008
March 1992

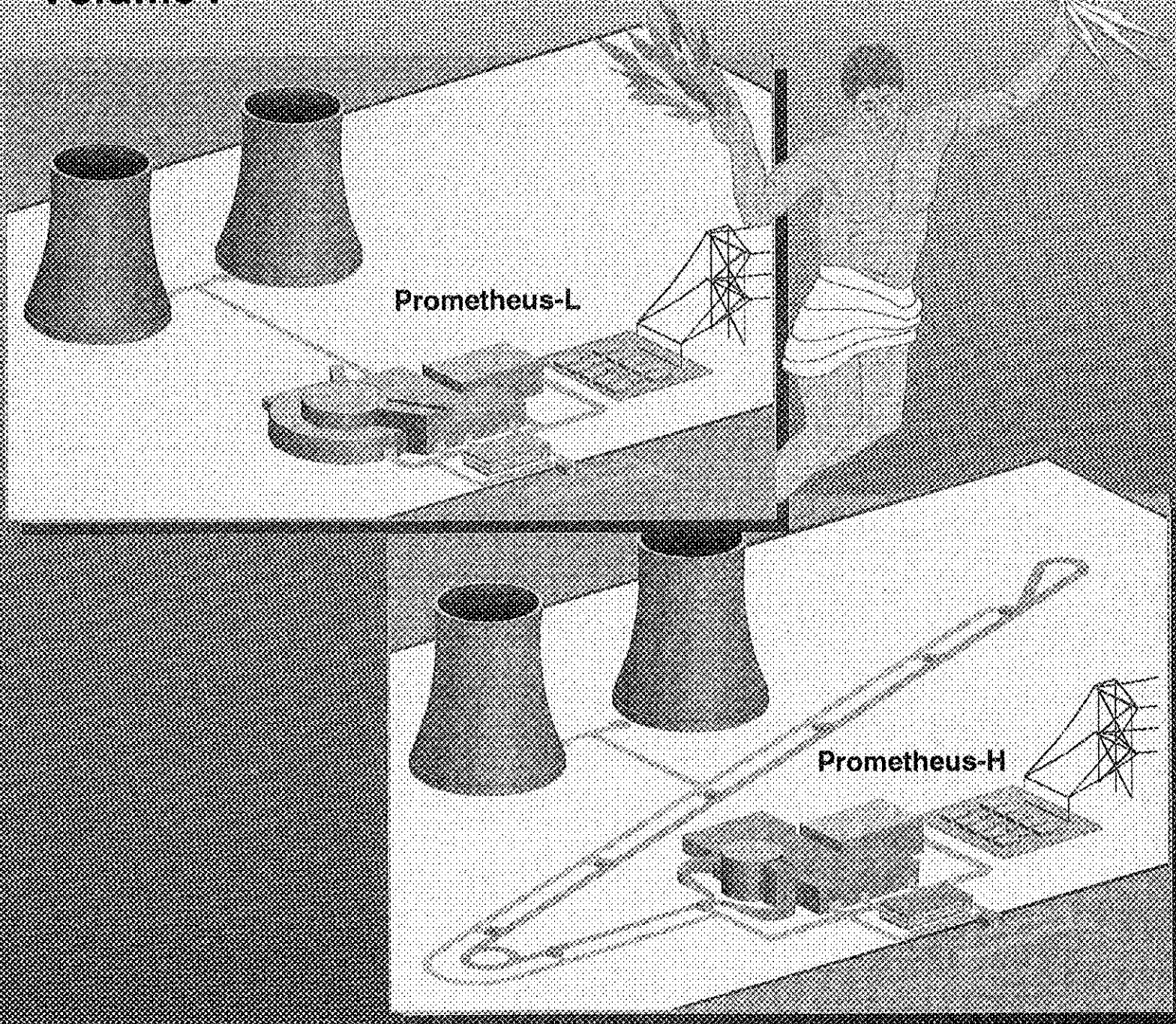

McDonnell Douglas Aerospace Team

Canadian Fusion Fuels Technology Group • Ebasco Services, Inc. • KMS Fusion, Inc.
SPAR Aerospace, Ltd. • TRW Space & Technology Group • University of California at Los Angeles

Final Report

DOE/ER-54101
MDC 92E0008

INERTIAL FUSION ENERGY REACTOR DESIGN STUDIES

PROMETHEUS-L
PROMETHEUS-H

FINAL REPORT
MARCH 1992

The manuscripts for this document were prepared for publication in March 1992.
The review of the document by DOE delayed publication until July 1993.

Volume I

Copy No. 196

McDonnell Douglas Aerospace
P.O. Box 516
St. Louis, MO 63166-0516

Canadian Fusion Fuels Technology Project
Mississanga, Ontario, Canada

Ebasco Services, Inc.
New York, NY

KMS Fusion, Inc.
Ann Arbor, MI

SPAR Aerospace, Ltd.
Brampton, Ontario, Canada

TRW Space and Electronics Group
Redondo Beach, CA

University of California-Los Angeles
Los Angeles, CA

This work was supported by the US Department of Energy, Office of Fusion Energy, under contract DE-AC02-91ER54101.

CONTRIBUTING AUTHORS

McDONNELL DOUGLAS AEROSPACE

Lester M. Waganer, Daniel E. Driemeyer, V. Dennis Lee

Robert L. Calkins | Henry B. Wald | Forrest R. Williams

CANADIAN FUSION FUELS TECHNOLOGY PROJECT

Ronald S. Matsugu, Otto K. Kveton

K. Kalyanam | Savtantar K. Sood

EBASCO SERVICES, INC.

Stephen L. Ostrow, Stephen F. Marschke

Paul J. Estreich | Marvin J. Parnes

KMS FUSION, INC.

Douglas J. Drake[1]

SPAR AEROSPACE, LTD.

Julian W.F. Millard

John Ballantyne, Chris English | Terry Haines, Clive Holloway | Don Perrot, Andy Turner

TRW SPACE AND ELECTRONICS GROUP

Gary J. Linford | **Steven W. Fornaca** | **Alfred W. Maschke**

UNIVERSITY OF CALIFORNIA, LOS ANGELES

Mohamed A. Abdou, Nasr M. Ghoniem, Mark S. Tillack

James E. Eggleston, Anter El-Azab, Zinovy R. Gorbis, Insoo Jun | Farrokh Issacci, A. Rene Raffray, Shahram Sharafat | Alice Y. Ying, Mahmoud Z. Youssef, Li Zhang

1. Now associated with Interscience, Inc., Germantown, MD

ACKNOWLEDGMENT

The McDonnell Douglas team wishes to thank a great number of people who supported and contributed to this overall effort. Their time and effort are greatly appreciated.

Oversight Committee

Ronald C. Davidson, Chairman	Princeton Plasma Physics Laboratory
Charles C. Baker	Oak Ridge National Laboratory
Roger O. Bangerter	Lawrence Berkeley Laboratory
E. C. Brolin	Princeton Plasma Physics Laboratory
Daniel R. Cohn	Massachusetts Institute of Technology
Donald L. Cook	Sandia National Laboratories
Donald J. Dudziak	North Carolina State University
William Hogan	Lawrence Livermore National Laboratory
David B. Harris	Los Alamos National Laboratory
Robert A. Krakowski	Los Alamos National Laboratory
Thomas E. Shannon	Oak Ridge National Laboratory
Charles P. Verdon	University of Rochester

Target Working Group

Roger O. Bangerter, Chairman	Lawrence Berkeley Laboratory
George Allhouse	Sandia National Laboratories
John Lindl	Lawrence Livermore National Laboratory
William Mead	Los Alamos National Laboratory
Charles P. Verdon	University of Rochester

ARIES Project Staff

Ronald L. Miller	Los Alamos National Laboratory

Lawrence Berkeley Design Staff

Edward Lee	Lawrence Berkeley Laboratory
Andy Faltens	Lawrence Berkeley Laboratory

We would also like to acknowledge the contributions of other people who made this report possible.

David B. Harris, LANL, who facilitated the review process at his facility
Phillip Lang, LANL, Technical Review
Linda M. Merritt, MDA, Principal Text and Graphics Coordinator and Senior Editor
David E. Morgan and J. Warren Stultz, MDA, Technical Editors
Joanne Matheson , SPAR Aerospace, Ltd, Secretarial Support
Bruce Sayer, SPAR Aerospace, Ltd, Graphics Support
Thomas Chao, Alan Chen, Winn Hong, Billy Jimenez, and Faiz Sherman: UCLA Technical Support
Julie Austin, UCLA Secretarial Support
Matt Durkan, UCLA Administrative Support

TABLE OF CONTENTS

TABLE OF CONTENTS (CONT.)

LIST OF PAGES – VOL. I

LIST OF FIGURES – VOL. I

LIST OF TABLES – VOL. I

ABBREVIATIONS AND ACRONYMS

ADS	Air Detritiation System
ALARA	As Low As Reasonably Achievable
ANL	Argonne National Laboratory
ARIES	Advanced Reactor Innovations and Evaluation Study
ASE	Amplified Spontaneous Emission
ASWS	Auxiliary Service Water System
ATA	Advanced Test Reactor
AVLIS	Atomic Vapor Laser Isotope Separation
BCSS	Blanket Comparison and Selection Study
BHP	Biological Hazard Potential
BOP	Balance of Plant
BQ	Beam Quality
BRP	Blanket/Reflector/Plena
BW	Bandwidth
CANDU	Canadian Deuterium Uranium (Fission Reactor)
CAS	Compressed Air System
CASCADE	LLNL IFE reactor concept using rotating ceramic-granuale blanket
CCWS	Closed Cooling Water System
CCW	Component Cooling Water
CD	Cryogenic Distallation
CDS	Central Difference Scheme
CEA	Commissariat A L'Energie Atomique
CEBAF	Continuous Electron Beam Accelerator Facility
CECE	Combined Electroysis and Catalytic Exchange
CERN	Centre for European Research, Nuclear
CET	Chemical Equilibrium Thermodynamic Code
CFFTP	Canadian Fusion Fuels Technology Project
CH	Hydro-Carbon based material
COE	Cost Of Electricity
CRAM	(beam) Crossed Raman Accumulator
CTMS	Cooling Tower Makeup System
CS	Constant Spot
CSS	Condensate Storage System
CVD	Chemical Vapor Deposition
CVI	Chemical Vapor Infilteration
CWS	Circulating Water System
DAC	Derived Air Concentrations
DBTT	Ductile-to-Brittle Transition Temperature
DCG	Derived Concentration Guide
DD	Direct Drive (target)
DEMO	Demonstration Power Plant
DESY	Deutsches Elektron-Synchrotron
DOD	Department of Defense
DOE	Department of Energy
DPA	Displacements Per Atom
DPP	Demonstration Power Plant
DRTF	Darlington Tritium Removal Facility
DSTI	Dual-Sided Target Irradiation
DT	Deuterium-Tritium
DTX	Dose-To-Flux
E/O	Electro-Optical
EADS	Exhaust Atmosphere Detritiation System
EBEEL	Electron Beam Excited Excimer Laser
EBEL	Electron Beam Excimer Laser
EBSEDL	Electron Beam Sustained Electric Discharge Laser
EDEL	Electric Discharge Excimer Laser

ABBREVIATIONS AND ACRONYMS (CONT.)

EDS	Electrical Distribution System
EEDS	Exchaust Effluent Detritiation System
EGDS	Exhaust Gas Detritiation System
ELD	Excimer Driver Laser
ELMO	Excimer Laser Master Oscillator
ELP	Excimer Laser Preamplifier
ELPA	Excimer Laser Power Amplifier
EMRLD	Excimer Mid-range Raman-shifted Laser Device
ENEA	European Nuclear Energy Agency
EP	Exhaust Purfication
EPA	Environmental Protection Agency
EPR	Experimental Power Reactor
EPRI	Electric Power Research Institute
ER	Energy Research
ESECOM	Environmental, Safety, and Economic Aspects of MFE COmmittee
ESCWS	Essential Services Cooling Water System
ETF	Engineering Test Facility
ETHEL	European Tritium Handling and Experimental Laboratory
ETR	Engineering Test Reactor
FCU	Fuel Cleanup Unit
F	Fluence
FEL	Free Electron Laser
FET	Field Effect Transistor
FFTF	Fast Flux Test Facility
FINESSE	Fusion Integrated Nuclear Experiments Strategy Study Effort
FMEA	Failure Modes and Effects Analysis
FODO	Focus-Drift-DeFocus-Drift
FPCCS	Fuel Processing Closed Coolant System
FPS	Freeze Protection System
FPS	Fuel Processing System
FPY	Full Power Year
FRC	Fiber Reinforced Composite
FRRA	Forward Rotational Raman Amplifier
FSMS	Fuel Storage and Management System
FSS	Fuel Storage System
FW/B	First Wall/Blanket
FW	First Wall
FWS	First Wall System
GB	Grain Boundary
GBCS	Glove Box Cleanup System
GBFEL	Ground-Based Free Electron Laser
GC	Gas Chromatographic
GDP	Glow Discharge Polymerization
GIA	Grazing Incidence Angle
GIMM	Grazing Incidence Metal Mirror
HI	Heavy Ion
HIBALL	Heavy Ion Beams and Lithium Lead
HID	Heavy Ion Driver or Driven
HIF	Heavy Ion Fusion
HIFSA	Heavy Ion Fusion Systems Assessment
HIP	Hot Isostatic Pressing
HITEX	High Temperature Isotopic EXchange
HR	High Reflectivity
HVAC	Heating, Ventilation, Air Conditioning
HYLIFE	High-Yield Lithium-Injection Fusion Energy
IADS	Inert Atmospheric Detritiation System

ABBREVIATIONS AND ACRONYMS (CONT.)

IB	Inverse Bremsstrahlung
ICCOMO	Inertial COfinement systems performance and COst MOdel
ICF	Inertial Confinement Fusion
ICFSS	Inertial Confinement Fusion System Study
ICRP	International Commission on Radiological Protection
ID	Indirect Drive (target)
IDLD	Indirect Drive, Laser Driven (targets)
IDLH	Immediately Dangerous to Life or Health
IDPR	IFE Experimental Power Reactor
IEEE	Institute of Electrical and Electronic Engineers
IEPR	IFE Experimental Power Reactor
IFE	Inertial Fusion Energy
IFERDS	Inertial Fusion Energy Reactor Design Study
ILSE	Induction Linac System Experiment
IS	Inherent Safety
ISI	Induced Spatial Incoherence
ISR	Ion Storage Ring
ISS	Isotope Separation System
IT	Impurity Treatment
ITER	International Thermonuclear Experimental Reactor
IVVS	In-Vessel Vehicle System
JAERI	Japan Atomic Energy Research Institute
JET	Joint European Torus
KfK	Kernforschungszentrum Karlsruhe
LA	Large Aperture
LAM	Large Aperture Module
LANL	Los Alamos National Laboratory
LBL	Lawrence Berkeley Laboratory
LD	Laser Driver or Driven
LIA	Linear Induction Accelerator
LIACEP	Linear Induction Accelerator Cost Evaluation Program
LIBRA	Light Ion Beam Fusion Reactor Conceputal Design Study
LINAC	LINear ACcelerator
LLE	Laboratory for Laser Energetics
LLNL	Lawrence Livermore National Laboratory
LLW	Low Level Radioactive Waste
LMF	Laboratory Microfusion Facility
LOCA	Loss of Coolant Accident
LOE	Level Of Effort
LOFA	Loss of Flow Accident
LRO	Local Raman Oscillator
LSA	Level of Safety Assurance
LTA	Long Term Activation
LTE	Local Thermodylnamic Equilibrium
LV	Low Voltage
M	Blanket or Nuclear Power Multiplication
MARS	Mirror Advanced Reactor Study
MB	Multiple Beam
MBL	Multiple Beam Linac
MCF	Magnetic Confinement Fusion
MD	Molecular Dynamics
MDA	McDonnell Douglas Aerospace
MDESC	McDonnell Douglas Electronic Systems Company
MDMSC	McDonnell Douglas Missile Systems Company
MFE	Magnetic Fusion Energy
MHD	Magneto-Hydromanmic

ABBREVIATIONS AND ACRONYMS (CONT.)

MINIMARS	Mini-Mirror Advanced Reactor Study
MOPA	Master Oscillator Power Amplifier
MPC_a	Maximum Premissible Concentration in Air
MSM	Master-Slave Manipulator
MTA	Maintainability Task Analysis
MTBF	Mean Time Between Failure
MTTR	Mean Time To Repair
MUF	Mass Utilization Factor
MV	Medium Voltage
NASA	National Aerospace and Space Administration
NECDB	Nuclear Energy Cost Data Base
NET	Next European Torus
NIOSH	National Institute for Occupational Safety and Health
NLO	Non Linear Optical
NMFECC	National Magnetic Fusion Energy Computer Center
NPB	Neutral Particle Beam
NPBIE	Neutral Particle Beam Integrated Experiment
NPR	New Production Reactor
NPRD	Non-electrical Parts Reliability Data
NRC	Nuclear Regulatory Commission
NRF	Neutron Reflection Factor
NRL	Naval Research Laboratory
OEL	Optimized Excimer Laser
OFE	Office of Fusion Energy
ORNL	Oak Ridge National Laboratory
PC	Pulse Compression
PF	Pulse Forming
PFL	Pulse Forming Line
PFN	Pulse Forming Network
PHA	Preliminary Hazards Analysis
PKA	Primary Knock-on Atom
PPPL	Princeton Plasma Physics Laboratory
PRA	Preliminary Risk Analysis
PRF	Pulse Repetition Frequency
PSA	Pressure Swing Adsorption
PWR	Pressurized Water Reactor
PVA	PolyVinyl Acetate
R&D	Research and Development
RA	Resonance Absorption
RA	Resonant Absorption
RAC	Raman Accumulator Cell
RADS	Recirculating Air Detritiation System
RAM	Reliability, Availability, Maintainability
RCRA	Resource, Conservation, and Recovery Act
RCS	Replacement Collision Sequences
RECON	A UCLA Heat and Mass Transfer Computer Model
RF	Radio Frequency
RHR	Reactor Heat Removal
RMCS	Remote Manipulator and Control System
RMS	Remote Monitoring System
RMSD	Remote Manipulator Systems Division (SPAR)
RPE	Reactor Plant Equipment
RPM	Revolutions Per Minute
RR	Repetition Rate
RT	Rayleigh-Taylor (instability)
RT	Room Temperature

ABBREVIATIONS AND ACRONYMS (CONT.)

SB	Single Beam
SBFEL	Space-Based Free Electron Laser
SBL	Single Beam Linac
SBS	Stimulated Brillouin Scattering
SCR	Silicon Controlled Rectifier
SDI	Strategic Defense Intitative
SDIO	Strategic Defense Intitative Organization
SENRI	A Japanese Fusion Reactor Design Study
SEP	Socie'te' Europeenne de Propulsion
SIRIUS	A Symmetric Direct Drive Laser Fusion Reactor Study (Univ of Wisc)
SLAC	Stanford Linear Accelerator
SNL	Sandia National Laboratories
SOLASE	Experimental Inertial Reactor Study (at Univ of Wisc)
SOW	Statement Of Work
SP	Single Pulse
SPAR	Spar Aerospace, Ltd
SPTF	Single Pulse Test Facility
SRRS	Stimulated Rotational Raman Scattering
SRS	Stimulated Raman Scattering
SSC	Superconducting Super-Collider
SSTI	Single-Sided Target Irradiation
STEM	Storage Tubular Extendible Member
STP	Standard Temperature and Pressure
TARM	Telescoping Articulating Remote Maniupulator
TBCCWS	Turbine Building Closed Cooling Water System
TBR	Tritium Breeding Ratio
TCPSA	Thermally Coupled Pressure Swing Adsorption
TCPSA	Thermally Coupled Pressure Swing Adsroption
TDRF	Threshold Dose Release Fractions
TEXTOR	Tritium Experiment for Technology Oriented Research
TFTR	Tokamak Fusion Test Reactor
TPD	Two Plasmon Decay
TPR	Tritium Production Rate
TRIUMF	Tri-University Meson Facility
TRM	Total Remote Maintenance
TSA	Thermal Swing Adsorption
TSDS	Tritium Storage and Delivery System
TSTA	Tritium System Test Assembly
TVD	Total Variation Diminishing
TWA	Time Weighted Averages
TWI	Target Debris-Wall Interaction
TWG	Target Working Group
UCLA	University of California at Los Angeles
UHS	Ultimate Heat Sink
US	United States
UV	Ultraviolet
VLS	Vapor-Liquid-Solid
VPCE	Vapour Phase Catalytic Exchange
VS	Ventilation System
WD	Water Distillation
WD	Water Detritation System
WJSA	W.J. Schafer Associates
XDL	Times Diffraction Limit
ZS	Zoomed Spot

TABLE OF CONTENTS – EXECUTIVE SUMMARY

EXECUTIVE SUMMARY

This report addresses the conceptual design and analysis of two commercial central station electric power plants. These plants use Inertial Fusion Energy (IFE) technologies employing the latest advances in KrF excimer laser and heavy ion drivers. These two drivers are integrated with an advanced reactor cavity concept to offer power plants with the highest level of safety assurance and low environmental impact. Advanced thermal conversion systems yield highly efficient plants capable of high reliability and capacity. Current target technologies are extrapolated in both performance and manufacturing capabilities. Fuel cycle systems are built upon a solid foundation of existing IFE technologies. The two power plant designs represent a wealth of information to help assess and develop a strategy and development plan for a future of energy independence. In that spirit, the reactor designs were named Prometheus in honor of the Greek god who gave fire to mortals.

In late 1990, the Department of Energy, Office of Energy Research, selected a design team to conduct these two conceptual design studies. The team was lead by McDonnell Douglas Aerospace (MDA) and included Canadian Fusion Fuels Technology Project; Ebasco Services, Inc.; KMS Fusion, Inc.; SPAR Aerospace, Ltd.; TRW Space and Electronics Group; and the University of California at Los Angeles. The team also had the consulting services of Dr. Mohamed Abdou. An Oversight Committee was appointed to advise and assist the team in conduct of the study. A Target Working Group was formed to provide normalized, unclassified target data to the team.

During the design development, key physics and engineering issues were addressed, analyzed, and results documented. Additional research and development needs have been identified to help resolve issues. Both generic technology and design specific issues were identified and documented. Design specific issues include target coupling with the beam energy, target heating from cavity environment, heavy ion beam channel formation, cavity structural response, film flow stability, and silicon carbide/metal piping transition interface. Issues are identified and described as to: applicability, impact, design specificity, level of concern, operating environment, and relevance to Magnetic Fusion Energy (MFE).

Critical Issues for IFE development are also identified which are broader in scope and have a higher level of importance. These critical issues may encompass several key issues. The design team described 16 critical issues as follows:

1. Demonstration of Moderate Gain at Low Driver Energy
2. Feasibility of Direct Drive Targets
3. Feasibility of Indirect Drive Targets for Heavy Ions
4. Feasibility of Indirect Drive Targets for Lasers
5. Cost Reduction Strategies for Heavy Ion Drivers
6. Demonstration of Higher Overall Laser Driver Efficiency
7. Tritium Self-Sufficiency in IFE Reactors
8. Cavity Clearing at IFE Pulse Repetition Rates
9. Performance, Reliability, and Lifetime of Final Laser Optics
10. Viability of Liquid Metal Film for First Wall Protection
11. Fabricability, Reliability, and Lifetime of SiC Composite Structures
12. Validation of Radiation Shielding Requirements, Design Tools, and Nuclear Data
13. Reliability and Lifetime of Laser and Heavy Ion Drivers
14. Demonstration of Large-Scale Non-Linear Optical Laser Driver Architecture
15. Demonstration of Cost Effective KrF Amplifiers
16. Demonstration of Low Cost, High Volume Target Production Techniques

The key features of the two Prometheus power plants are summarized in Table ES-1. The site plans for the two plants are shown in Figures ES-1 and ES-2.

Table ES-1
The Prometheus Power Plants Have Valuable and Attractive Features

Common Features
- Low Activation Structural Material (SiC) in First Wall and Blanket
- More Environmentally Attractive Shield Material in Place of Concrete
- Helium Coolant Minimizes Stored Energy and Chemical/Activation Hazards
- Lower Pressure Helium Coolant Increases Inherent Blanket Safety
- Lead First Wall Protectant/Coolant Reduces Corrosion and Fire Hazard
- Double-Walled Steam Generators Maintain Low Tritium Permeation to Environment
- Reactor Plant Equipment is Easily Maintained with Remote Maintenance
- Plant Level of Safety Assurance is Rated as One
- Waste Disposal is Considered to be Class C or Better

Laser Plant Features
- Electric Discharge Lasers Offer High Reliability
- Illumination Requirements Are Maintained with Loss of One or More Amplifiers
- NLO Architecture Improves Optics Lifetime/Reliability and Beam Quality
- SBS Cells and Delay Lines Provide Efficient Beam Pulse Shapes to Target
- New GIMM Design is Long-Lived
- Direct Drive Target Offers High Gain at Reasonable Driver Energies

Heavy Ion Plant Features
- Single Beam LINAC w/Storage Rings is Simple, Flexible, and Less Expensive
- Low 4 GeV Ion Energy Reduces the Number of Required Beams
- Triplet Coil Sets Ballistically Focus Beams on Focal Spot Outside Blanket
- Channel Transport Offers Minimal Blanket Penetrations and Maximizes Shielding
- Indirect Target Uses Radiation Case to Protect DT Capsule During Acceleration

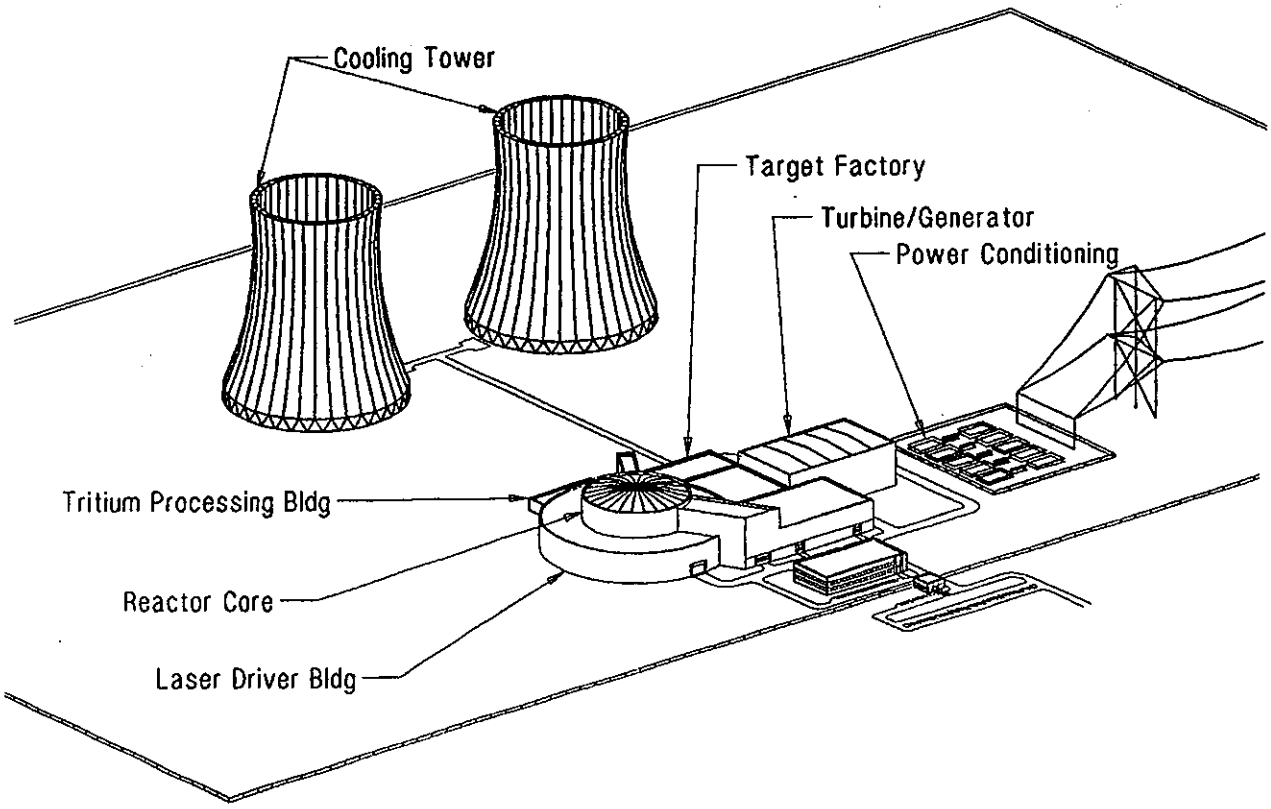

Figure ES-1. Prometheus-L Plant Site Trimetric View

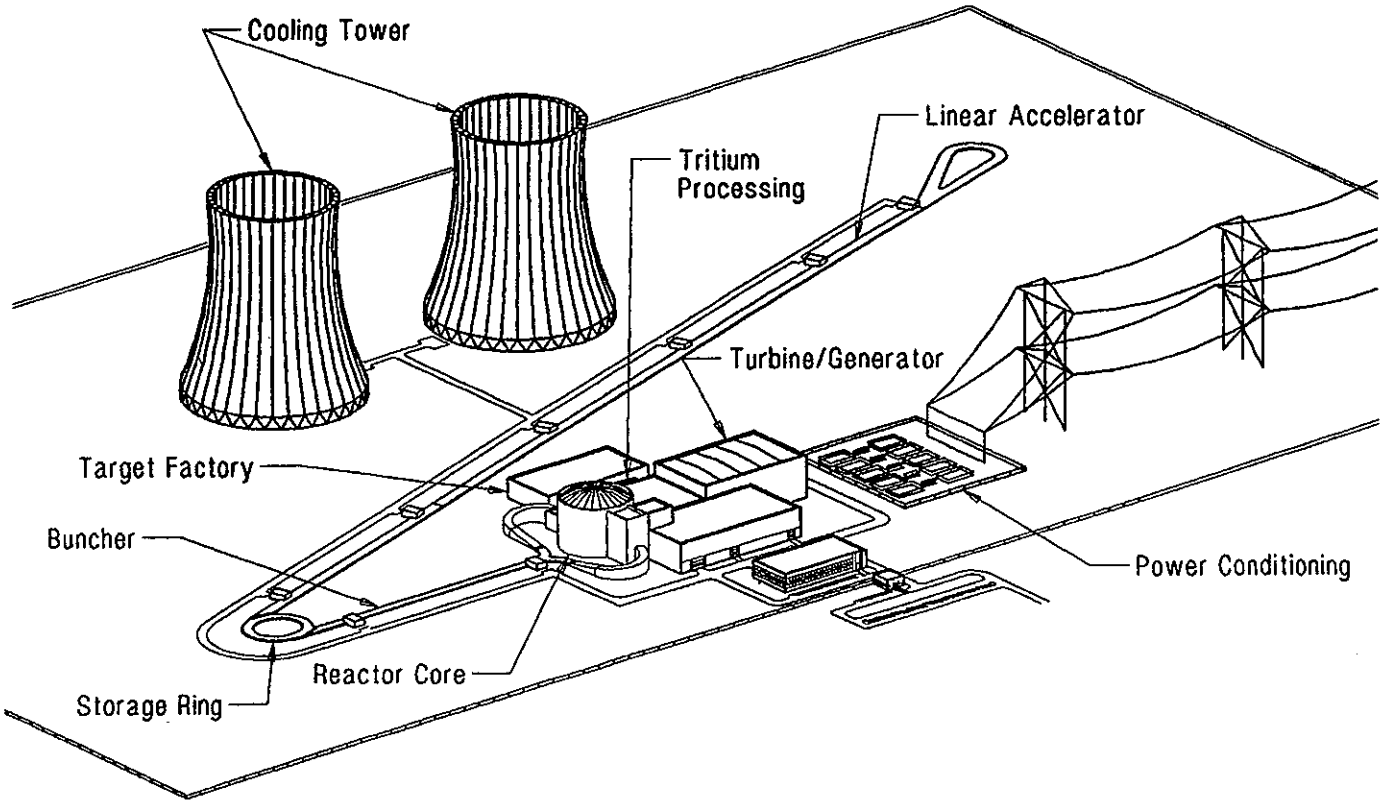

Figure ES-2. Prometheus-H Plant Site Trimetric View

Both Prometheus IFE power plants were designed to supply a net power output of 1000 MWe. Key parameters of the two power plants are presented in Table ES-2. The laser driver is less efficient than the heavy ion driver in producing the required energy to the target, which increases the thermal power, gross electric power, and recirculating power requirements for the laser-driven plant. The nominal pulse rate is 5.65 Hertz. The type and number of laser amplifiers are selected to enable the achievement of a nominal plant availability of 79.4%. The cost of electricity for this laser-driven plant is estimated to be 72.0 mills/kWh expressed in 1991 dollars.

The system efficiency for the heavy ion driver is higher in producing the required energy delivered to the target. This effect translates into a lower recirculating power requirement, physically smaller systems, and lower capital costs in most cost accounts. The nominal pulse rate for the heavy ion plant is 3.54 Hertz. The heavy ion driver has an advantage in inherent availability that raises the plant availability to 80.8%. The resultant cost of electricity is estimated to be 62.6 mills/kWh expressed in 1991 dollars.

The capital costs for the major plant elements of the laser and the heavy ion plant options are compared in Figure ES-3. The Structures and Site Facilities' heavy ion costs are lower mainly due to the smaller Reactor Building size. The reduced fusion, thermal, and electric power requirements for the heavy ion option, resulting from the more efficient driver, have lower related Reactor Plant Equipment, Turbine Plant Equipment, and Electric Plant Equipment costs as indicated. Reactor Plant costs also benefit from the simplified beamline interface for the heavy ion system. The more complex indirect-drive heavy ion target results in a slightly higher Target Manufacturing Plant Equipment cost, but the lower repetition rate keeps the overall cost comparable to that for the laser-driven plant. Interestingly, the resultant costs for the two Driver Plant Equipment approaches are virtually identical despite drastically different design approaches and delivered energy (4 MJ laser, 7.8 MJ heavy ion). The result is a 10 mills/kWh cost of electricity advantage for the heavy ion option as compared to the laser option.

The power plant designs were based upon today's known technology and physics extrapolated some 20-30 years into the future. Safety and environmental attractiveness were key design requirements to enhance the public's perception of fusion. Technical credibility is stressed in order to gain acceptance of the fusion community. Innovative concepts were encouraged to help foster and nurture developmental areas that may enhance the overall economics of fusion.

Table ES-2 Major Design Parameters and Features of the Prometheus Plants

Parameter	Prometheus-L (Laser)	Prometheus-H (Heavy Ion)
Net Electric Power (MWe)	972	999
Gross Electric Power (MWe)	1382	1189
Driver Power (MWe)	349	137
Auxiliary Power (MWe)	36	28
Cavity Pumping Power (MWe)	25	25
Total Thermal Cycle Power (MWt)	3264	2780
Blanket Loop Power (MWt)	1782	1597
Wall Protection Loop Power (MWt)	1267	1162
Usable Driver Waste Heat (MWt)	193	NA
Usable Pumping Waste Heat (MWt)	22	21
Thermal Conversion Efficiency	42.3%	42.7%
Recirculating Power Fraction	30%	16%
Net System Efficiency	31%	36%
Fusion Power (MW)	2807	2543
Neutron Power (MW)	2027	1818
Surface Heating Power (MW)	780	725
Fusion Thermal Power (MWt)	3092	2797
Thermal Power to Shield (MWt)	43	38
Cavity Radius (m)	5.0	4.5
Cavity Height (m)	15.0	13.5
First Wall Protection/Coolant Media (In/Out Temp., °C)	Liquid Lead (375/525)	Liquid Lead (375/525)
Breeder Material	Li_2O Pebbles	Li_2O Pebbles
Structural Material, Wall and Blanket	SiC	SiC
Blanket Heat Transfer Media (In/Out Temp., °C)	1.5 MPa Helium (400/650)	1.5 MPa Helium (400/650)
Cavity Pressure (mtorr, Pb)	3.0	100
Neutron Wall Load, Peak/Ave (MW/m^2)	6.5/4.3	7.1/4.7
Energy Multiplication Factor	1.14	1.14
Tritium Breeding Ratio	1.20	1.20
Target Illumination Scheme	Direct Drive, Symmetric	Indirect Drive, Two-Sided
Number of Beams	60	18 in LINAC (12 main + 6 in 2 prepulses)
Driver Output Energy (MJ)	4.0	7.8 (7.0 to target)
Overall Driver Efficiency (%)	6.5	20.6
Type and Number of KrF Amplifiers	Electric Discharge, 960	N/A
Beam Combining Technique	Raman Accumulators	N/A
Pulse Compression Technique	Stimulated Brillouin Scattering	N/A
Ion Accelerated	N/A	Lead
Charge State	N/A	+2
Final Energy (GeV)	N/A	4.0
Type of Accelerator	N/A	Single Beam LINAC
Final Beam Transport Efficiency(%)	100	90
Target Gain	124	103
Target Yield	497	719
Repetition Rate (pps)	5.65	3.54
Plant Availability (%)	79.4	80.8
Cost of Electricity (mills/kWh, 1991$)	72.0	62.6

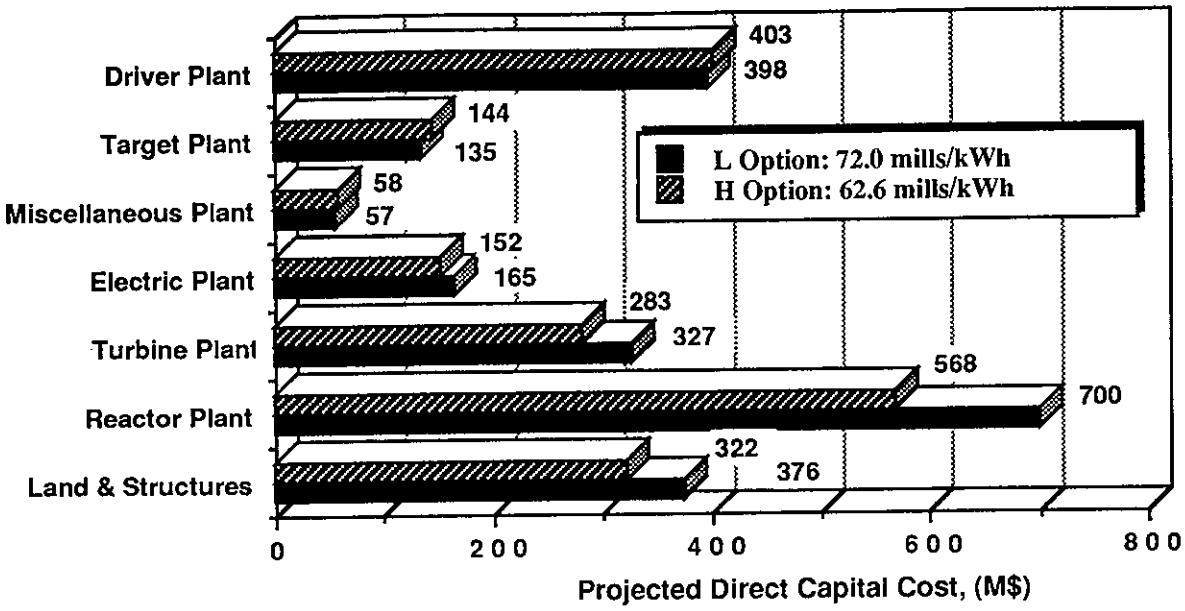

Figure ES-3. Capital Cost Comparison Between the Laser and Heavy Ion Plant Designs

A single reactor cavity concept was judged acceptable for servicing both the laser and the heavy ion reactor power plants. A cylindrical reactor cavity is used to maximize the maintainability of the first wall and blanket and keep a reasonable balance of peak to average neutron wall loading. Modular construction and support techniques were analyzed to assure development of a maintainable design. The cavity aspect ratio was determined by a trade study.

SiC was chosen as the major structural material within the high radiation environment of the reactor cavity to provide low activation and safety enhancement. The first wall is protected by a thin film of liquid lead that is evaporated by each microexplosion and is recondensed between explosions, thus providing protection and vacuum pumping. The first wall is constructed as tubular panels of porous composite SiC structure, which is cooled with liquid lead. Behind the first wall, a lithium oxide solid breeder is cooled with a low pressure, high temperature helium coolant. A low pressure helium purge extracts the tritium generated in the breeder. The tritium breeding ratio of the blanket is 1.20. All the lead and helium coolant piping within the bulk shielding is a SiC low-activation material. The lives of the wall and the blanket are five and ten years, respectively. The peak to average neutron wall load is 6.5/4.3 and 7.1/4.7 for the laser and heavy ion reactors.

Detailed calculations of the nuclear performance of the first wall, blanket and the shield were performed by UCLA. The bulk shield was analyzed for both a concrete and a composite shield of B_4C, Pb, SiC, Al, and H_2O. The composite shield was

chosen to provide a lower and more predictable activation level. In the case of the laser, the beamlines are protected by shielding all the way out beyond the final optics. The heavy ion final focus coils are also protected by internal shielding.

An elevation view of both the laser driver and the reactor buildings is shown in Figure ES-4. The Reactor Building is 86 meters in diameter, dictated by the length of the shielded beamlines. The Driver Building contains all the laser systems and surrounds the Reactor Building. The laser driver option uses 960 electric discharge lasers to provide a highly reliable power amplifier system. Non-linear optical (NLO)

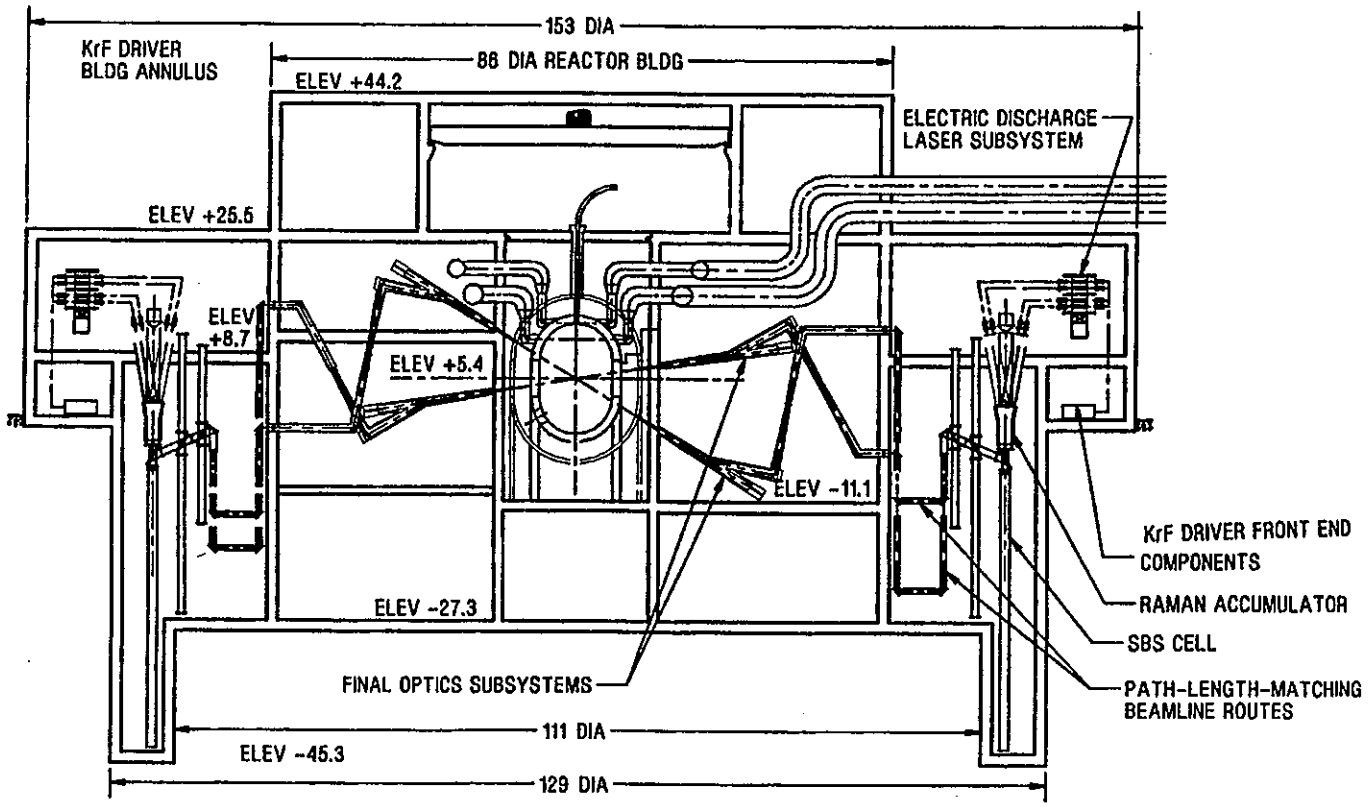

Figure ES-4. Prometheus-L Reactor Building Provides Space for Shielded Beamlines. Driver Building Surrounds Reactor Building.

laser elements provide the beam combining and compression functions to deliver high quality beams on the target. The laser driver delivers 4.0 MJ of 250 nm wavelength energy in 60 symmetrical beams onto a 6-mm diameter target. Beams are combined and quality is enhanced with Raman Accumulator cells with an 88% conversion efficiency. Beams are compressed with Stimulated Brillouin Scattering (SBS) cells. Optical delay switch yards maximize the utilization of the unused energy in the SBS to provide a proper prepulse shape for the target. The 60 beams pass through an optical focus at a neutron pinhole to minimize neutron activation in the driver building. One of the final optical elements is a final focus mirror to focus and turn the beams. A grazing incidence metal mirror (GIMM) is the final optical element that lies in the direct line of sight of the center of the cavity. Innovative design and choice of material offer the possibility of a life-of-plant for this component in a high radiation environment. This is especially difficult as this component is only 20 meters from the center of the cavity. The vapor pressure of the lead in the cavity must be approximately 3 mtorr or less for propagation of the laser beams through the cavity to the target.

An innovative design was chosen for the heavy ion driver. Heavy ion LINAC drivers have previously been thought to be very capital intensive, resulting in an unattractive cost of electricity. Several developments were investigated to reduce the driver costs. A single, rapidly pulsed beam LINAC was chosen as the baseline design. Eighteen beams are accelerated to 4 GeV and then are stored in storage rings for a time less than a millisecond. At the appropriate time, beams are extracted and sent to bunchers to compress the beams. Six of the 18 beams are designated as prepulse beams to prepare the target for the remaining 12 beams. Beams are divided into two sets and delivered to opposite sides of the reactor cavity. This final focus system is displayed in the elevation view of the heavy ion Reactor Building shown in Figure ES-5. The main heavy ion pulse beams are arranged in an 8.54° conical array with the precursor beams on axis. All beams are ballistically focused to a spot size of 3 mm radius at the back of the blanket. The two precursor beams establish 3 mm radius, self-formed transport channels across the cavity to the target. This channel transport concept has the obvious advantage of minimal penetration through the blanket, affording full and uninterrupted blanket coverage.

Two entirely different target concepts are used in the two design studies. The laser driver is using a direct-drive, symmetrically illuminated target with 60 beams. The target capsule is roughly 6 mm in diameter. Laser beams are focused beyond the target to fully illuminate the target and provide a 1% illumination uniformity. The target is a CH plastic shell with beta-layered, solid DT on the interior surface. The target gain is predicted to be 124, based on the beam energy of 4 MJ. The direct drive targets are protected with a sabot during the electromagnetic injection process. The target and sabot are separated prior to reactor cavity entry.

Note: This figure is shown at the same scale as the laser building, Figure ES-4.

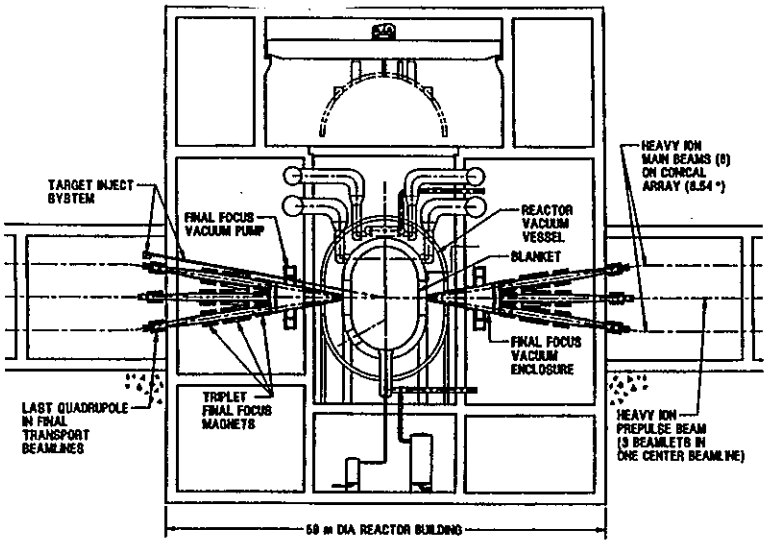

Figure ES-5. Prometheus-H Reactor Building Is Relatively Compact

The heavy ion, indirect-drive target uses a similar DT capsule, but it is enclosed in a radiation case. The case is cylindrical with an energy converter region in each end to convert the heavy ion energy into X rays bathing the interior of the case and the DT capsule. The case has high-Z material (lead) to enhance the capture and distribution of the X rays. The two opposing heavy ion beams are focused on the two end energy converter regions of the target. A gain of 103 is expected for a beam energy of 7 MJ. The indirect drive targets are injected with a pneumatic system and no sabot.

The energy conversion system used in both IFE systems is an advanced Rankine cycle. Two coolant streams, first wall lead and blanket helium, are used as shown in Figure ES-6. Waste heat from the KrF amplifier gas flow system is utilized to improve the laser system efficiency. Steam-driven helium circulators minimize the power required to circulate the helium coolant.

Features of Plant and Design Studies

- Because of the choice and utilization of the materials, the plant is rated at the highest level of safety assurance.
- The drivers contribute to the high level of reliability and availability.
- Innovative driver technologies and design concepts offer cost-effective pathways to economic fusion.

- Two IFE target design approaches have been employed to evaluate their relative merits.
- Non-linear optical laser system architecture offers performance improvements over more conventional systems.
- A single beam LINAC plus storage rings provides a lower cost HI IFE facility option.
- Key Technical Issues and R&D Needs identify areas for development.
- Critical Needs help focus emphasis toward more generic developmental areas.
- Evaluation and comparison of the two studies will help assess IFE program goals.

Power Flows for Laser and Heavy Ion Systems

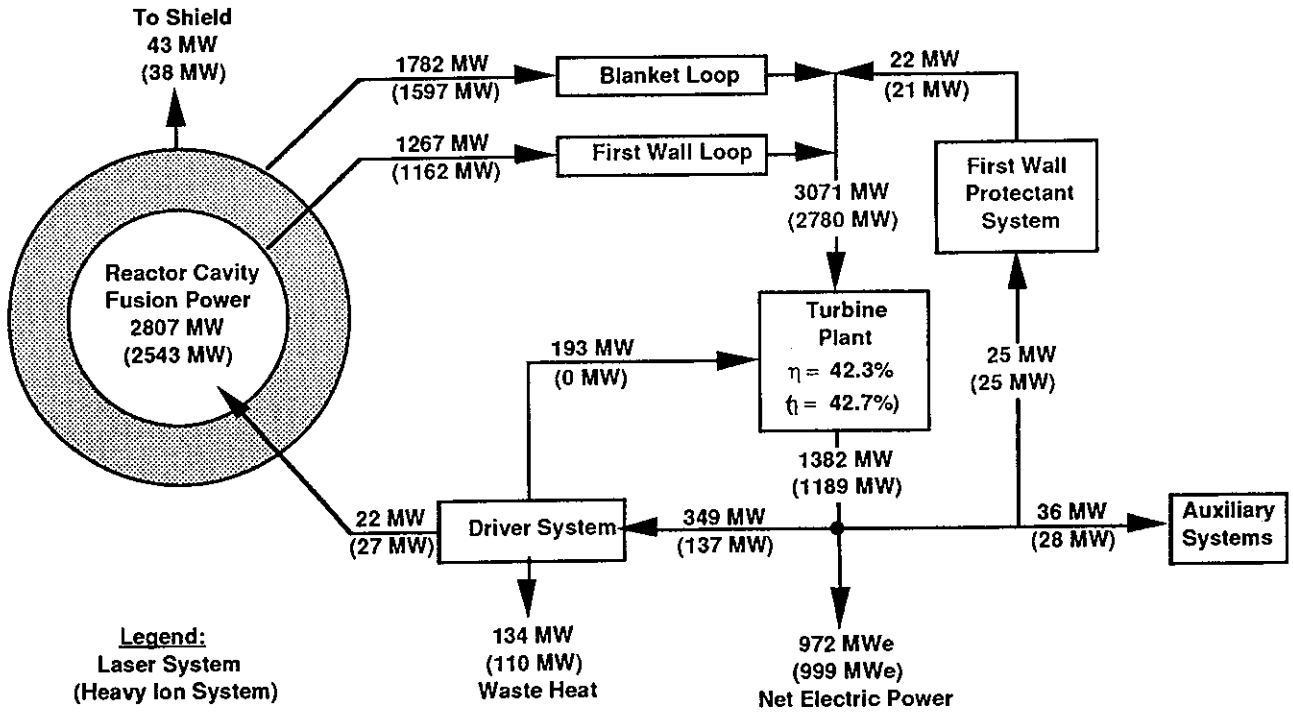

Figure ES-6. Overall Plant Power Flow for Prometheus Baseline Designs

TABLE OF CONTENTS – CHAPTER 1

CHAPTER 1
INTRODUCTION

The Department of Energy, Office of Fusion Energy, contracted with McDonnell Douglas Aerospace (MDA) and its subcontractors to develop and assess two separate Inertial Fusion Energy (IFE) reactor design studies. A parallel effort with identical goals and direction was also funded and contracted to W. J. Schafer and Associates. DOE wanted in-depth design studies similar to those previously accomplished in Magnetic Fusion Energy (MFE) to advance the state-of-the-art of IFE physics, technology, and engineering. These studies will provide a basis for future R&D planning to achieve successful commercialization of inertial fusion. The teams were encouraged to seek innovative design approaches and cost-effective solutions while improving the safety and environmental impact aspects of the reactor designs. Since there are several attractive IFE driver technologies, the teams had the opportunity to choose two drivers to be used in two conceptual reactor design studies. The driver technologies chosen by both teams during the pre-proposal efforts were the KrF laser and the heavy ion beam.

The 18-month MDA study ran from September 1990 to March 1992. Difficulties in the subcontract approvals delayed full team involvement until February 1991; however, all project milestones were met.

The program objectives were clearly defined in the contractual statement of work (SOW). The main objectives are summarized below:

- Adopt common groundrules for design development and comparison tasks
- Conduct parametric trades studies using developed systems codes
- Develop conceptual designs for two IFE reactor power plants
- Estimate plant capital and operating costs
- Assess critical technical issues and define R&D requirements
- Compare two IFE reactor designs
- Document the results

Accomplishment of these objectives in a timely and cost-effective manner required an experienced, multi-disciplined team of individuals and companies intimate with the IFE technologies and reactor design. McDonnell Douglas Aerospace assembled an exemplary team with outstanding capabilities.

Company/University	Area of Responsibility
McDonnell Douglas	Program management, systems integration, system analysis, costing
Canadian Fusion Fuels Technology Project (CFFTP)	Design of the fuel system, tritium inventory assessment
Ebasco Services	Energy conversion, safety and environmental impact assessment, balance of plant definition
KMS Fusion	Target and target-related systems, target factory
SPAR Aerospace Ltd.	Remote maintenance systems; reliability, availability, maintainability
TRW, Space & Electronics Group	KrF and heavy ion driver systems
University of California, Los Angeles	Reactor cavity design and analysis - first wall, blanket, shield, final optics (lifetime), safety
Dr. Mohamed Abdou	Technical Consultant on comparison and evaluation methodology, reactor design approach, economics, safety and environmental assessment

The Department of Energy commissioned an Oversight Committee to help provide technical guidance for the study team. Two subteams were formed. One subteam provided the overall reactor technical, economic/safety, and economic groundrules while the other subteam, the Target Working Group, provided unclassified, normalized data on laser and heavy ion target performance. These groups provided the study team with a set of recommended guidelines. Throughout the effort, the study team worked closely with the members of the Oversight Committee to clarify and enhance the reactor and target guidelines.

The study team enhanced and amplified the furnished guidelines to form a credible technical basis upon which to develop the conceptual design on a consistent basis with previous MFE and IFE designs as well as the W. J. Schafer-developed designs. Details of these requirements, guidelines and assumptions will be furnished in Chapter 3.

The ability of a study team to conduct system level trade studies to select the optimal system choices and operating parameter space is totally dependent upon having a credible systems analysis code. The code must be able to model with a reasonable fidelity the physics, technical performance, system efficiency, and cost of all the reactor plant systems and facilities. Fortunately, our team had the MDA ICCOMO systems

analysis code from the Heavy Ion Fusion Systems Assessment (HIFSA) project[1] to build upon. Updates of the driver modeling were developed from data obtained from LANL and TRW on the laser driver and from LBL and TRW on the heavy ion driver. This code enabled trade studies that did not just find local minima or maxima of a particular system, but rather represented system effects which influenced the whole of the reactor plant usually in terms of the cost of electricity (COE).

The selection of the system options and the design parameter point was based upon a balance of several considerations. The system level trade study results were used to obtain the relative cost and performance factors. These were evaluated and compared to the technical and physics risk and the safety/environmental impact of the options being considered. Once the system options were selected, the systems analysis code provided further system optimization.

The conceptual design development for the two reactor designs was conducted in a phased manner to better utilize the available personnel and resources. The KrF driver reactor was completed first, with the heavy ion driver next. Dr. David Harris of Los Alamos provided assistance on the angular-multiplexed, large-area, e-beam pumped, laser amplifiers. The other laser driver option considered was the non-linear optical (NLO) system with smaller discharge lasers. The NLO system with discharge lasers was chosen as the baseline design because of the higher reliability and improved safety of the discharge lasers and the design flexibility of the NLO system.

An overriding concern in the heavy ion driver reactor designs is the cost of the driver that usually dominates the plant costs. The more conventional approach for the linear accelerator (linac) is to accelerate multiple beams to control space charge effects present in the beams; however, this approach is usually very expensive. LLNL is investigating the use of a recirculating linac to reduce its cost, but the recirculating LINAC represents a technology with a high degree of technical risk. Al Maschke of TRW conceived an approach to use a single beam LINAC rapidly pulsed to deliver multiple beams. These beams are temporarily stored in individual storage rings until they are simultaneously delivered to the reactor and target. We believe this approach represents a significant cost reduction in the LINAC and will provide the basis for a cost-effective reactor.

The Target Working Group (TWG) provided the study teams with technical guidelines of direct and indirect drive (DD and ID) targets for the laser driver and indirect drive for the heavy ion beam driver. This technical data consisted of gain and power curves, illumination requirements, pulse shaping, and pulse duration. Building upon the data provided, it was determined that the direct drive laser target and the indirect drive heavy ion target would be best suited for use in the design studies.

The reactor cavity is a key element in the overall design of an inertial fusion power plant. The design of the cavity elements is significantly different from those of magnetic fusion. There is much more design freedom because of the lack of the constraints imposed by toroidal and poloidal field coils and the shaping of the cavity wall to coincide with critical field lines. The inertial cavity designer is freed from those severe constraints. However inertial confinement imposes new design constraints in terms of pulsed operation, severe electromagnetic and blast effects, and beamline penetrations. The previous inertial fusion cavity design approaches were evaluated for incorporation along with other promising new design concepts. The adopted reactor cavity design is a blend of new concepts, modifications of previously proposed IFE designs, and adaptations of MFE technologies. A layer of liquid lead protects a silicon carbide (SiC) first wall structure containing coolant channels of flowing liquid lead. In addition to protecting the first wall, the liquid lead vacuum pumps the chamber, providing the requisite base pressure between target implosions. Behind the first wall is a low-pressure, helium-cooled breeding blanket. The breeding material, Li_2O, is housed in a low-activation SiC blanket structure. The vacuum vessel and shield are composed of ferritic steel, H_2O, B_4C, Pb, and SiC. This is a very low activation design which is beneficial in terms of environmental impact. The low pressure helium coolant provides a high degree of safety due to passive containment of the coolant in the event of a coolant tube rupture.

The reactor cavity design team assessed all the reactor cavity design options for both driver options, fully anticipating that two separate designs might evolve. Rather, it was found that the design for the KrF driver has the more severe requirements in terms of lower cavity pressure and more beam penetrations. Therefore the resultant design for the KrF driver will be appropriate for the heavy ion driver case.

The remainder of the reactor equipment systems and balance of plant (BOP) systems were developed with the intent of being used in both reactor concepts with suitable modifications. The driver building design will be unique for each driver concept.

One of the most important outputs of the study is the identification and assessment of the resultant technical issues. The project team first identified specific technical issues that must be addressed and solved for each reactor system. Research and development needs were defined for each of the technical needs. To provide additional information, the list of key issues was reviewed, summarized, and condensed to those critical issues that were of most importance to the advancement of commercial inertial fusion energy.

A quantitative methodology for the comparison and evaluation of the two reactor designs was developed. The general evaluation parameters are as follows:

- Physics Feasibility
- Engineering Feasibility
- Economics
- Safety and Environmental Impact
- R&D Requirements

The two reactor concepts are quantitatively scored in each category which is appropriate at this developmental stage. As fusion technology advances, both the physics and the engineering feasibility questions will be answered by the necessary R&D efforts. Time to accomplish the R&D is also implicitly included in the R&D requirements. Thus the evaluation of the reactor concepts will ultimately be measured by economics and safety/environmental impact. Even the safety/environmental impact could be assessed in economic terms. For the present, it is prudent to retain all the evaluation parameters. Because of the diverse nature of the parameters and their relative perception by factions, there will not be an overall total weighted score. It will be left to the reader to judge the relative merits of each concept in each general evaluation area.

The endeavor of developing two separate IFE reactor conceptual designs within the same study using identical groundrules and requirements has been enlightening. The study may provide DOE and the fusion community with innovative and cost-effective solutions. However, many of the key technical issues remain to be identified and resolved.

Reference for 1

1. D. S. Zuckerman, et al., "Induction Linac Driven Heavy Ion Fusion System Model," Fusion Technology, Vol 13, #2, 1986.

This page intentionally left blank.

TABLE OF CONTENTS – CHAPTER 2

CHAPTER 2
STUDY OVERVIEW

This chapter provides a brief overview of the basis for and the results of the two IFE conceptual design studies of commercial central station power plants conducted for the Department of Energy, Office of Energy Research.

2.1 Introduction

In late 1990, the Department of Energy, Office of Energy Research, awarded a contract to McDonnell Douglas Aerospace (MDA) and its team of subcontractors to develop two inertial fusion energy conceptual designs of commercial central station power plants. Two different drivers were selected by the MDA contract team during the proposal period; namely, a KrF excimer laser and a heavy ion induction LINAC. The conceptual design effort included the defintion and optimization of the driver system, reactor system, target factory, balance of plant systems, and plant facilities.

In addition to the design study contract awarded to the MDA team, a second and parallel design study with the same objectives was awarded to a design team headed by W. J. Schafer Associates (WJSA). The WJSA team also chose the same set of drivers as the basis for their reactor power plant designs.

To assure comparable designs and a degree of normalization of physics, technology, and economics, DOE commissioned an Oversight Committee. The Committee established common groundrules and guidelines for the two study teams. All studies were to be unclassified with wide distribution to the fusion community. Since inertial fusion has evolved from the classified arena of Defense Programs, much of the target data and target interactions with the drivers and reactor cavities are sensitive in nature. To accomplish the objective of an unclassified study, DOE formed a Target Working Group (TWG) to assemble unclassified parametric data for use by the teams as common design data and groundrules. A kickoff meeting for the two design teams was held to introduce the guidelines. Frequent technical interchange with the Oversight Committee and the Target Working Group refined the guideline data. A supplement of the guideline document was issued to help answer some questions. Chapter 3 summarizes these provided guidelines. Members of the Oversight Committee and the Target Working group also attended the regular project design review meetings and provided helpful technical critiques and guidance.

A brief description of the statement of work may assist the reader in understanding the presentation style of the report and the data contained within the report. There are six main project tasks in addition to tasks associated with regular meetings and reports. These are:

- Establish project groundrules, requirements, and criteria sufficient to meet the intent of comparability and provide design guidance to the team.
- Develop a systems code to help select and design major system and subsystem options and determine specific design points for the design teams to begin the detailed design process. This code would also be used to conduct system level parametric trade studies.
- Develop conceptual engineering designs for the KrF and the heavy ion beam drivers and the inertial fusion power reactors and establish descriptions of the support facilities, plant systems, and major components.
- Prepare capital and operating cost estimates and the projected cost of electricity for the two power plants.
- Identify and analyze the major technical issues confronting the two designs and the associated research and development needs for the two systems.
- Evaluate and compare the two IFE plant designs to each other.

This Study Overview chapter is a brief synopsis of the entire study and its results. At the end of this chapter, a section will discuss the conclusions to be drawn from this study.

2.2 Key Objectives, Requirements, and Assumptions

The primary objective of the Prometheus study is to develop two conceptual designs for commercial fusion electrical power plants based on inertial confinement; one with the KrF laser driver (Prometheus-L) and the other with the heavy ion beam driver (Prometheus-H). In addition, the study has emphasized the following goals: (1) advancement of the state-of-the-art in IFE power plant design; (2) improvements in physics and engineering credibility and enhancement of potential economic, safety, and environmental attractiveness of IFE reactor power plants; (3) identification and characterization of key technical issues and the R&D required to resolve them; and (4) comparison of the two IFE reactor design concepts.

A set of requirements and guidelines was developed from the onset of the project to help meet the above objectives and goals. The requirements and guidelines were developed partly by an oversight committee, particularly in areas related to targets and target-driver coupling, and partly by the study management. Details of the study requirements, guidelines and assumptions are presented in Chapter 3 and are briefly summarized below.

- The IFE plant is to serve as a commercial central station electric power plant; the only product is electricity.
- The reactor is operated on the deuterium-tritium fuel cycle; fuel self-sufficiency conditions in a mature power economy must be satisfied.
- The net electric power output is 1000 MW.

- The data base of physics, technology and economics will be extrapolated by about 30-40 years.
- The design is for tenth-of-a-kind commercial power plant.
- The plant lifetime is 40 years for engineering design and 30 years for economic analysis.
- The study should perform and document tradeoff studies for key design choices.
- The study is to focus on key IFE reactor components such as target, driver, cavity, and fuel cycle. Effort on balance-of-plant should be limited.
- Safety and environmental aspects of the design should be emphasized.
- Target factory is on site.

Target and Driver Guidelines - The Oversight Committee and the Target Working Group (TWG) provided the study with specific guidelines and information regarding the target and driver. Examples of these are the yield versus driver energy for direct- and indirect-drive targets with KrF and heavy ion beams, illumination uniformity requirements, and requirements on power balance and beam alignment. The details of such guidelines and information are given in Chapter 3. Because this information is specific and spans several areas, no summary is given here.

2.3 Systems Modeling and Trade Studies

Optimization of an inertial fusion power plant involves trade studies of several major systems including reactor plant, driver plant, target plant, and balance of plant. The rationale for choosing between design options for these major systems and for selecting an operating point for a given set of options involves complicated trade-offs between many issues including economics, safety, engineering feasibility, technical risk, etc. In many instances, design choices can be made without considering how they might impact the overall system performance. However it often is useful (and sometimes essential) to consider an overall figure of merit when selecting design options. The Inertial COnfinement systems performance and COst MOdel (ICCOMO) was updated to assist the design process for this study. This code has evolved over many years. The models were originally developed as part of the STARFIRE reactor design study.[1] Later they were adapted to IFE as part of the HIFSA project.[2] The code contains parametric scaling and cost models for all major fusion power plant subsystems and design options, and as such, it evolved along with the design. It includes both KrF laser and heavy ion LINAC drivers, reactor cavity systems, and main heat transport systems, target energetics and manufacturing plant, fuel stream and waste processing, and all remaining balance-of-plant systems.

The IFE power plant performance is directly tied to the product of the driver efficiency, η, and the target gain, G, at a given driver energy. The basis for this is illustrated by the simple power flow diagram shown in Figure 2.3-1. Economic power generation requires that ηG exceed $1 / \varepsilon M'$, where ε is the plant thermal efficiency and M' the

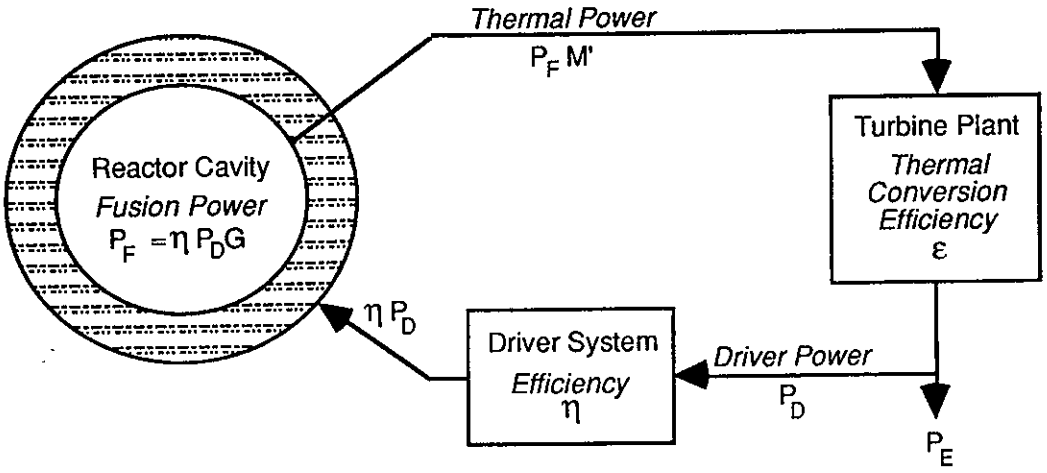

Figure 2.3-1. Simple Power Flow Diagram for an Inertial Fusion Power Plant

effective blanket power multiplication, typically by a factor of two or more. Advanced thermal conversion efficiencies of 40% and effective blanket multiplications of 1.1 thus imply a minimum ηG of ~6 for economic power generation. A 6% efficient driver requires target gain greater than 100. If the driver efficiency improves to 20%, a gain greater than 30 will suffice.

The systems modeling provides a basis for deciding how large an ηG is economically warranted. The target gain curves provided for this study are shown in Figure 2.3-2 for the KrF laser and heavy ion beam drivers. The constant focal spot (CS) gain curve is the TWG-recommended arithmetic mean of the Optimistic Gain curve and the Conservative Gain curve provided (see Figure 3.3-2 and the related discussion for details). These figures show that target gain typically increases with driver energy. This improves ηG, but implies a more costly driver. For a fixed-size plant, however, there can be a net cost savings because the driver is pulsed less frequently and therefore requires less input power. The size, hence cost, of the supporting plant equipment (reactor, steam generators, turbines, etc.) is thus reduced. The systems code quantifies this trade-off by parametrically modeling the size and cost of all major power plant systems. Incremental driver cost can then be weighed against the cost savings provided by higher target gain to determine the optimum size driver for the anticipated target gain curves.

The trade studies were also valuable in choosing between design options for some subsystems. This was particularly true for the heavy ion driver where the single beam LINAC was compared to a more conventional multiple beam system. This comparison involved a complex tradeoff between driver efficiency, which favored the multiple beam approach, and driver cost, which favored the single beam. The systems code quantified this trade and led to the selection of a single beam LINAC with storage rings for the baseline Prometheus-H driver concept. Finally, the systems code was useful in assessing the sensitivity of overall system performance to changes in key system performance assumptions. Cases were run at the minimum and maximum expected

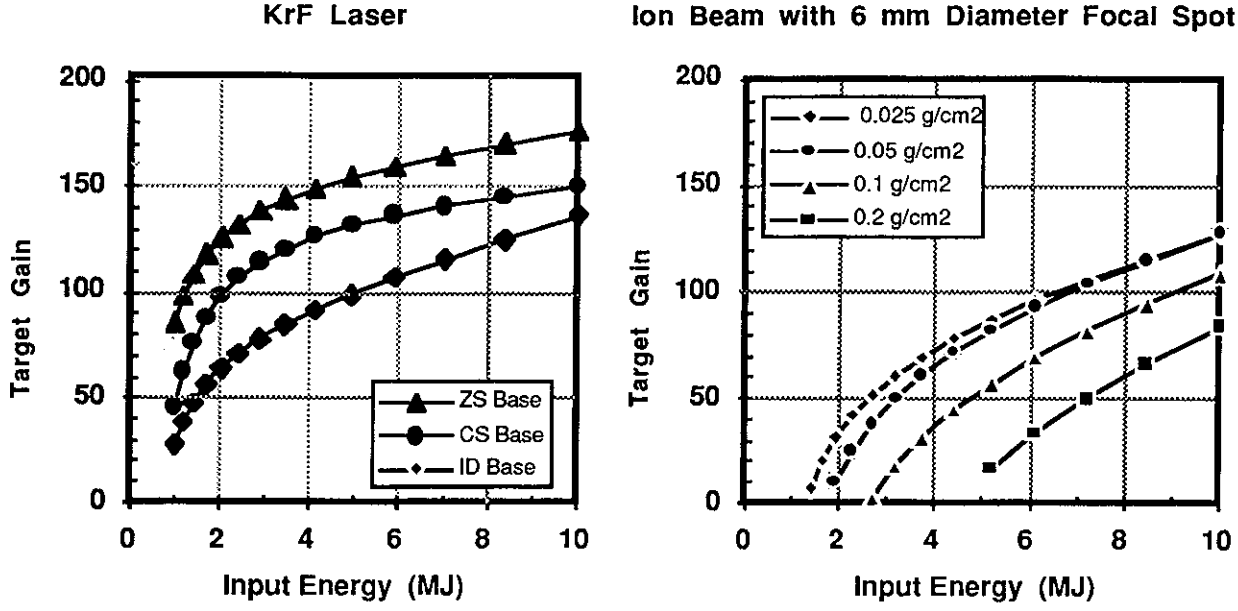

Figure 2.3-2. Comparison of Baseline Gain Curves for KrF Laser and Heavy Ion Systems. Laser Curves are for Direct Drive (Zoomed and Constant Focal Spot) and Indirect Drive Targets. Heavy Ion Curves Show Variation with Ion Range.

range of key parameters. These studies help provide a measure of the relative importance of research and development work in various areas.

2.3.1 Prometheus-L Design Point Selection - Figure 2.3.1-1 compares projected system performance for the three baseline laser target gain curve options. This figure highlights the strong preference for direct drive option predicted by the baseline gain curves provided for this study. The minimum cost of electricity is ~10% higher for indirect drive and the requisite driver energy increases from 4 to 6 MJ. The driver is thus more complex (2160 discharge lasers as compared to 960 for the direct drive case) and costly (~$250M). This is a direct result of the ηG penalty for the baseline indirect-drive gain curve. For the projected Prometheus-L driver efficiency of 6.5%, the 4 MJ direct drive system has an ηG of 8.2 compared to only 7.0 for the 6 MJ indirect drive case. Illumination symmetry requirements complicate the reactor plant design for direct drive, however the detailed design analyses led to the conclusion that for 60 beams, the cost implications of direct drive illumination are not significant. This was further reinforced by TWG guidance that indirect drive illumination, while not symmetric, would also require roughly 60 beams arrayed on two 60° half-angle cones. Direct drive targets were thus selected for the Prometheus-L system design.

Figure 2.3.1-1 also highlights the basis for selecting a 4 MJ driver energy. The COE is relatively flat between 3 and 5 MJ; however, the number of discharge lasers jumps from 960 to 2160 at 5 MJ in order to keep their output energy below 6 kJ that was selected as an upper limit on discharge laser technology. This complicates the driver design for no performance payoff. Conversely, at 3 MJ the same 960 discharge lasers

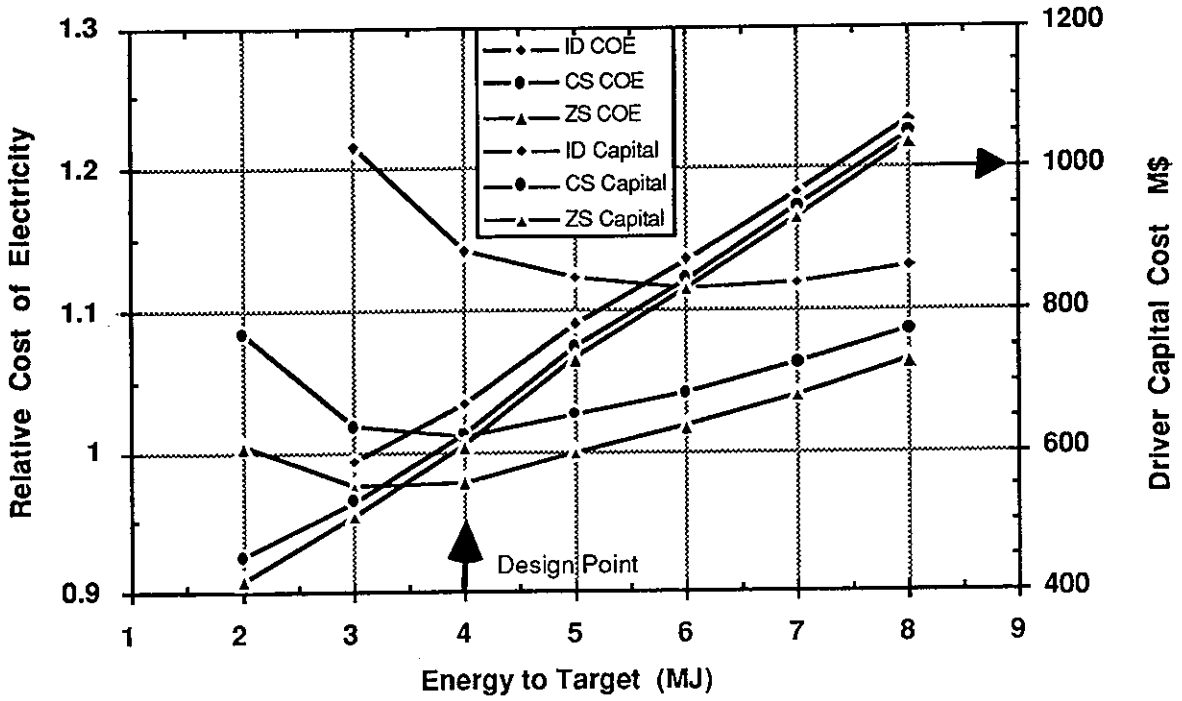

Figure 2.3.1-1. System Performance Comparison for the Three Laser System Target Options Using Baseline Gain Curves. Solid Curves Show COE, Dashed Curves Show Driver Capital Cost.

need only produce 4.4 kJ as compared to 5.9 kJ at 4 MJ. This is attractive from a laser design standpoint, but the pulse repetition rate increases from 5.6 pps to 8.2 pps at 3 MJ. This repetition rate does not provide sufficient cavity clearing time between pulses for the 3 mtorr laser pressure requirement. As a result, a 4 MJ driver energy was selected for the Prometheus-L design point.

The possibility of zooming the focal spot to improve target gain as suggested by the TWG was also considered. To assess the attractiveness of this possibility, the trade study shown in Figure 2.3.1-1 was conducted assuming no added driver cost to provide for zooming. The result of this study shows that a zoomed focal spot potentially leads to ~3% lower COE. For the Prometheus NLO laser architecture, the only viable way to zoom the focus involves modifying the rf-driven frequency chirpers for the SBS cells to enable them to introduce a time-varying wavefront curvature. This requires an annular rf field variation around the chirper that significantly complicates its design and would add to the capital cost. The benefit of focal spot zooming was deemed not sufficient to warrant this added complexity.

The results of the Prometheus-L sensitivity studies of the major parameters are highlighted in Figure 2.3.1-2. The data displayed in the figure is summarized in Table 2.3.1-1 together with the parameters that were varied and their range of variation. The adopted baseline gain curve was recommended by the TWG as the mean of the provided Optmistic and the Conservative Gain curves. Hence, these two

were used as the maximum and miniumum gain curve values. This figure shows that COE depends most strongly on the gain curve assumption and the discharge laser intrinsic efficiency. The projected COE is 10% higher at the minimum value considered for these two parameters and drops 5% below the baseline value at their upper limit. These are sensitive parameters because there is very little ηG margin for the KrF laser driver since the overall efficiency is only 6.5%.

Table 2.3.1-1. COE Sensitivity to Variations in Key Prometheus-L Design Parameters

Parameter	Baseline Value	Minimum Value	Change in COE (%)	Maximum Value	Change in COE (%)
Gain Curve (Conservative, Optimum)	126	86	+10.6	165	-4.8
Laser Intrinsic Efficiency (%)	15	10	+10.3	20	-4.7
Optical Damage Limit (J/cm^2)	10	5	+3.2	15	-1.1
Num Dischg Lasers, Energy (kJ)	960, 6	240, 20	+0.6	2160, 2	+0.3
Number Final Beamlines	60	30	-1.7	90	+1.7
Cavity Radius (m)	5	4.5	-2.2	5.5	+2.3

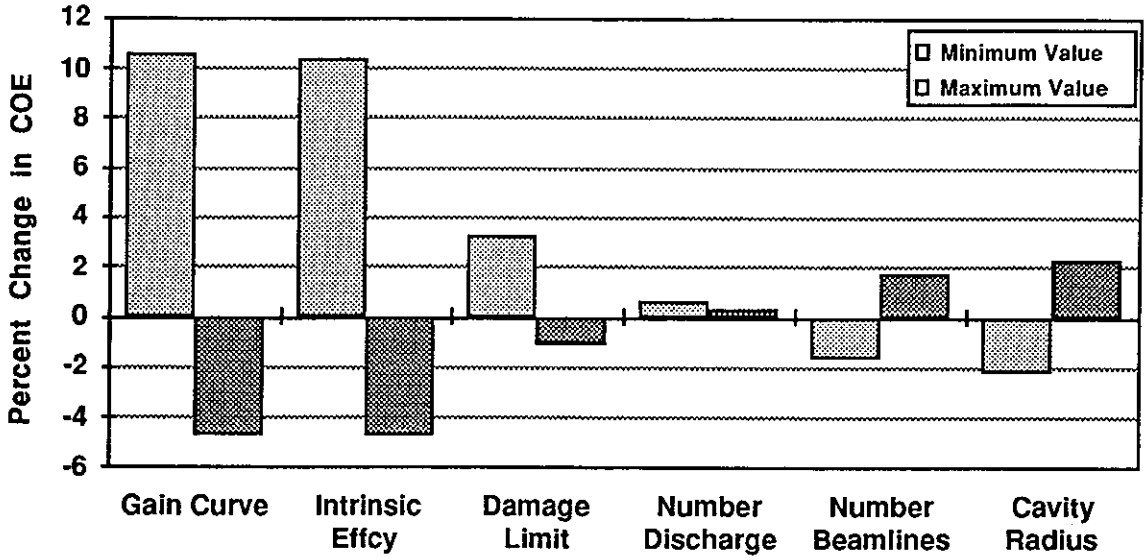

Figure 2.3.1-2. COE Sensitivity to Prometheus-L Design and Performance Assumptions

Sensitivity to optical damage limit shows that lowering it to 5 J/cm^2 causes a 3% increase in COE, while raising it to 15 J/cm^2 only decreases COE by 1%. There is thus little incentive to improve optical coatings beyond the 10 J/cm^2 point and this is why a 10 J/cm^2 fluence limit was adopted for the present study. Studies of discharge laser output power show that COE is virtually independent of this parameter even though the number of discharge lasers varies from 2160 down to 240. This is because the lasers are producing the same amount of total energy (4 MJ) in either case. Hence, the pulsed power energy requirement is the same and it is the major cost contributor. Finally, a decrease in the number of beamlines from 60 to 30 or a reduction in cavity radius from 5 to 4.5 m would each lower COE by 2%. Conversely, COE would

increase by 2% for 90 beamlines or if a 5.5 m cavity radius was needed to lower cavity vapor pressure.

2.3.2 Prometheus-H Design Point Selection - The primary issue for the heavy ion beam system design trade studies involved the choice between a multiple beam LINAC and the single beam system with intermediate storage rings. The parametric scaling and cost basis for this comparison is discussed in detail in Section 4.1.2, but the result is repeated in Figure 2.3.2-1. This comparison uses lattice scaling suggested by Ed Lee[3], since it was thought to be most favorable for multiple beam systems. The final single beam design uses an alternative lattice scaling discussed in Section 6.2 that leads to lower capital cost and higher single beam efficiencies than those presented here. Nevertheless, this figure still highlights the significant advantage projected for the single-beam approach in spite of its lower efficiency, 15% as compared to 37% for the multiple beam. Driver capital costs are roughly half those for the multiple beam system and this leads to a 12% reduction in COE. The single beam system was, therefore, selected for the baseline driver in the Prometheus-H design study.

It should be noted, however, that the multiple-beam system remains a viable driver option. Its COE is comparable to that for the KrF laser system, and the alternative transport lattice scaling discussed in Section 6.2 also leads to significantly lower MB capital costs than those presented here. In addition it avoids technical issues associated with beam stability and particle loss in the storage rings. These are critical R&D concerns for the single beam approach and they are highlighted in Section 5.

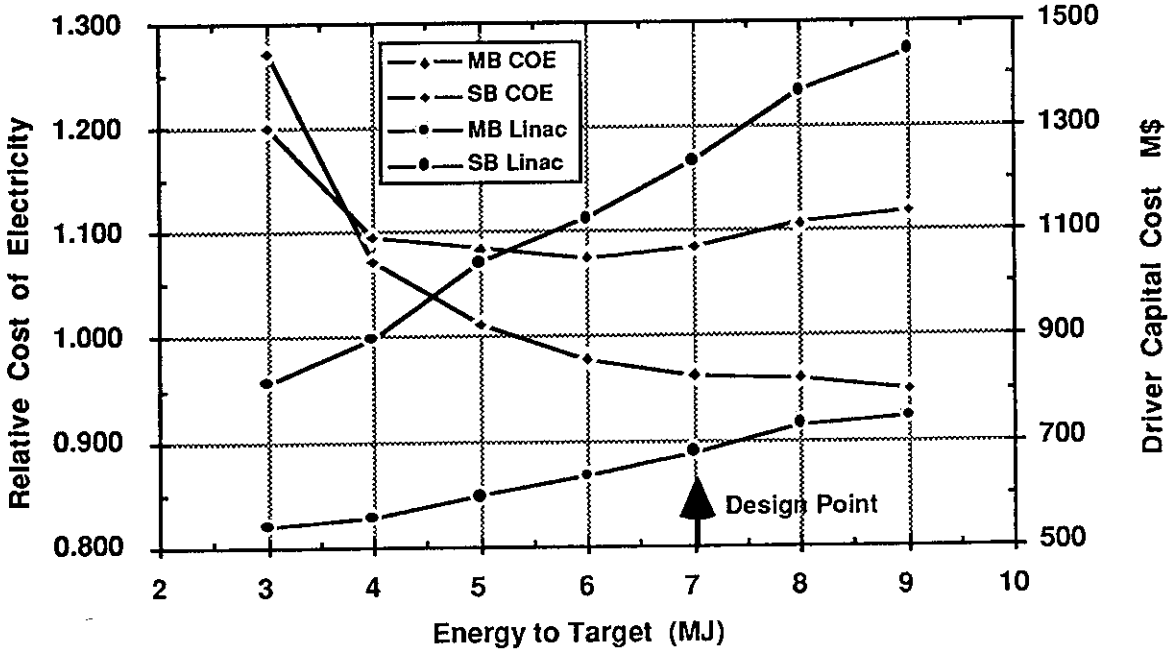

Figure 2.3.2-1. Comparison of Projected COE and Driver Capital Cost for Multiple and Single Beam LINACs. Systems are all 4 GeV, +2 Lead with 3 mm Radius Focal Spot.

A number of other significant design parameters, such as ion range, ion type/charge, spot size, illumination, ion energy, and incident beam energy, were evaluated in arriving at the reactor and HI beam driver design point. Section 6.2.2 discusses these factors and trade studies in detail. However the trade study to determine the incident beam energy on the target is worthy of discussion here. Figure 2.3.2-1 illustrates that the COE continues to decrease, with increasing energy delivered to the target although the gains above 7 MJ are becoming increasingly small. The cost of the driver continue to increase above this level. And as the energy increases, the gain curves indicate a continued improvement in the utilization of the energy within the target. This effect causes the lowering of the COE regardless of the capital cost increases. The increase in incident energy comes at the expense of more beamlets and magnet quads in the accelerator system, hence more complexity and risk. It was felt that pushing the design point past 7 MJ on target (7.8 MJ out of the driver) would represent a significant developmental risk for the driver system and entail significant technical risk with declining economic benefits. Further driver development may allow this design envelope to extend to higher energy levels on target at a future date.

The results of the Prometheus-H sensitivity studies are highlighted in Figure 2.3.2-2. The data displayed in the figure is summarized in Table 2.3.2-1 together with the parameters that were varied and their range of variation. These results highlight several key aspects of the Prometheus-H driver design. The primary one involves the improved cost and performance characteristics provided by the reduced ion kinetic energy. As is indicated, COE is 18% higher for a 7 GeV design due to the increased length of accelerator required at this energy. The number of beamlets is reduced from 18 to 6 at 7 GeV, but the single beam approach, coupled with the alternate transport scaling, eliminates most of the complication (hence cost) of added beamlets at 4 GeV. The results also indicate that there is little motivation to further reduce ion energy. COE is 3% lower at 3 GeV but 32 beamlets are required at this energy which complicates the final transport and lowers driver efficiency by 13%.

It is worthwhile here to note that the alternative lattice transport scaling really opens a more attractive heavy ion LINAC design window that previously was not accessible due to the large number of required beamlets. This can be understood by referring to the gain curves shown in Figure 2.3-2. The gain falls off rapidly for ion energies above 5 GeV and is almost a factor of 2 lower for the 10 GeV ions typically proposed in the past. In addition, lower energy ions are much less sensitive to variations in focal spot size. The results show that a 7 GeV system is twice as sensitive to spot size variations as the 4 GeV design point. This is important because it minimizes the effect that the poorly understood transport channel reimaging properties may have on system performance.

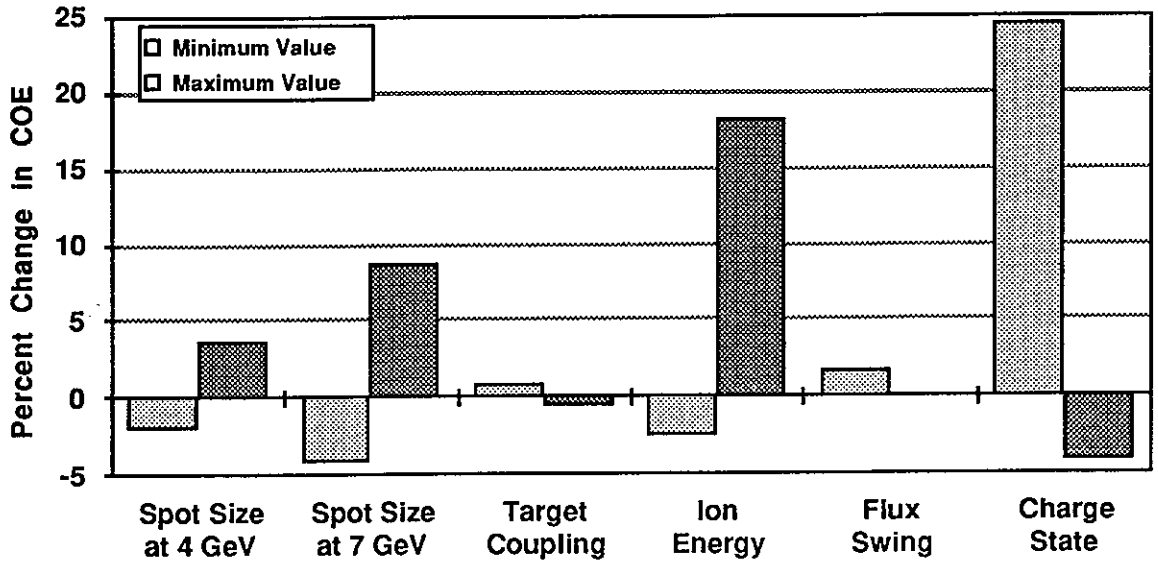

Figure 2.3.2-2. COE Sensitivity to Prometheus-H Design and Performance Assumptions

Table 2.3.2-1. COE Sensitivity to Variations in Key Prometheus-H Design Parameters

Parameter	Baseline Value	Minimum Value	Change in COE, Effcy*	Maximum Value	Change in COE, Effcy*
Focal Spot Radius (mm)	3	2	-2.1	4	+3.6
Spot Radius Change at 7 GeV**	3	2	-4.3	4	+8.6
Final Beam Transport Effcny (%)	90	80	+0.8	100	-0.6
Ion Kinetic Energy (GeV)	4	3	-2.7, -13.0	7	+18.2, +21.4
Core Flux Swing (T)	1.5	1.0	+1.7, +8.4	2.0	+0.1, -9.3
Ion Charge State	+2	+1	+24.5, +2.8	+3	-4.2, -4.4

* Change in driver efficiency is indicated only for parameters that influence it significantly

** Changes are normalized to 7 GeV system with 3 mm radius spot which is 18% higher than 4 GeV COE

Insensitivity to transport channel properties are reinforced by the weak COE dependence on final beam transport efficiency (beam energy loss in the transport channel). A doubling of energy loss (from 10 to 20%) only increases COE by 1%. The results also indicate very weak COE dependence on Metglas flux swing. A low flux swing of 1.5 T was selected for the baseline design to reduce induction core energy losses since this was thought to be a key factor in the design of a single beam LINAC where the cores are recycled several times per pulse. Indeed, the driver efficiency changes by ± 9% as flux swing is varied from 1 to 2 T, however this causes only a 1% change in COE.

Finally, the results highlight that there is still a significant advantage to higher charge states for the single beam system, but that the payoff is limited beyond +2. The cost of electricity is 24% higher for singly charged ions while it drops by 4% for charge state 3. Unfortunately, the number of beamlets increases to 36 for +3 ions that may offset the

indicated cost advantage once the engineering details of final transport and focusing are evaluated.

In spite of concerns about beam stability in the storage rings, the Prometheus-H design point represents a tantalizing development goal for heavy-ion drivers. This is underscored by Table 2.3.2-2 that compares the projected Prometheus-L driver costs with those for a 4 GeV, 7 MJ multiple beam driver design using the Lee lattice scaling[3] that was the starting point for this design study. This comparison highlights the potential advantages of the configuration. The single beam accelerator column reduces accelerator structure costs by $200M and focusing magnet costs by $320M. In addition, the alternate transport lattice scaling reduces the number of beamlets from 34 to 18; that leads to cost savings of $120M in the final transport and focus sections. Pulsed power costs are assumed to be ten times those for the MB system per joule, but the overall SB pulsed power cost is only $20M higher because the system only provides energy for one beamlet at a time. All of these savings are at the expense of a stack of 14 storage rings that are projected to cost ~$20M.

The net result is a $700M reduction in projected cost and a significant simplification in required LINAC technology development. It should be noted that this comparison is not entirely fair because the MB system would not have considered a design at 4 GeV due to the large number of required beamlets. However, this raises another important point, namely that the proposed design has extended the heavy-ion LINAC design window to a more attractive region of parameter space. The 4 GeV ion energy provides improved target performance due to the reduced range at this energy, and it reduces LINAC costs because it corresponds to a shorter accelerator. Significant issues need to be resolved concerning the storage rings, but the starting point is much more appealing than any previously envisioned for induction LINAC drivers.

Table 2.3.2-2. Projected Single and Multiple Beam LINAC Cost Comparison for 4 GeV, 7 MJ Drivers

Component	SB Cost (M$)	MB Cost (M$)
Injector System	10.0	40.0
Accelerator Structure	100.5	292.4
Focusing Magnets	61.4	387.6
Cryogenic System	12.3	18.2
Storage Rings	18.5	0.0
Final Transport	76.2	194.1
Pulsed Power	214.1	194.4
Vacuum System	13.7	13
Instrum & Control	27.0	58.5
Maint Equipment	33.1	33.1
Misc Equipment	10.8	23.4
Tunnel and PFN Bldg	38.3	49.8
Total System Cost	615.9	1304.5

Note: These costs are for a first production unit, not tenth of a kind.
SB = Single Beam, MB = Multiple Beam, PFN = Pulse Forming Network.

References for 2.3

1. C.C. Baker, et al., "STARFIRE - A Commercial Tokamak Fusion Power Plant Study," ANL/FPP-80-1 (1980).

2. February 1988 special issue, *Fusion Technology,* **13**, 2 (1988).

3. Dr. Edward Lee, Lawrence Berkeley Laboratory, Private Communication.

2.4 Prometheus-L Reactor Plant Design Overview

The Prometheus-L power plant is a KrF excimer laser-driven commercial central station power plant. These designs are based upon an extrapolation of today's technology advanced some 20-30 years into the future. The necessary technology and engineering basis is assumed to have been developed previously. The design emphasizes safety, environmental attractiveness, economic competitiveness, soundness of physics and engineering data, and a high degree of reliability, maintainability, and availability.

The data base upon which to design the two power plants is rich in reactor concepts both from the IFE and MFE communities. Many reactor designs have preceded these design studies, each with innovative and valuable system concepts worthy of consideration. A following chapter, Chapter 4, will thoroughly discuss the rationale for choosing the key design options addressed in these studies. Additional trade study data, design rationale, and detailed definition and analyses for the reactor systems are presented in Chapter 6, Conceptual Design Selection and Description. This section is intended to provide the reader with a brief overview of the key features of the KrF laser-driven inertial fusion power plant that evolved out of the design study. Section 2.5 provides a similar review for the heavy ion beam-driven power plant.

2.4.1 General Plant Features - An overall site plan for the Prometheus-L reactor power plant is shown in Figure 2.4-1. The reactor building is located at the center of the complex with the fusion reactor cavity at its center. Surrounding the reactor building is an annular laser hall housing the laser driver subsystems including 60 identical sets of the final electric discharge laser amplifiers, Raman accumulators, Stimulated Brillouin pulse compression cells, and pulse shaping and delay line optics shown in Figure 2.4-2. The annular arrangement was selected to simplify beamline layout for the symmetric direct drive illumination geometry. The laser system architecture builds on reliable, moderate energy (~6 kJ), electric discharge lasers coupled with non-linear optical (NLO) systems for final beam combination and pulse compression. This is an attractive, flexible, and low-risk approach to the driver design as discussed in Section 2.4.3.

Figure 2.4-1 also indicates the other ancillary facilities necessary for an inertial fusion power plant. The steam generator building houses six sets of steam generators for both the blanket coolant loop (1.5 MPa He at 650°C outlet temperature) and the first wall protectant/coolant loop (liquid lead at 525°C outlet temperature). These systems are discussed in Section 2.4.4. A tritium processing building provides for recovery of unburned fuel and target debris (carbon and hydrogen) from the liquid lead loop and removal of fresh fuel from the blanket purge loop (1 MPa He = 0.2% H_2). An auxiliary building provides for processing of spent blanket modules (ten-year lifetime) and first wall panels (five-year life). Analyses indicate that the resulting waste material will all qualify for Class C or better disposal.

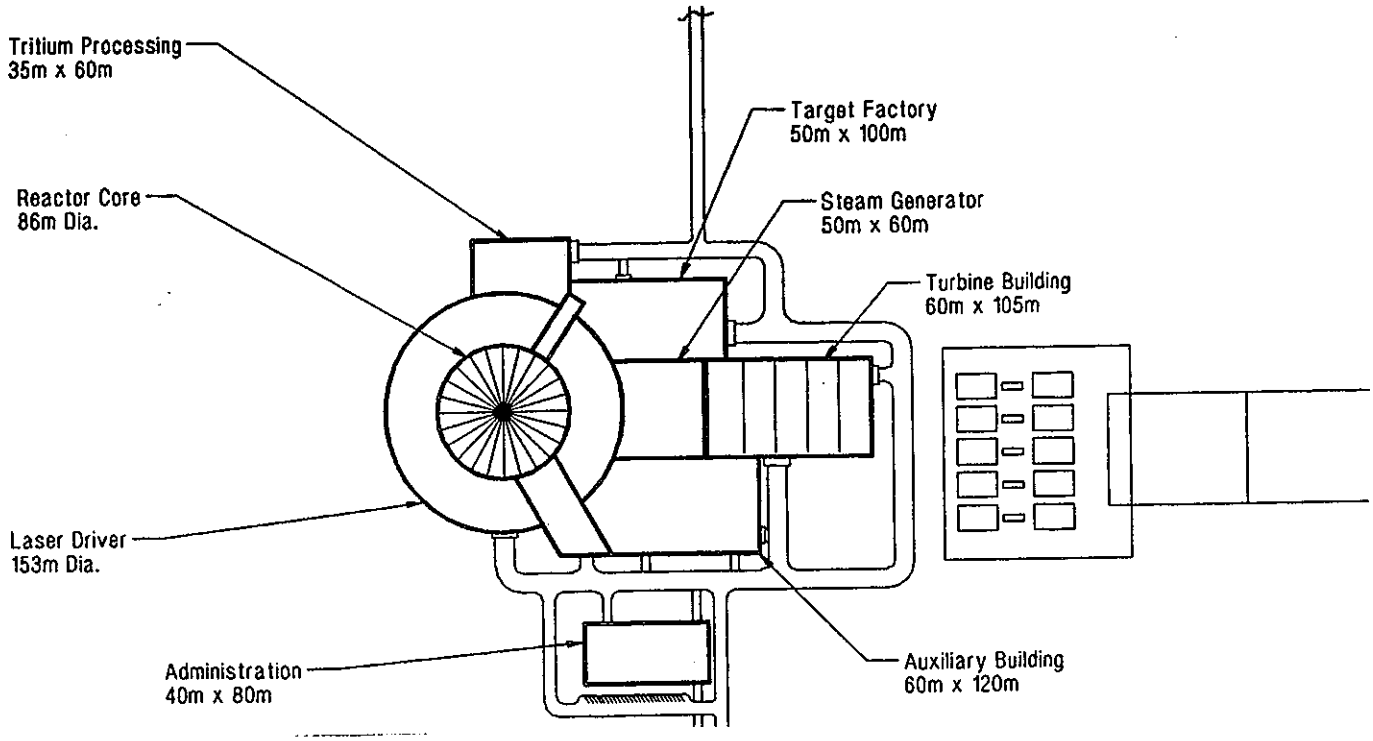

Figure 2.4-1. Prometheus-L Site Plan

The turbine building houses the 1,400 MWe main steam turbine for the power plant. It employs an advance Rankine steam cycle to achieve 42.3% overall efficiency. The recirculating power fraction is high at 29% for the Prometheus-L system due to the low 6.5% driver efficiency. This is offset to some extent by using the laser gas waste heat for feedwater heating in the turbine plant. Finally, a target factory is also included for manufacturing the 180 million targets used annually by the power plant. This eliminates the need to ship tritium off-site for target processing and leads to a self-contained on-site fuel cycle. The targets are simple hydrocarbon (CH) shells, diffusion-filled with DT, and then cooled to cryogenic temperatures. Beta heating is used to provide for uniform layering of the fuel inside the capsule. A total tritium inventory of ~7 kg (7×10^7 Ci) is anticipated in the target factory. Release concerns are minimized by dividing this inventory into several separate chambers.

The major Prometheus-L design parameters are summarized in Table 2.4-1. The plant produces a net power output of 972 MWe to the electric grid from a total thermal power of 3,091 MWt, for a net system efficiency of 31%. The gross power of 1,382 MWe is derived from 3,264 MWt that is composed of 3,049 MWt from the fusion power core and 215 MWt of waste heat from the driver and lead pumping systems. Thirty percent of the gross power supports in-plant requirements for the laser driver (342 MWe), auxiliary systems (36 MWe), and liquid lead pumping (25 MWe). Helium-flow through the blanket is provided by steam-driven circulators. The fusion core

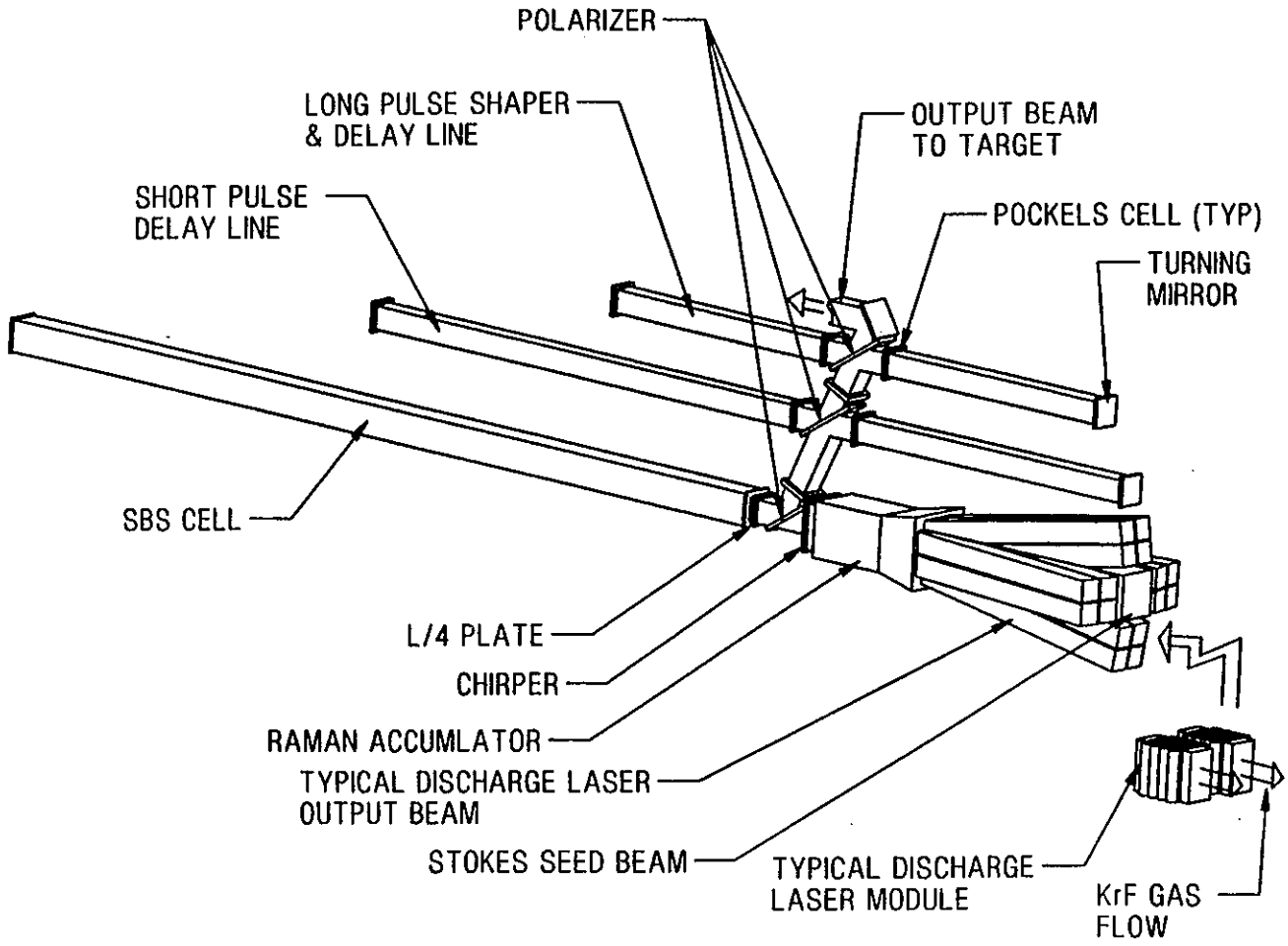

Figure 2.4-2. Raman Accumulator/SBS Cell/Delay Line

power results from a target yield of 497 MJ at a pulse repetition rate of 5.65 per second with an energy multiplication factor of 1.14. The liquid lead first wall loop handles 1,267 MWt of this power with the remainder going to the blanket loop. The power in the first wall loop is significantly higher than the surface heating of 780 MWt due to neutron interactions in the lead coolant channels.

The reactor cavity features a first wall (FW) system employing liquid lead that both cools the silicon carbide FW structure and bleeds through the porous inner wall to provide a protective film on the FW surface. The blanket features a SiC composite tube sheet structure sandwiched around layers of packed bed Li_2O breeder. The blanket has separate helium purge and helium coolant streams.

The reactor cavity radius and height of 5.0 and 15.0 m, respectively, are determined from the need to conduct the surface heat energy through the first wall support structure into the coolant, with a surface temperature that enables the lead vapor pressure in the cavity to reach the level required for laser propagation without breakdown (~3 mtorr) before the next pulse. This is driven by the available surface

Table 2.4-1 Prometheus-L Major Design Parameters and Features

Parameter	Value
Net Electric Power (MWe)	972
Gross Electric Power (MWe)	1382
Driver Power (MWe)	349
Auxiliary Power (MWe)	36
Cavity Pumping Power (MWe)	25
Total Thermal Cycle Power (MWt)	3264
Blanket Loop Power (MWt)	1782
Wall Protection Loop Power (MWt)	1267
Usable Driver Waste Heat (MWt)	193
Usable Pumping Waste Heat (MWt)	22
Thermal Conversion Efficiency	42.3%
Recirculating Power Fraction	30%
Net System Efficiency	31%
Fusion Power (MW)	2807
Neutron Power (MW)	2027
Surface Heating Power (MW)	780
Fusion Thermal Power (MWt)	3092
Thermal Power to Shield (MWt)	43
Cavity Radius (m)	5.0
Cavity Height (m)	15.0
First Wall Protection/Coolant Media (In/Out Temp., °C)	Liquid Lead (375/525)
Breeder Material	Li_2O Pebbles
Structural Material, Wall and Blanket	SiC
Blanket Heat Transfer Media (In/Out Temp., °C)	1.5 MPa Helium (400/650)
Cavity Pressure (mtorr, Pb)	3.0
Neutron Wall Load, Peak/Ave (MW/m^2)	6.5/4.3
Energy Multiplication Factor	1.14
Tritium Breeding Ratio (TBR)	1.20
Target Illumination Scheme	Direct Drive, Symmetric
Number of Beams	60
Driver Output Energy (MJ)	4.0
Overall Driver Efficiency (%)	6.5
Type and Number of KrF Amplifiers	Electric Discharge, 960
Beam Combining Technique	Raman Accumulators
Pulse Compression Technique	Stimulated Brillouin Scattering
Final Beam Transport Efficiency (%)	100
Target Gain	124
Target Yield	497
Repetition Rate (pps)	5.65
Plant Availability (%)	79.4
Cost of Electricity (mills/kWh, 1991$)	72.0

area so the cavity is elongated slightly by inserting a one-radius high cylindrical section between the hemispherical ends. This shortens the recondensation time without introducing a large difference between the peak and average wall loading.

Safety and environmental impact were strongly considered during the design option selection and design definition stages of the program. The design team favored the use of the low activation SiC material as the principal structural material in the first wall

and blanket region. Use of this material also extended to the primary coolant piping from the plenum regions out through the primary bulk shield. Care was taken to only include a minimum of ferritic materials within the bulk shield and then only in the vacuum vessel. Helium was chosen as the main heat transfer media to reduce the danger of fires and explosions present with liquid metals. The pressure of the helium coolant was lowered from the more conventional high pressure of 50 atmospheres to 15 atmospheres to reduce the safety consequences of a blanket tube leakage or rupture. To accomplish a viable wetted wall protection system, a liquid metal film on the surface is required. Lead provides excellent heat transfer capability, neutron multiplication, no fire hazard, and minimal decay heat. Lead has a toxicity and radioactivity concern but these have been carefully analyzed and considered to be acceptable. A composite shield composed of aluminum structure, B_4C, Pb, SiC and water is used to provide a predictable, low activation shield that will reduce decommissioning costs. Electric discharge lasers were chosen over the large e-beam pumped KrF lasers to eliminate the hazard associated with the foil rupture and release of the high temperature KrF gases. More numerous (960) electric discharge lasers operated at lower output energies (~6 kJ) permit safer, more reliable reactor operation.

With the attention to selection of materials, innovative design approaches and careful design practices, Prometheus-L is rated as a Level of Safety Assurance (LSA) = 1, which means safety is assured by passive mechanisms of release limitations no matter what the accident sequence. The radioactive inventories and materials in Prometheus-L preclude a fatal release regardless of the reactor's condition. This definition is extracted from the ESECOM study[1]. The usage of low-activation materials, such as SiC, allows all waste material to be classed as Class C or better.

2.4.2 Target Features - Both the direct drive (DD) and indirect drive (ID) targets were considered for the Prometheus-L power plant. Target illumination requirements provided by the TWG were used to determine beamline geometries and pulse comparison and shaping systems. Target performance was parameterized in the form of the gain curves shown on Figure 2.3-2. An assessment of the supplied target data showed that direct drive targets were more favorable in terms of lower operational cost and better performance at the same driver energy. However, the chosen driver and reactor designs can easily accommodate either target configuration.

The unknown factor in this decision is the risk associated with the technical performance of both types of targets. Quantitative assessments of target physics feasibility are difficult. Extrapolations are required in incident energy, number of illuminating beams, power balance and pointing of the beams, gain of the target, and from stationary to moving targets. The design team heard differing opinions as to the inherent risk in each target concept, but the TWG provided assurance that supplied gain curves and associated data had been normalized to account for those risk factors. Thus the team elected to adopt the direct drive, symmetrically illuminated target for the baseline design.

A target factory or plant is located on site adjacent to the Reactor Building to provide a ready supply of targets with a minimum tritium inventory. The direct drive target will be a hydrocarbon (CH) shell approximately 6 mm in diameter, the inner shell filled with a mixture of frozen DT. Figure 2.4-3 schematically illustrates the direct drive target configuration. Droplet generators combined with micro-encapsulation processes will form the shells with the necessary surface finish. A diffusion process will fill the shell with DT within 24 to 36 hours. The DT will be frozen, forming on the inner shell walls. Beta heating will be used to achieve the necessary uniform DT layer. The targets will be inspected, mated to an injection sabot, and held in a short queue to be injected into the cavity.

The target injection system is an electromagnetic synchronous accelerator that accelerates the capsule and sabot with 100 g's to a velocity of 200 m/s. The sabot protects the capsule from abrasion in the 20 meter long accelerating tube, provides thermal protection in the holding and acceleration processes, and provides the accelerating forces via an imbedded ferromagnetic insert. The robust CH shell and inner DT layers should easily withstand the acceleration forces. Analyses have also shown that the heating during the transit time across the reactor cavity will be acceptable for the direct drive target. The target velocity and position will be determined after the exit from the injector in order to predict the target position relative to the center of the cavity. Repeatability of the positioning of the target at the center of the cavity was addressed and the resulting positional requirements are thought to be within current technology capabilities. The final mirrors and/or grazing incidence metal mirrors (GIMMs) can be adjusted in angle to account for slight variations in target position. Estimates indicate that the target will be within a millimeter of the final focus position from the time the excimer laser master oscillator initiates the 60 laser beams until beam arrival.

2.4.3 KrF Laser Driver Features - The laser driver architecture chosen for the Prometheus-L design is based upon a moderate energy (~6 kJ) electric discharge excimer laser amplifier module coupled with non-linear optical (NLO) systems for beam combination and pulse compression. This approach yields a safer and more reliable design with design flexibility and capabilities to meet the target demands for beam quality and illumination requirements. The Prometheus-L laser driver delivers 4.0 MJ of laser energy at ~250 nm. This energy is delivered with 60 beams symmetrically arranged to converge simultaneously on the target. The NLO system architecture incorporates special optical delay lines to tailor each arriving beam to have a long (80 ns), low energy precursor beam followed by a shorter (6 ns), high energy main pulse. Beam profiles are tailored to be flat-topped to fully illuminate the target from all 60 locations. The beams interact with the target to compress and heat the target to fusion conditions.

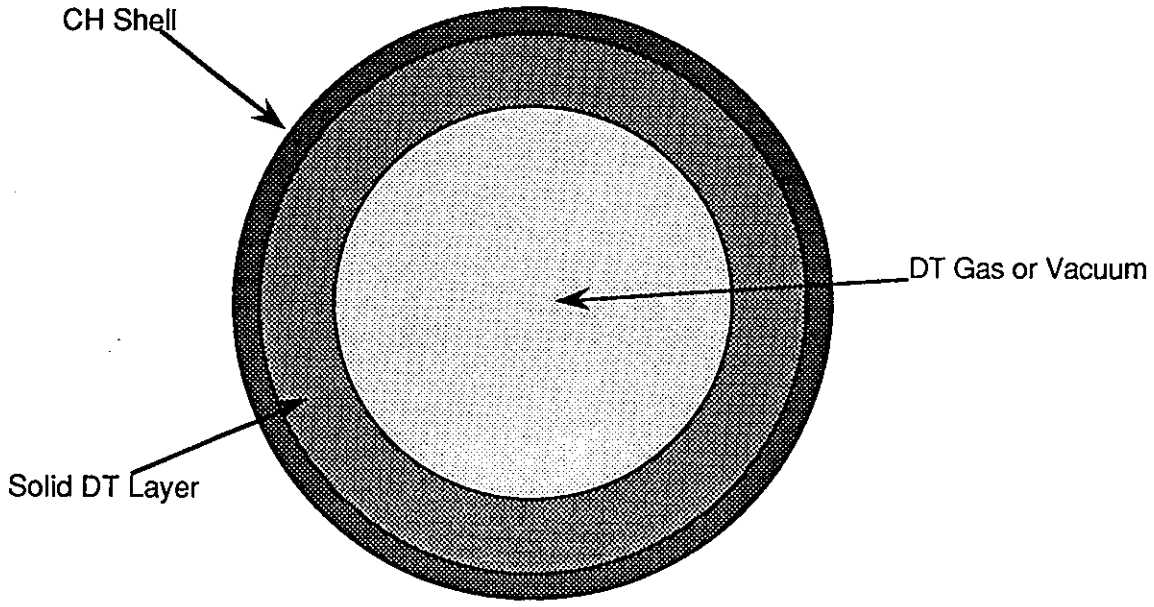

Figure 2.4-3. Schematic of Laser Direct-Drive IFE Target Structure.

The primary pulse of laser energy is provided by 960 electric discharge laser power amplifiers (16 for each of 60 beamlines), each producing ~6 kJ in a nominal (250 ns) pulse. These amplifiers are driven from a common master oscillator through a series of beam splitters and pre-amplifiers. Figure 2.4-4 illustrates a module of 16 power amplifiers combined in a common module for a single beamline. The KrF working gas is circulated through the lasing cavities and the waste heat is removed to maintain proper thermal conditions in the lasing cavity. This waste heat is used in the thermal conversion process to improve the effective driver efficiency.

The relatively low quality beam outputs from the 960 excimer laser power amplifiers (ELPAs) are directed into 60 Raman Accumulator Cells (RAC) to combine the energy of the individual ELPAs into that required for each beamline. The Raman Accumulators are 1.8 m square aperture x 5 m long cavities filled with D_2. One of the attractive features of the RAC is that it converts relative low quality, high power pump beams into a high quality, high power output beam. The output beam from each RAC is now 81 kJ and 250 ns long. This is achieved at a high conversion efficiency of 88%. The Raman accumulator process is schematically shown in Figure 2.4-5.

The next step in the Prometheus-L optical train is to compress the 250 ns beams exiting the Raman Accumulators into shorter beam pulses suitable for the primary and precursor interactions with the target (~6 ns for the main pulse and ~80 ns for the prepulse). This is accomplished with the use a stimulated Brillouin scattering (SBS) cell. The leading edge (10 ns) of the long duration pulse from the RAC is "chirped" or frequency-shifted by an amount equal to the Brillouin shift in the SF_6 gas used as the SBS gain medium. The duration and modulation depth of the "chirped" signal permit

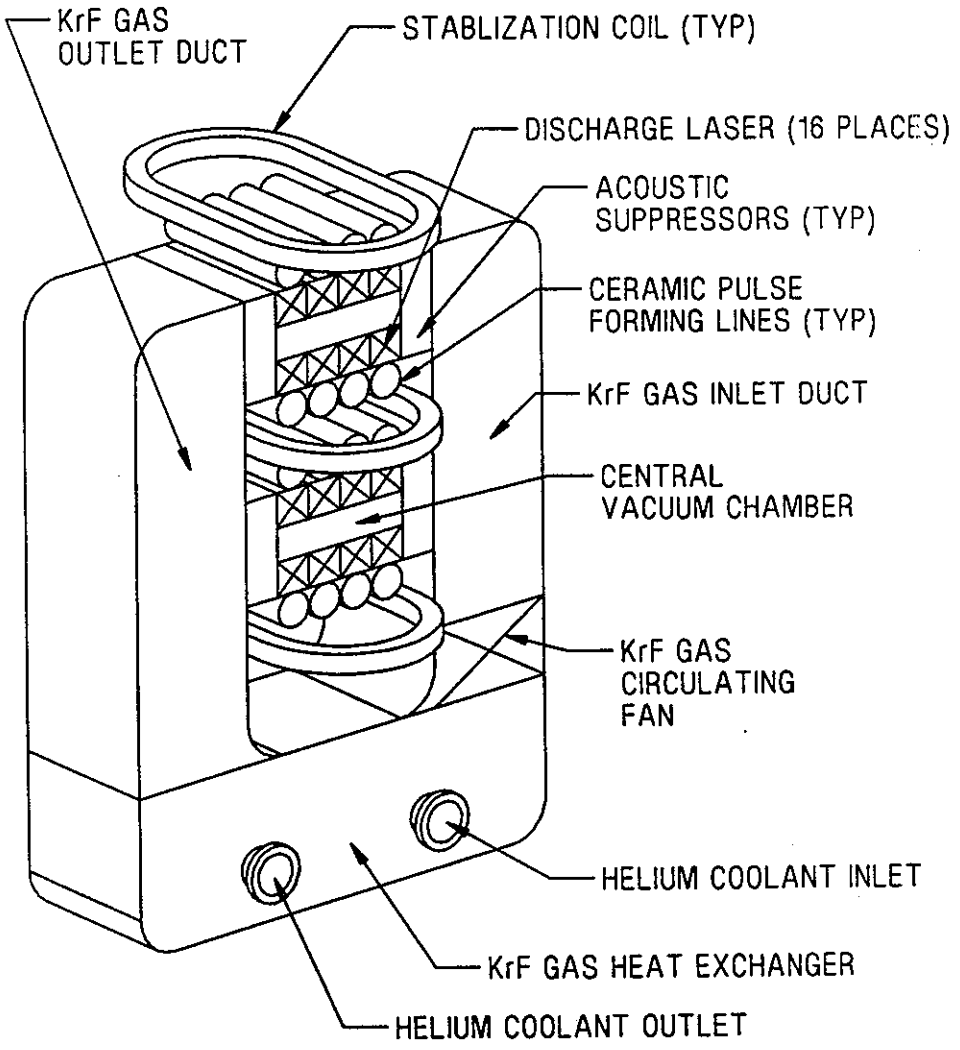

Figure 2.4-4. Electric Discharge Laser Subsystem

control of the shape and pulse duration of the resulting compressed pulse. The entire 250 ns beam with the "chirped" 10 ns leading edge travels the 37.5 m length of the SBS cell and reflects off an internal mirror aligned normal to the beam. As the "chirped" leading edge and the remainder of the beam reflects back onto itself, the frequency-shifted photons in the leading edge experience high optical gain from the SF_6 gas pumped by the incoming beam. This results in a highly compressed beam, suitable for the main pulse. The process is depicted in Figure 2.4-6.

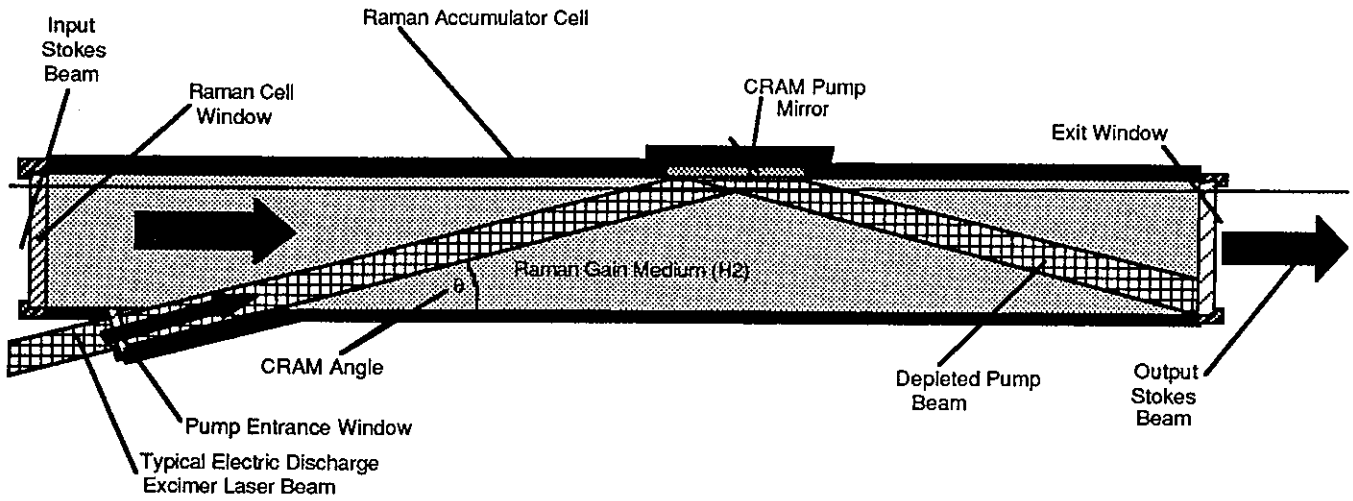

Figure 2.4-5 Injection of the Stokes seed into the Raman accumulator cell permits the efficient extraction of the excimer pump beams into a 81 kJ beam having an aperture of 1.2 x 1.2 m.

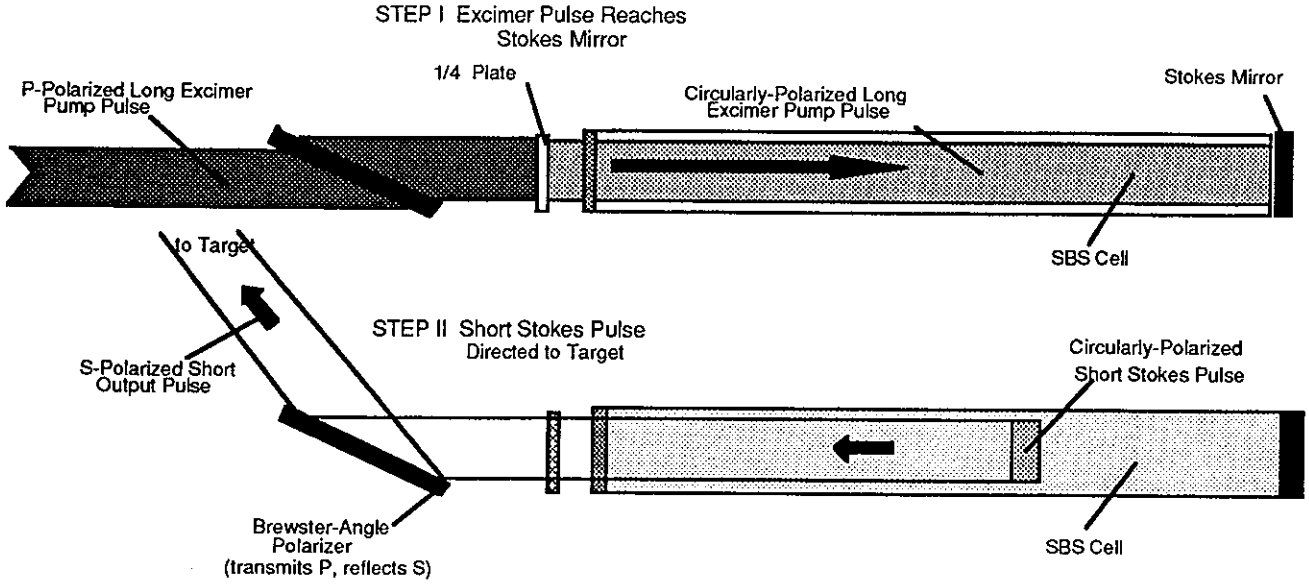

Figure 2.4-6 By frequency-"chirping" the leading edge of the SBS pumping pulse and reflecting it back upon the incoming pulse within an SF cell, it is possible to compress the RAC output pulse from 250 ns (or 500 ns) down to short pulse durations.

Although the SBS cell has some control over the pulse shape and energy content of the emerging beams, additional temporal tailoring of the beam is required. The residual energy in the unextracted portion of the original 250 ns pulse is used to generate a prepulse beam. An optical switchyard of delay lines inverts the sequence of the leading and trailing pulses from the SBS cell to form proper prepulse and main pulse durations and energy content while achieving high energy conversion efficiency in the SBS cell. An illustration of the entire optical train from each set of 16 ELPAs through the Raman Accumulator, SBS cell, and delay lines for one of the 60 beamlines was shown previously in Figure 2.4-2.

The 60 beams are directed from the SBS cells and delay lines through the reactor building wall, down shielded beamlines to the reactor cavity as shown in Figure 2.4-7. To protect upstream optics and driver plant equipment, a neutron pinhole is provided upstream of the final turning mirror. A grazing incidence metal mirror (GIMM) is used at a distance of 20 meters from the center of the reactor cavity. This long-lived component will be located in the direct line-of-sight of the target. The final focus mirror will not be in the direct line-of-sight of the target but will still be in a high radiation zone. Neutron traps are provided to help minimize radiation down the beamlines. The GIMMs and the final focus mirrors are equipped with fast-acting actuators to align the beams on the targets. Tracking systems will provide information from the targets at the end of the injector and, if needed, within the reactor cavity.

Considerable effort was directed toward identifying the physical processes governing the transmission of the optical beams through the reactor cavity. The predominant constituent in the gas atmosphere within the reactor cavity is lead vapor. Trade studies were conducted to determine the optimum combination of wall protectant temperature, cavity radius, repetition rate, beam losses by various mechanisms, and vacuum pumping requirements. The studies showed that the lead protectant operating at its highest possible temperature (525°C) for compatibility with external stainless steel piping and a cavity radius of 5.0 meters would result in a 3 mtorr Pb vapor pressure. This vapor pressure is not anticipated to cause significant loss in beam energy content or quality during transit across the cavity.

2.4.4 Reactor Cavity Features - The reactor cavity for the Prometheus-L design includes the first wall system, blanket, coolant manifold, vacuum vessel, and shield. The main purpose of the cavity is to contain the radiation and blast effects from the inertial fusion reaction, transform that nuclear energy into a more useful form of energy, and to breed tritium for sustaining fuel supplies. Since the reactor cavity is exposed to a very harsh radiation environment, it is the component that would have the most impact on the safety and environmental impact associated with the plant.

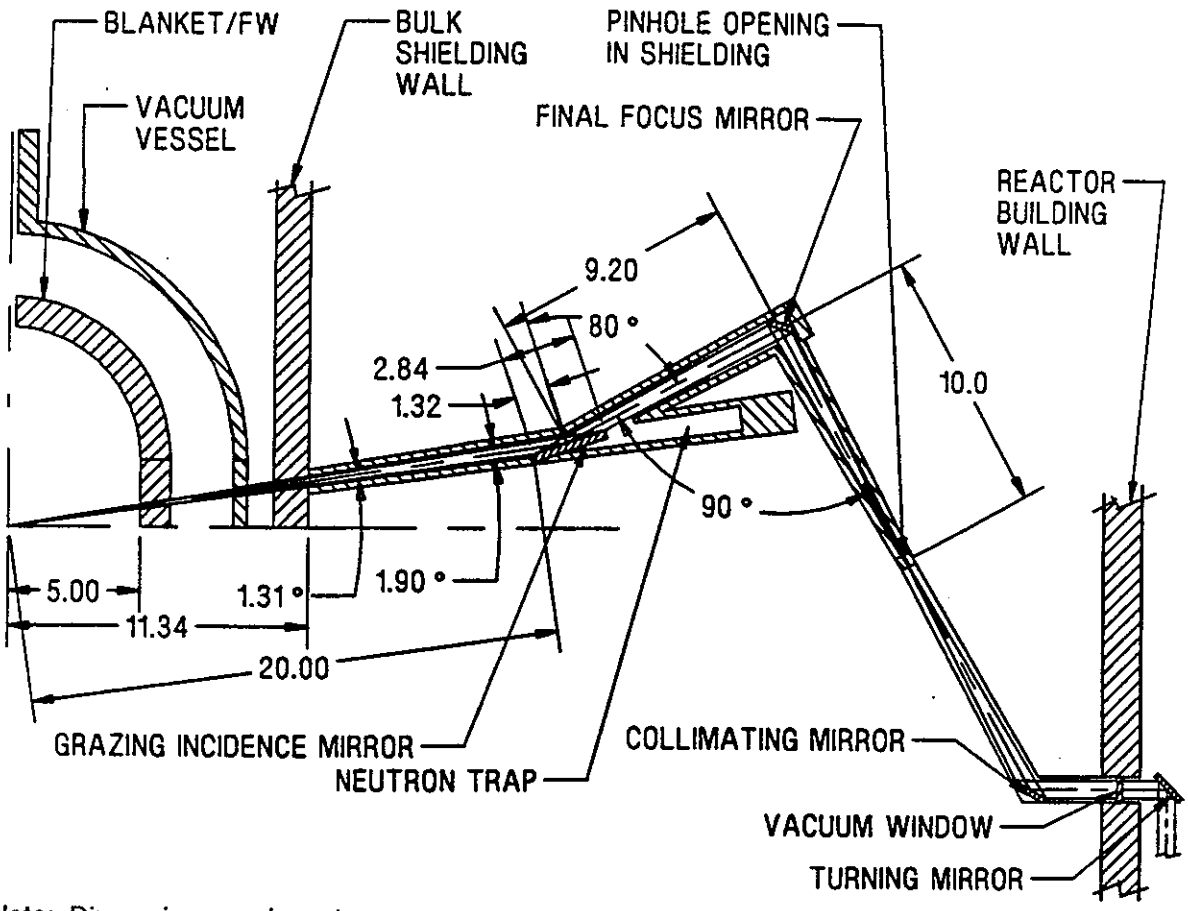

Note: Dimensions are in meters.

Figure 2.4-7. Final Optics Configuration-Reactor Building

Safety and environmental impact played a significant role in the choices of materials and the design approaches employed. Many concepts and materials were evaluated for inclusion. Silicon carbide (SiC) composite material was chosen as the primary structural material for the first wall, blanket, and coolant piping. This material offers low level activation for both long-term and short-term activation products that minimizes the waste disposal difficulties and provides low decay heat. Lead offers excellent heat transfer properties and good neutron multiplication although it has both toxicity and radioactivity concerns. Even with these concerns, it is thought to be superior to other liquid metals in the reactor cavity. A composite shield material is employed to significantly reduce the activation in the bulk shield and the component shielding. A few applications require more traditional metals such as aluminum and steel and, in those cases, the alloys are tailored to reduce the activation properties.

A cylindrical cavity with hemispherical ends was chosen to improve the maintainability of the reactor components. A wetted wall with a layer (0.5 mm) of liquid lead on the surface was chosen as the first wall protection scheme, shown in Figure 2.4-8.

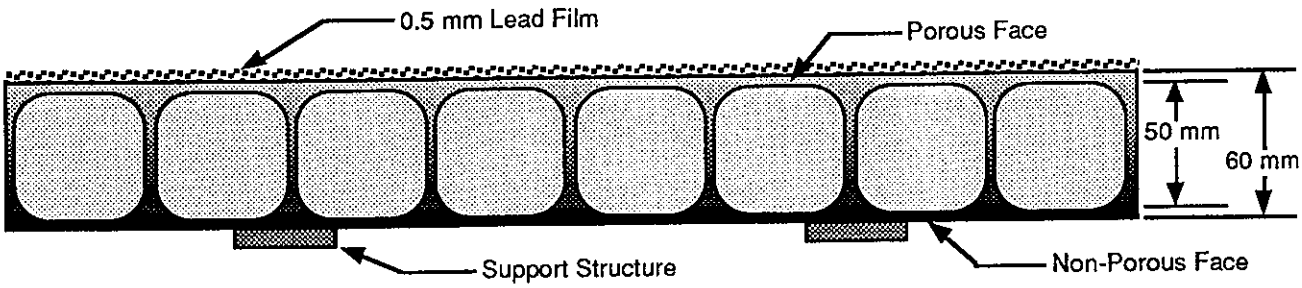

Figure 2.4-8. First Wall Panel; Cross Sectional View

Rectangular coolant channels for the liquid lead cool the surface and bulk material. The composite SiC material is also graded in density from fully dense at the back face to 10% porosity at the front face. This porosity allows the lead to migrate from the coolant channels to the surface. A portion of the lead film is vaporized by the target explosion and subsequently recondensed on the surface. A separate Pb film injector is used near the top of the cavity to establish and maintain a film in contact with the wall surface in that area. The lead coolant is introduced at the top of the cavity and it flows downward to the bottom of the cavity.

SiC occupies a minimal FW volume fraction (~10%) to ensure good neutron multiplication. The thickness of SiC behind the liquid film is 5 mm to assist heat conduction into the coolant flow. The heat deposited in the first wall system is 1,267 MWt which is over 40% of the generated thermal power. Removal of this heat requires a mass flow rate of 54,422 kg/s with an inlet bulk temperature of 375°C and an outlet bulk temperature of 525°C.

Lead recondensation on the first wall surface is the primary vacuum pumping mechanism in the cavity. The surface temperature of the lead determines the vapor pressure. With a repetition rate of 5.65 Hz, it is calculated that the base pressure of the cavity will be 3 mtorr. The non-condensible gas load created by the He, unburned D and T, and the H from the target capsule is pumped with cryogenic vacuum pumps and roots blower backing pumps.

The expected lifetime of the first wall panel is estimated at five years. This is primarily due to radiation damage in the SiC and to surface damage and fatigue caused by the pulsed operation. The first wall modules are attached to the front face of the blankets.

The blanket region is directly behind the first wall systems. The chosen design builds upon the existing blanket data and design base developed by MFE. The general blanket arrangement is shown in Figure 2.4-9. The structural material is SiC composite material, serving all the structural functions including coolant tubes, pebble bed container, outer blanket module wall, reflector region, and coolant plenum. Helium at 1.5 MPa is the coolant media extracting heat from the blanket region. The

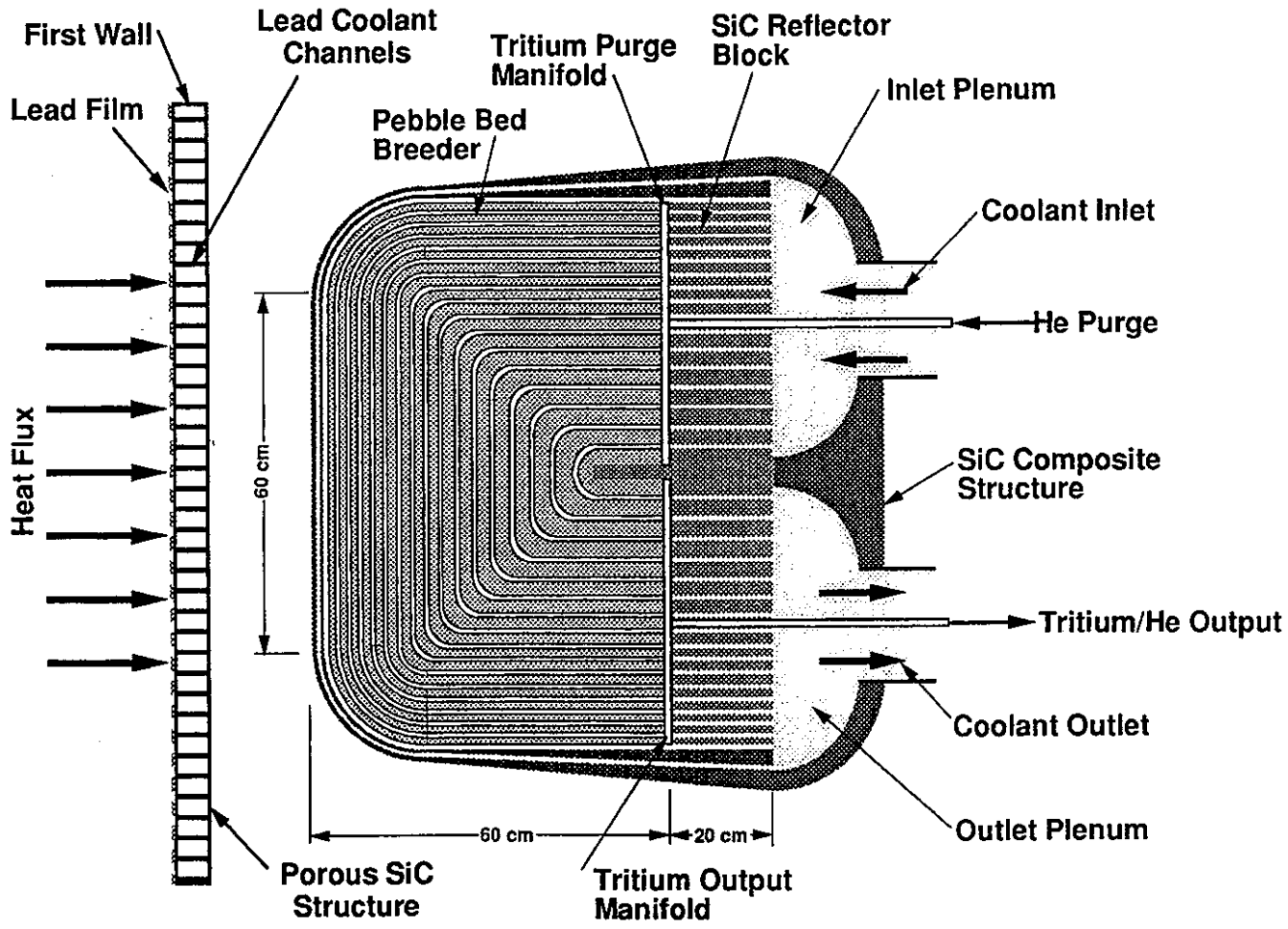

Figure 2.4-9 Schematic of a Blanket Module

tritium is bred in a Li_2O pebble bed breeding zone. A low pressure helium gas removes the tritium gas for processing.

The blanket system removes 1,782 MWt of power from the system. The inlet temperature of the helium is 400°C and the exit temperature is 650°C. There is an overall energy multiplication ratio of 1.14 within the first wall and the blanket. The blanket tritium breeding ratio is 1.2. The tritium inventory of the blanket is calculated to be 100 g. The peak and average neutron wall loads are equivalent to 6.5 and 4.3 MW/m^2 respectively. The lifetime of the blanket is expected to be ten years or greater.

The blanket is constructed in longitudinal modules. Penetrations are allowed for the entrance of the laser beams and the vacuum ports. Plenums are provided in the annular space outside the blanket region. Adequate space is allowed for remote maintenance of the blanket and first wall piping.

A ferritic vacuum vessel is provided outside the blanket and plenum region to help contain the reactor vacuum conditions. This region is approximately 0.5 meters thick.

All of the previously addressed systems have been constructed in radial fashion outward from the basic first wall shape, as shown in Figure 2.4-10. The bulk shielding

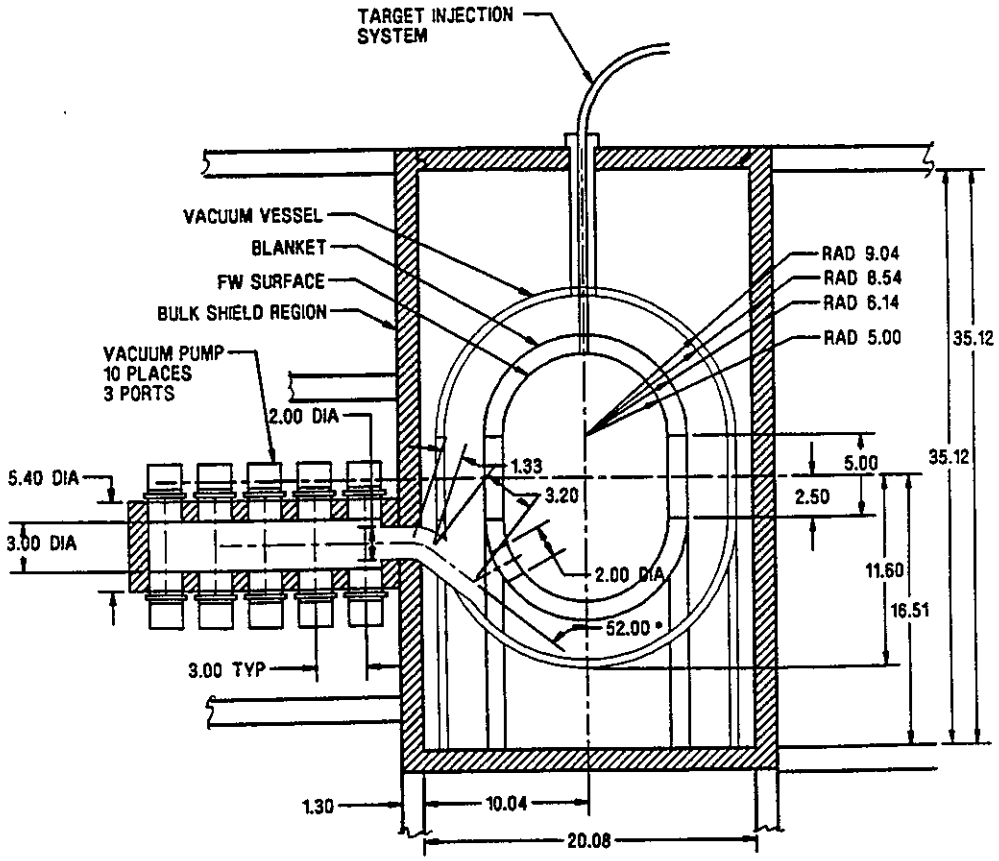

Figure 2.4-10 Elevation of Reactor Cavity Region Without Beamlines

was placed close to the vacuum vessel with a 1-m space for maintenance access, support structure, and plumbing. The basic bulk shielding shape adopted was a simple right circular cylinder 20 meters in diameter and 35 meters high (inside dimensions). The adopted composite shield composed of Al, SiC, B_4C, Pb, and water is 1.3 meters thick. That figure also shows the shielding provided around the three vacuum plena. Similarly, Figure 2.4-7 illustrates the 25-cm thick shielding provided around individual beamlines. At the end of the beamline, neutron trap and thicker shielding is provided to stop neutrons with direct line-of-sight to the cavity interior.

A shielding trade study was conducted to determine if the best approach was to place the shielding as close as possible to the source or to move the shield back to the wall beyond the final mirrors. The trade study indicated it was most cost effective to place the bulk shield in as close as possible and shield each beamline out to the "pinhole" openings. This approach minimizes structural activation within the building environment and walls.

2.4.5 Reactor Integration Features - Reactor integration combines the major system elements of the reactor plant into a synergistic whole system. As shown in Figure 2.4-1, the reactor building is circular and contains the reactor cavity, the vacuum pumps, the lead steam generators, and the 60 beamline enclosures. The configuration of the laser beams shown in Figure 2.4-11 illustrates the difficulty in locating any components in close proximity to the reactor vessel. However, there is a symmetry exhibited every 12°. With computer-aided drawing tools, individual beam locations were defined to determine the proper locations of other components. Section 6.3 has more detail on these arrangements.

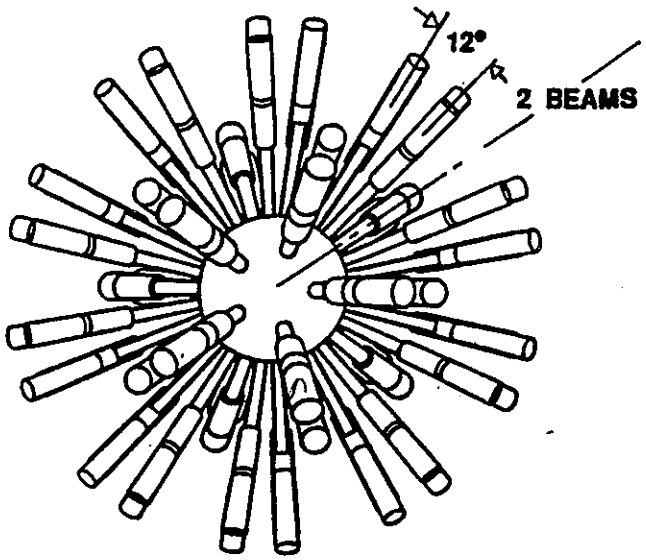

Figure 2.4-11. 3-D Beamline/Reactor Cavity Interface – Plan View

The general arrangement for the Driver Building was chosen to be an annular arrangement surrounding the Reactor Building. This is a more cost effective approach than a more conventional rectangular building. It also affords a common set of beamline geometries for each beamline location. The central Reactor Building will be serviced through service passageways above the Laser Building. The target injector will be located at the top of the reactor cavity and inject the targets downward into the cavity.

The energy conversion system is based on an advanced Rankine cycle. The Prometheus-L thermal conversion system uses three main sources of heat, the primary helium coolant with 1,782 MWt, the primary lead coolant with 1,267 MWt, and waste heat recovery of the driver at 193 MWt. Credit is also given for recovered lead pump work of 22 MWt. A steam-driven helium circulator is employed because it has a higher efficiency than a motor driven circulator. Power requirements for this circulator are not quoted separately, but the overall thermal efficiency is reduced to 42.3% to account for the power requirements.

2.4.6 Summary of Prometheus-L Reactor Plant Key Features - The reactor power plant design contained herein is indicative of what could be constructed within 20-30 years given assumed extrapolations of IFE physics and engineering technology. The plant could be constructed for a total direct capital cost of 2.2 billion dollars in 1991$ and a total cost, including indirect costs, of 4.1 billion dollars. The estimated cost of the electricity would be approximately 72.0 mills/kWhr that is comparable to most estimates of fusion power plants and new advanced fission power plants.

The plant is inherently safe, earning the best LSA rating of one. Use of low activation materials results in waste disposal estimated to be Class C or better for the plant. An extremely safe and environmentally acceptable reactor cavity has been designed. The usage of SiC as the structural material lowers the waste disposal concern and raises the level of safety assurance. An innovative first wall approach provides a very long-lived first wall. The blanket approach builds on the MFE data base in solid breeders and adapts the concept to the unique aspects of IFE. A new concept in shielding helps lower the level of activation in the shield.

The reliability and maintainability of the plant have been stressed to assure high availability. The reactor cavity has been designed to be remotely maintained with access from the top of the vessel. This enables low maintenance times for replacement of the first wall or the combination of the first wall and blanket. The laser driver final optical elements are designed to be life-of-plant, or a major fraction thereof, with short mean-times-to-repair. The calculated inherent availability of the laser driven reactor plant is 79.4%.

The technology and physics of the direct drive targets has potential for significant improvements. The design study has contributed toward defining illumination requirements and techniques, manufacturing processes, and definition of the target factory.

A viable laser driver option has been identified and defined with innovative approaches to greatly improve the requisite beam quality, power level, beam pointing, pulse compression, and reliability.

We feel this design is a valuable contribution toward understanding IFE's needs to move toward the goal of commercial fusion energy.

Reference for 2.4

1. J. P. Holdren, Chair, et. al., "Report of the Senior Committee on Environmental, Safety, and Economic Aspects of Magnetic Fusion Energy," UCRL-53766, 25 September 1989.

2.5 Prometheus-H Reactor Plant Overview

The Prometheus-H Power Plant is a heavy ion beam-driven commercial central station power plant. This design is also an extrapolation of today's technology advanced some 20-30 years into the future. The design emphasizes the same characteristics as the Prometheus-L Power Plant; namely, safety, environmental attractiveness, economic competitiveness, soundness of physics and engineering data, and a high degree of reliability, maintainability and availability.

The data base that supports the heavy ion power plant design builds on that for the laser system. The reactor cavity is similar to that for the Prometheus-L design. It is scaled down due to the higher cavity pressure permitted for heavy ion beam propagation through the cavity environment and to the lesser required thermal power. The higher cavity pressure is a direct outgrowth of the proposed use of self-pinching cavity transport channels, discussed in Section 4.2.3. The heavy ion driver selected by the study is a single beam LINAC coupled with intermediate, high current storage rings. This approach transfers much of the development challenge from the LINAC to the storage rings. This is attractive because it potentially leads to a cost per joule of delivered energy for the heavy ion driver that is roughly half that for the laser system as discussed in Section 4.1.2.

As noted previously, Chapter 4 discusses the rationale for choosing design options for the heavy ion power plant. Additional trade studies, design point selection basis, and detailed design definition and analyses for the reactor and balance-of-plant systems are presented in Section 6, Conceptual Design Selection and Description. This section is intended to provide the reader with a brief overview of the key features of the heavy ion beam-driven inertial fusion power plant that evolved out of the design study.

2.5.1 General Plant Features - A site plan for the Prometheus-H power plant is shown in Figure 2.5-1. The main complex is similar to that for the Prometheus-L design, but the driver building is a narrow (~10 m wide, 2.2 km long) tunnel housing the linear accelerator. The LINAC is folded at the approximate midpoint by introducing a hairpin bend. This reduces the overall size and cost of the driver facility by permitting certain support systems (e.g., cryogenic and maintenance) to be shared between accelerator legs. The accelerator is a single beam, rapidly cycled (30 kHz in a burst mode) design coupled into a stack of 14 high current storage rings that are also shown in the figure. The LINAC is actually cycled 18 times per pulse with two of the storage rings collecting three beamlets each to form a single prepulse beam for each side of the target. The beams are switched out of the storage rings into two multiple beam buncher accelerators that compress the pre and main pulses to a duration acceptable for target implosion. Upon exiting the bunchers, the group of 14 beams is divided into two sets consisting of six main and one prepulse beam and directed down

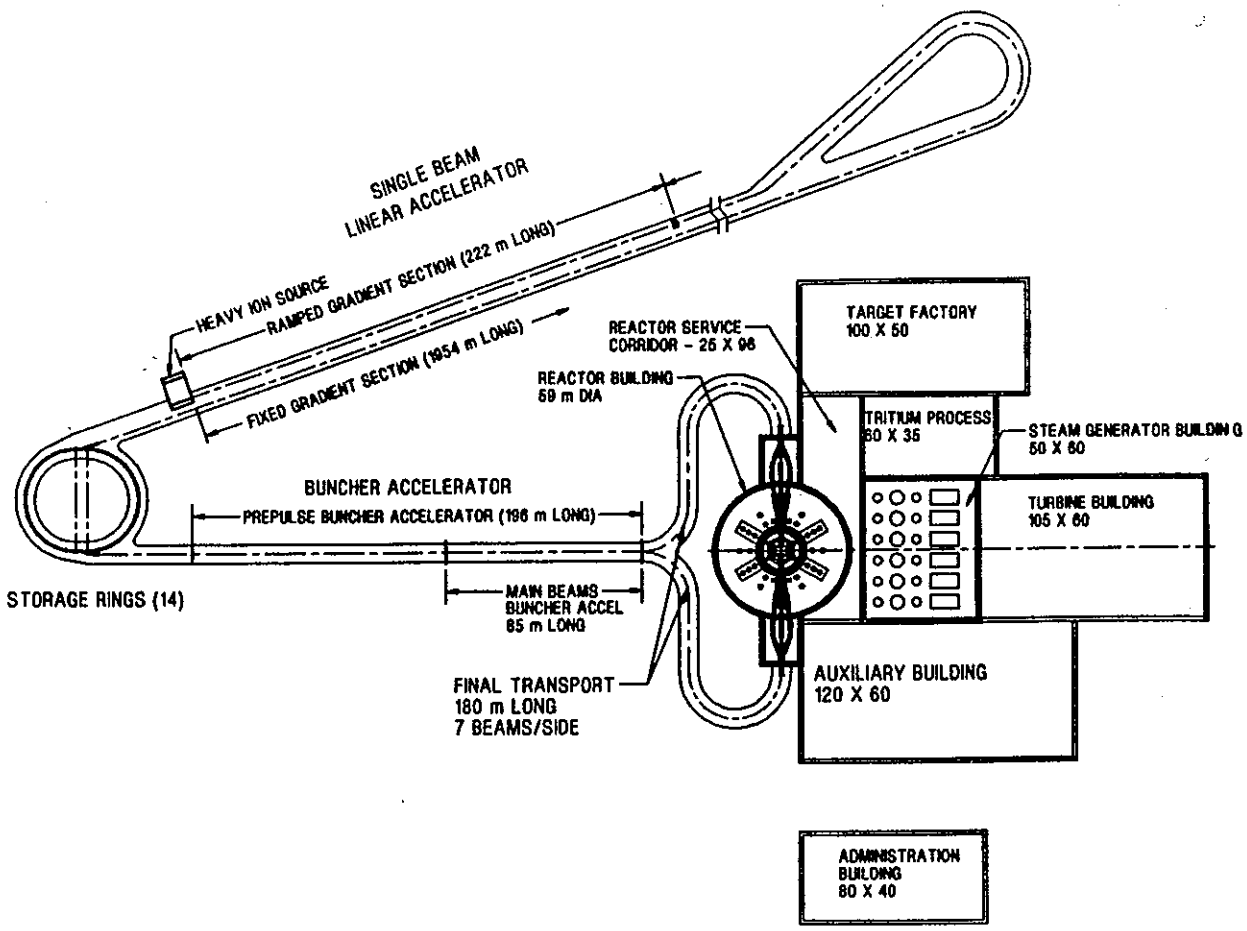

Figure 2.5-1. Heavy Ion Reactor Plant Site Plan

a final drift compression section to the Reactor Building. This is an attractive, low-cost approach to the heavy ion driver design as discussed in Section 6.

Figure 2.5-1 illustrates the other ancillary facilities necessary for the power plant. As in the laser system, the steam generator building houses six sets of steam generators for the lead and helium primary coolants. However, as indicated in Table 2.5-1, the total thermal cycle power is reduced from to 2780 MWt for this system (compared to 3264 MWt for the laser design) due to the improved heavy ion driver efficiency. This reduces the size of the main steam turbine generator from 1400 to ~1200 MWe. Sixteen percent of this gross power supports in-plant requirements for the heavy ion driver (137 MWe), auxiliary systems (28 MWe), and liquid lead pumping (25 MWe). The net power delivered to the electric grid is therefore 999 MWe.

Helium flow through the blanket is again provided by steam-driven recirculators. The tritium processing, target factory, and auxiliary buildings are comparable to their laser counterparts although their internal details are different due to the dissimilar process flows and manufacturing requirements for the heavy ion targets. It should be noted

Table 2.5-1 Prometheus-H Major Design Parameters and Features

Parameter	Value
Net Electric Power (MWe)	999
Gross Electric Power (MWe)	1189
Driver Power (MWe)	137
Auxiliary Power (MWe)	28
Cavity Pumping Power (MWe)	25
Total Thermal Cycle Power (MWt)	2780
Blanket Loop Power (MWt)	1597
Wall Protection Loop Power (MWt)	1162
Usable Driver Waste Heat (MWt)	NA
Usable Pumping Waste Heat (MWt)	21
Thermal Conversion Efficiency	42.7%
Recirculating Power Fraction	16%
Net System Efficiency	36%
Fusion Power (MW)	2543
Neutron Power (MW)	1818
Surface Heating Power (MW)	725
Fusion Thermal Power (MWt)	2797
Thermal Power to Shield (MWt)	38
Cavity Radius (m)	4.5
Cavity Height (m)	13.5
First Wall Protection/Coolant Media (In/Out Temp., °C)	Liquid Lead (375/525)
Breeder Material	Li_2O Pebbles
Structural Material, Wall and Blanket	SiC
Blanket Heat Transfer Media (In/Out Temp., °C)	1.5 MPa Helium (400/650)
Cavity Pressure (mtorr, Pb)	100
Neutron Wall Load, Peak/Ave (MW/m^2)	7.1/4.7
Energy Multiplication Factor	1.14
Tritium Breeding Ratio (TBR)	1.20
Target Illumination Scheme	Indirect Drive, Two Sided
Number of Beams	18 in LINAC (12 main + 6 in 2 prepulses)
Driver Output Energy (MJ)	7.8 (7.0 transmitted to target)
Overall Driver Efficiency (%)	20.6
Ion Accelerated	Lead
Charge State	+2
Final Energy (GeV)	4.0
Type of Accelerator	Single Beam LINAC
Final Beam Transport Efficiency (%)	90
Target Gain	103
Target Yield	719
Repetition Rate (pps)	3.5
Plant Availability (%)	80.8
Cost of Electricity (mills/kWh, 1991$)	62.6

that the target factory production capacity is only 63% of that for the laser system due to the reduced pulse repetition rate (3.54 versus 5.65 pps). The target factory cost is thus comparable to that for the laser system in spite of the fact that the heavy ion targets are more complex.

The heavy ion driver delivers 7 MJ of energy to the targets at a repetition rate of 3.54 pps. This results in a fusion yield of 719 MJ and a total power of 2792 MWt with the anticipated 1.14 energy multiplication factor. The liquid lead loop handles 1162 MWt of this power and the helium coolant loop transports 1597 MW while 38 MWt are deposited in the bulk shield as waste heat. An overall thermal cycle efficiency of 42.7% is achieved for this system as compared to 42.3% for the laser case because a larger percentage of the input heat is contained in the high temperature helium loop.

The Prometheus-H reactor cavity is essentially identical to that for the laser system. The main differences are a reduction in size from 5 to 4.5 m radius and a simplified beamline interface. These changes are a direct outgrowth of the proposed mode of cavity transport. The capability to form the proposed self-pinched heavy-ion transport channel is speculative at present, but the many engineering advantages this provides (few, small blanket penetrations, improved final focus magnet shielding, high chamber operating pressure) definitely warrant further investigation. This is highlighted by comparing Figures 2.4-7, 2.4-11, 2.5-4, and 2.5-5. The 60 individually shielded, ~1 m focal aperture laser beamlines in Figure 2.4-7 are replaced by two, 7-beam bundles of final focus magnets indicated in Figure 2.5-4. The actual focal spots are formed at the back side of the blanket and re-imaged onto the target through two 2-cm diameter openings in the blanket. This significantly reduces the amount of bulk shield material and combines with the smaller cavity size to provide a 30% reduction in reactor cavity cost for the Prometheus-H design.

2.5.2 Target Features - The TWG-referenced guidelines mentioned the use of both direct drive (DD) and indirect drive (ID) targets for the heavy ion driver but, because of the stiffness of the beams and the added complications of direct drive, the direct drive target was judged not to be worthy of further consideration. Moreover, direct drive heavy ion gain curves were never supplied.

The indirect drive target was adopted as the baseline target for the heavy ion driver. The revised target groundrules from the TWG stated that single-sided illumination of the ID target was technically possible for the target with negligible degradation of performance. For purposes of the study, it was recommended no degradation or enhancement was to be assumed for single-sided illumination. In a meeting with DOE in August 1991, members of the TWG advised the teams that the single-sided illumination option was judged to have too much technical risk to be considered as the

primary option. Thus the team elected to baseline the two-sided illumination for the ID target.

The indirect drive target employs a similar cryogenic DT capsule as the direct drive target. To provide a suitably uniform compression, a radiation case surrounds the DT capsule. The ends of the case have energy converter regions of a similar material. The heavy ion beams impinge upon the energy converter regions and convert the beam energy into X rays that bathe the inside of the case and the capsule. The radiation case will provide the radiation uniformity on the internal capsule. The capsule is suspended within the case by a very light weight support structure to withstand the injection acceleration forces yet not influence the target performance.

The Target Factory would be modified to add the step of mating the radiation case to the DT capsule and to delete the sabot process. The radiation case performs the same functions of protection as the sabot for the direct drive target.

The injection scheme for the indirect target will be based upon a pneumatic system. The support for the internal DT capsule has been determined to be able to sustain 200 g's of acceleration that establishes the length of the injector at 20 meters. A set of eight injector barrels will be used in a Gatling gun arrangement to enable the functions of loading, injecting, and evacuation be accomplished at the requisite target rate. The injector assembly will be aligned 10° off the beamline axis to provide adequate clearance with the beam final focus subsystem. Tolerances on the target final velocity will be very tight. Techniques of steering the beams will be a subject of investigation and development.

2.5.3 Heavy Ion Driver Features - The heavy ion driver must efficiently and cost-effectively deliver the required energy to the target within a focal spot radius on the order of 6-mm diameter from two sides of the cavity. The two key design choices considered for this study involved the accelerator configuration (single versus multiple beam) and the technique for delivering the beams to the target (channel transport versus some form of direct ballistic focus). The design team chose a single beam LINAC with storage rings for the accelerator configuration based on the clear economic advantage for this approach as discussed in Section 2.3. Channel transport was selected on a more qualitative basis. Channel transport offers many potential engineering advantages over focusing the beams directly on the target. Furthermore, analyses indicate that, when the beams are partially stripped, there is more than enough beam current to support the formation of a self-pinching transport channel. The concern lies in the capability to maintain a stable 5.6 m long channel in the surrounding cavity environment and the repeatability of aiming this channel at the proper spot on the target. These are critical issues that can only be addressed through future theoretical and experimental work. Section 4.3 discusses the detailed rationale

for selecting these technology options for the heavy ion driver. The remainder of this section presents a summary of the final heavy ion driver design.

The systems studies led to the selection of a 7 MJ target incident energy design point for the Prometheus-H design point. A 10% energy loss was budgeted for forming the beam transport channels and transmission to the target, so the LINAC is designed to output 7.8 MJ. Lead ions with a +2 charge state were chosen for compatibility with the first wall protection scheme. Detailed studies of transport lattice scaling determined that the required 7.8 MJ could be provided with 4 GeV ions using only 18 beamlets. Low ion energies are desirable because they provide improved target performance; however, the number of beamlets is a concern at low energies because it can become quite large (>50) for some lattice scaling choices. This is a particular problem for the single beam LINAC because of core recycling losses and beam stability and scattering loss in the high current storage rings. Section 6.2 discusses the trade studies that led to the 18 beamlet design point.

The resulting beamline configuration at various points along the driver is illustrated in Figure 2.5-2. Corresponding beam and LINAC parameters are summarized in Table 2.5-2. The driver consists of an injector, a ramped gradient section, a fixed gradient section, a stack of storage rings, a buncher accelerator section, a drift compression section, and a final focus section. These are shown in plan view in Figure 2.5-1. Switching sections will also be required to insert and extract the beams from the storage rings, but these were not specifically considered for this study.

The overall length of the LINAC is 2.2 km. Transport lattice scaling was chosen so the mean beam radius of 9.4 cm remains constant over this entire distance. Additional constraints were imposed on quadrupole axial packing fraction (< 80%) and aspect ratio (beam radius/quadrupole length < 0.25). These lead to a common magnet radial build as indicated in Figure 2.5-2; however, the magnet length and field strength must be adjusted to provide proper focusing. The quadrupole inner and outer radii were chosen as 1.65 and 3.3 times the mean beam radius based on guidance provided by LBL. An additional 12 cm was added to the magnet outer radius to determine the core inner radius. This provides space for cryogenic insulation, magnet dewar, insulator rings, accelerator structure, and vacuum access.

Ions are injected into the LINAC at an energy of 6 MeV. The beamlet current is 14 A at this point and the pulse length is 15.5 μs. The initial voltage gradient is low (~40 kV/m), but it rapidly increases to the design limit of 1 MV/m over the 223 m ramped gradient section. The local voltage gradient scales with beam energy in this section is based on accepted limits as discussed in Section 6.2. This section contains 300 quadrupoles, terminating at a beam energy of ~100 MeV where the limiting gradient is reached. The initial 70% quadrupole axial packing fraction is high (but less

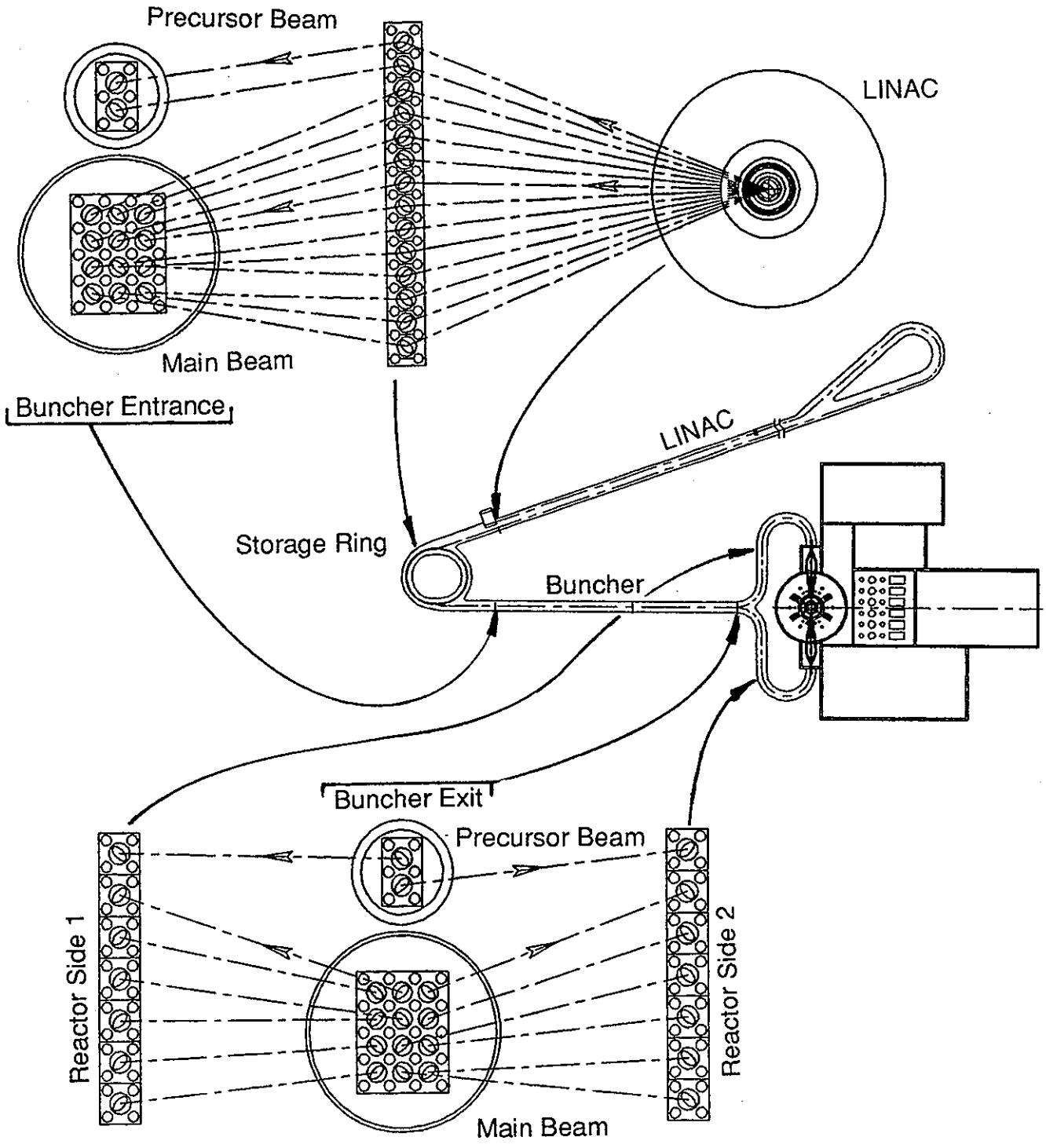

Figure 2.5-2. Beamline Configuration – Routing from LINAC to Reactor

Table 2.5-2. Parameter Summary for Prometheus-H Driver Design

Parameter, Unit	Injector	Trans	Final	Main Beamlets		Prepulse Beamlets	
				Buncher	Fnl Focus	Buncher	Fnl Focus
Beam Energy, MeV	6	99.4	4000	4000	4000	4000	4000
Beam Radius, cm	9.4	9.4	9.4	9.9	15.0	10.5	14.9
Lattice Half Period, m	0.50	1.33	4.85	4.67	3.55	4.50	3.56
Pulse Length, ns	15,500	1639	85.3	70.5	17.8	176.4	54.4
Bunch Length, m	36.5	15.7	5.1	4.2	1.07	10.6	3.27
Beamlet Current, A	14	132	2532	3065	12,130	3674	11,920
Packing Fraction, %	69.0	39.3	18.8	21.5	56.2	24.4	55.5
Magnet Length, m	0.344	0.523	0.911	1.00	1.99	1.10	1.98
Magnet Bore Radius, m	15.5	15.5	15.5	16.4	24.8	17.3	24.7
Magnet a/L Ratio	0.273	0.179	0.103	0.099	0.075	0.096	0.076
Core Inner Radius, cm	43.0	43.0	43.0	155.4	—	68.0	—
Core Thickness, cm	36.9	150.2	7.8	6.5	0.0	16.2	0.0
Depressed Tune, Deg	8	5.3	3.0	2.6	0.86	2.2	0.87

Parameter, Unit	Ramped Gradient	Fixed Gradient	Storage Ring	Main Buncher	Main Drift	Prepulse Buncher	Prepulse Drift
Number Beams	1	1	14	6	6	1	1
Section Length, m	223	1954	157	85	180	196	180
Tunnel Width, m	9.8	9.7	8.1	8.1	8.1	8.1	8.1
Core Volume, m^3	906	1629	—	60	—	193	—
Pulser Energy, MJ	0.13	1.9	0	0.49	0	0.59	0
Number Quadrupoles	300	578	34	18	39	41	37
Number Dipoles	—	—	32	—	19	—	20
Dipole Lengths, m	—	—	2.40	—	2.30	—	2.15
Magnet Powers, MW	0.9	1.734	0.198	0.054	0.348	0.123	0.342

than the 80% design limit) because focusing is needed every 0.5 m at this energy (lattice half period). The packing fraction decreases to 39% at the end of the ramped gradient section because the lattice half period grows to 1.33 meters.

The fixed gradient section (1 MV/m) continues from the 100 MeV point to the final energy of 4 GeV. This section is 1.95 km long and contains 578 quadrupoles. The pulse length decreases from 1.64 μs to 85 ns in this section, so the beamlet current increases from 132 A to 2.53 kiloamps. The quadrupole packing fraction drops to 19% at the end of the fixed gradient section because the lattice half period has grown to 4.85 meters. The quadrupole length also increases, from 0.52 to 0.91 meters, to offset the increased beam stiffness.

A flux swing of 1.5 T was selected to reduce induction core losses (proportional to ΔB) since they are recycled 18 times per pulse for this design. The corresponding core thickness increases from 37 to 107 cm in the ramped gradient section due to the increase in gradient. Thereafter, it decreases because the pulse length shortens as the beam energy increases. Driver efficiency was a concern for the single beam design, but the 1.5 T flux swing and low number of beamlets lead to a projected efficiency of 20.6% for the Prometheus-L driver using Metglas loss curves suggested by LBL. This is discussed in more detail in Section 4.1.

The target pulse is generated by operating the LINAC in a burst mode. The 18 beamlets are sequentially accelerated by cycling the induction cores on a 30 kHz timescale so the longest residence time within the storage rings is less than 1 ms. The beamlets are stacked vertically in 14 storage rings as indicated to provide a common bend radius and path length. Only 14 storage rings are needed because two storage rings collect three beamlets each to form a single prepulse for each side of the target. The twelve remaining rings each collect single beamlets that are used to form the main target pulse. This arrangement provides the recommended prepulse energy content of ~30%.

Once all beamlets are collected and properly time sequenced, they are released from the storage rings and sent to the two buncher accelerators as indicated in Figure 2.5-2. The prepulse buncher is 196 m long and induces a 4.9% velocity tilt on these beamlets. This causes the 256 ns long prepulse to compress to the required 30 ns over the 180 m drift distance to the target. The main pulse beamlets are sent through a shorter 85 m long buncher since they only require a 2.1% velocity tilt. This compresses their pulse length from 85 ns to the 7.3 ns required for target implosion over the same 180 m drift distance. The final time phasing and energy content of the prepulse and main beamlets is shown schematically in Figure 2.5-3. A multiple-beam transport lattice is employed in the buncher sections, as indicated, to minimize core volume.

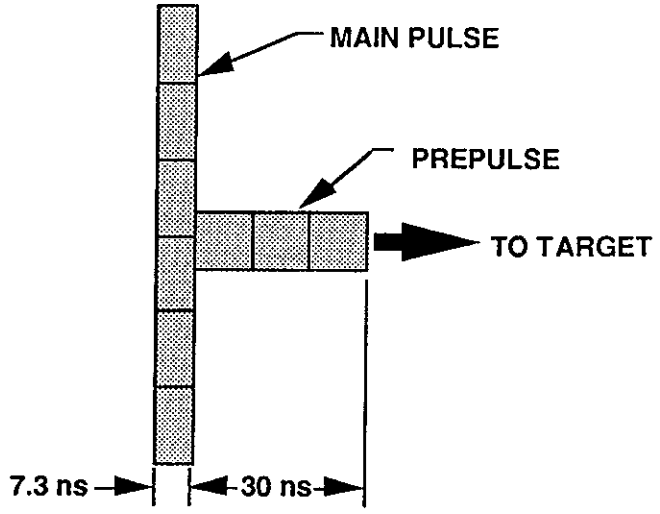

Figure 2.5-3. Heavy Ion Beam Prepulse and Main Pulse Schematic

After the beams exit the buncher section they are divided as indicated in Figure 2.5-2 with six main and one prepulse beamlet directed to each side of the reactor cavity. The beam radius is allowed to increase in the buncher and drift sections to ease matching with the final focus magnets. The physical arrangement of the final focus magnets and beamlines is illustrated in Figure 2.5-4. Triplet quadrupoles are used to focus the beams down on a point at the rear surface of the blanket. A lead vapor cell provides electrons that space-charge neutralize the beam at the exit of the last quadrupole. This permits the final 6-mm diameter focal spot to be attained.

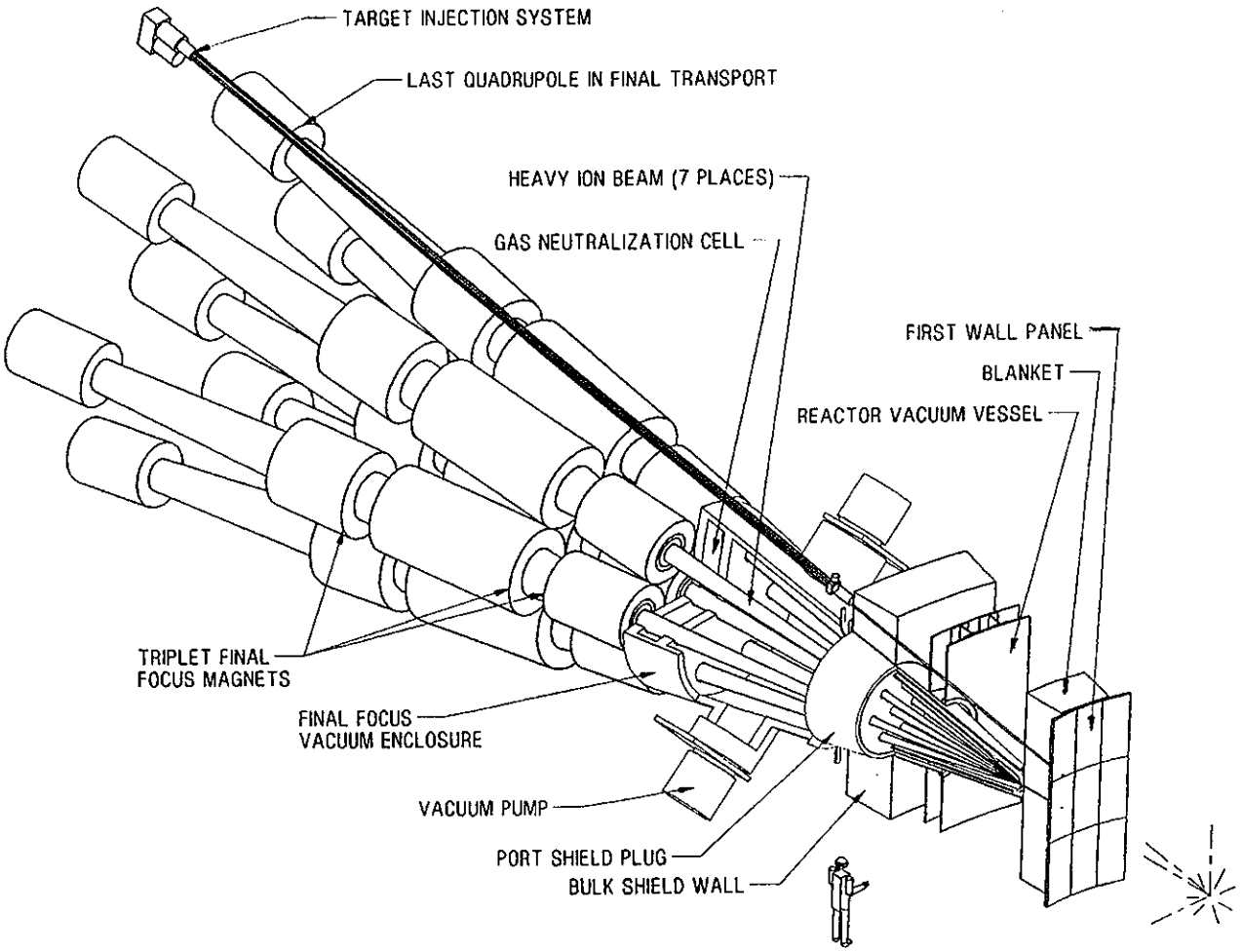

Figure 2.5-4. Physical Arrangement of Final Focus Coils, Plenum, and Shielding Penetrations

At the focal point, a lead vapor jet is provided that strips the beam ions to a high charge state. This is the mechanism for creating the transport channel. It also serves to isolate the reactor cavity pressure environment (~100 mtorr) from that required in the beamlines (~0.01 mtorr). The prepulse beamlet is located on the channel axis and arrives first at the lead gas jet as indicated in Figure 2.5-4. The six main beamlets follow immediately and they arrive in parallel. Both the prepulse and the main pulse have a significant current margin for self-pinching (greater than five times), so channel

formation is certainly feasible. The surrounding plasma's tendency to generate a reverse current that might destroy the channel is a concern. This is identified as a critical research and development issue in Section 5.

If transport channels are found to be viable, questions still remain concerning the ability to direct them at a target that is 5.6 m away with an accuracy of ±1 mm. The initial path of the pinched beam channel will be defined by its net momentum. The single prepulse beams can be steered directly and can easily be pointed with the required accuracy. The direction of the main pulse, however, depends on the momentum balance between the six main beamlets. The questions involve whether momentum imbalances cause steering of the channel or if the prepulse beam provides a focusing mechanism. These questions are a related part of the transport channel critical issue.

2.5.4 Reactor Cavity Features - Figure 2.5-5 depicts the final Prometheus-H reactor cavity configuration. The design is essentially the same as that for the laser system. The most notable difference is the simplified beamline interface. The laser driver requires 60 beam penetrations through the blanket that vary in diameter from 17 to 26 cm and force the outer wall of the building to be located at a diameter of

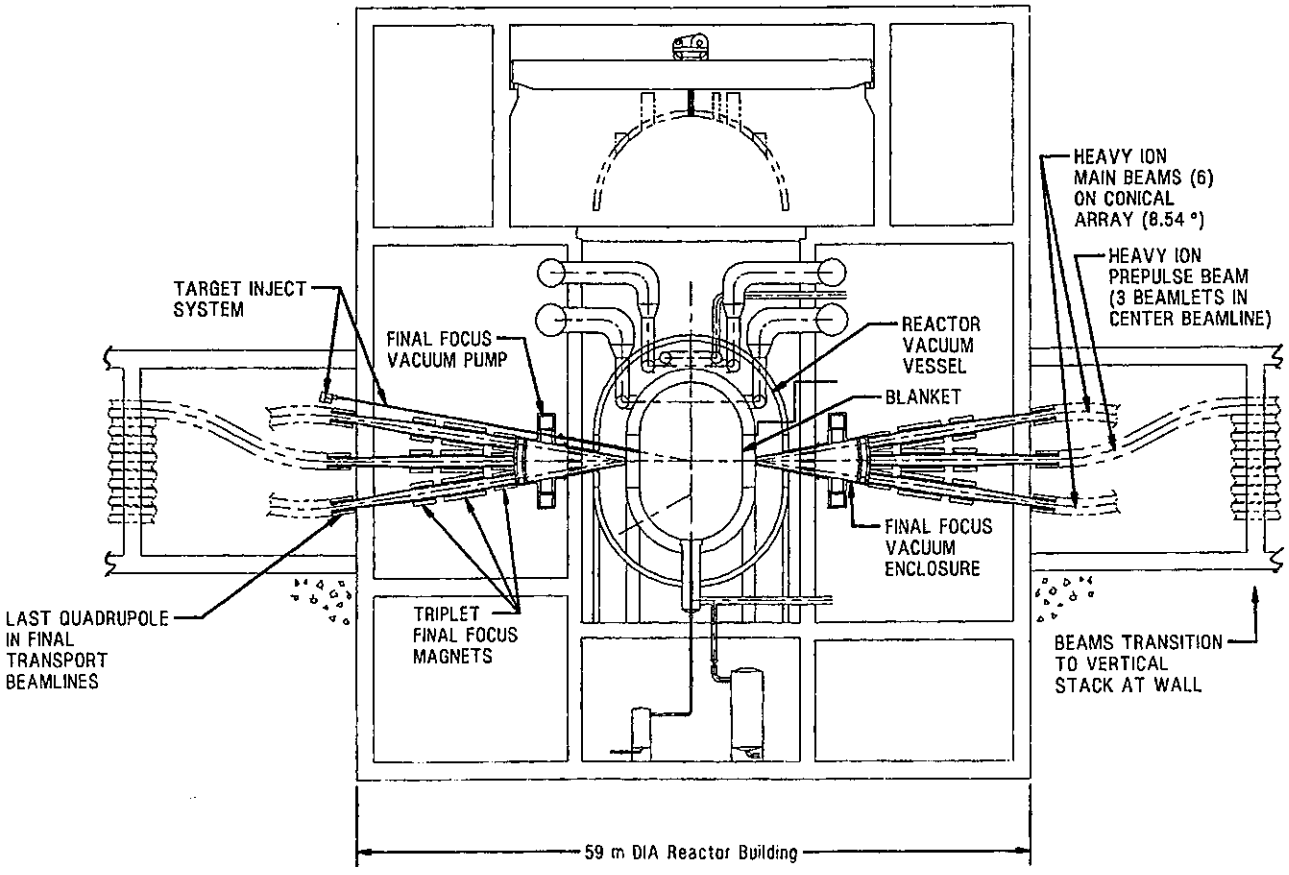

Figure 2.5-5. Prometheus-H Reactor Cavity Arrangement

86 meters to provide adequate separation distance for protecting the final optics from radiation damage. These are replaced by two, 2-cm diameter openings for the heavy ion driver as indicated in Figure 2.5-4. The localized nature of the heavy-ion beamlines permits shielding them using two adjoining enclosures as indicated in Figure 2.5-1. The overall building diameter is thus reduced to 63 meters.

The other configuration difference is the 0.5 m reduction in cavity radius. A smaller size cavity is possible based on cavity clearing calculations, but significant modifications in the wall and blanket design would be required to accommodate the increased wall loading and power density in the blanket. Reductions in component reliability and lifetime would also be expected under these conditions. For the 4.5 m final design point, the lifetime of the first wall and blanket remain roughly the same as predicted for the laser first wall and blanket. Furthermore, all structural, thermodynamic, safety, and environmental impact analyses conducted for the laser cavity are directly applicable to the heavy ion design. Some safety margins are reduced, but the conclusions are still valid.

The 4.5 m radius Prometheus-H cavity design thus achieves many of the cost benefits of smaller size without compromising the attractive design features. The building diameter is reduced from 86 to 63 meters because the need to protect final line-of-sight optics is eliminated. The final focus magnet arrangement allows close placement of ancillary equipment and service buildings and localized beamline shielding. The energy conversion system is based on the same general features and hardware as the laser plant. Piping sizes are identical to those for their laser counterparts. The only real difference is the elimination of a driver waste heat recovery system since this is not practical for the heavy ion driver.

Vacuum pumping requirements for the heavy ion system are less severe due to the increased cavity pressure. The vacuum ports are identical to the laser reactor chamber, but simple roots blowers were found to provide adequate pumping speed and capacity. There is a common vacuum chamber housing all the beamlines from the last quadrupole in the triplet set to the focal point. Pressure in this region is maintained by two cryogenic vacuum pumps due to the 0.01 mtorr requirement during final focus. Shielding around this enclosure is equivalent to that provided around the laser beamlines. Shielding is also provided on the blanket facing surface of the last focusing magnet and within the bores of these magnets, but thicknesses are minimal because the magnets are not exposed to primary radiation. This permits all focusing magnets to be superconducting with the possible exception of the central, prepulse triplet that does have direct line-of-sight into the cavity.

The majority of the driver building is a simple tunnel housing the single beam LINAC. The tunnel is enlarged for the storage ring, buncher accelerator and drift compression sections to accommodate the multiple transport channels in these sections. Considerable care was taken in arranging these sections to preserve the proper drift

lengths, beam bend radii, and quadrupole placements. Beamline layouts were chosen to facilitate the use of common magnet cryostats where identical parallel transport channels are required.

2.5.5 Summary of Prometheus-H Power Plant Key Features - The Prometheus-H power plant represents a very attractive design goal for heavy ion inertial fusion energy. The design embodies several potential ways to help reduce the cost and improve the engineering feasibility of heavy ion drivers. The driver plant equipment is estimated to cost $403M in 1991 dollars for a tenth-of-a-kind plant. This is significantly lower than that previously envisioned for induction LINAC drivers[2] and, in fact, corresponds to roughly half the cost per joule projected for the Prometheus-L driver.

In addition, the high efficiency of the heavy ion driver allows a reduction in the size of most of the remaining balance-of-plant systems, which translates into lower capital costs. As a result, the total direct capital cost for the Prometheus-H power plant is $1.94B; that is $230M lower than that for the laser system. Adding indirect costs increases these values to $3.63B and $430M, respectively. The projected cost of electricity for the heavy ion plant is therefore 62.6 mills/kWh; that is 13% below that for the Prometheus-L design. This is very competitive with costs projected for other advanced energy sources.

Many of the reactor and BOP features are common between the heavy ion and laser plants, but there are some distinct advantages that favor the heavy ion system. The self-formed transport channel concept significantly eases the job of designing a remote maintenance system for the first wall and blanket. It also improves the overall reactor engineering feasibility by providing a nearly uniform first wall and blanket. It mitigates concerns about the protective lead film integrity around openings, concerns about the design of effective shielding around multiple beamlines, and concerns about shielding the final focus magnets from the cavity radiation environment. Consequently, it enhances the level of safety assurance for the entire plant, although both the laser and heavy ion designs are anticipated to achieve the highest LSA rating of one. Finally the reliability and maintainability assessment indicates that the heavy ion plant will have an 80.8% plant availability; that is 1.4% higher than that predicted for the laser plant.

References for 2.5

1. J. P. Holdren, Chair, et. al., "Report of the Senior Committee on Environmental, Safety, and Economic Aspects of Magnetic Fusion Energy," UCRL-53766, 25 September 1989.

2. D. S. Zuckerman, et al., "Induction LINAC Driven Heavy Ion Fusion System Model," Fusion Technology, Vol 13, #2, 1986.

2.6 Key Technical Issues and R&D Requirements

Although significant progress has been made in inertial fusion energy research during the past decades, the field is still in its early stage of R&D and the present data base is very limited. Therefore, many uncertainties exist in the actual performance and operation of present fusion reactor conceptual designs. The expected consequences of these uncertainties vary in magnitude—on one extreme the uncertainties are so large that the feasibility of the reactor design is at stake, and on the other extreme, the uncertainties may simply require moderate redesign, reduced performance, or increased cost.

An extensive effort has been made in this study to identify and characterize the key physics and engineering issues for the two IFE conceptual reactor designs, Prometheus-L and H. However, many of the issues tend to be generic and are fairly independent of the specific design selections made in Prometheus. Therefore, the issues identified here are of general importance to IFE. Furthermore, an effort has been made in this study to indicate the relevance of the issues to MFE.

The key issues identified in this work are large in number and they cover specific technical issues ranging in complexity and importance. Each of these key issues impacts key aspects of feasibility, safety, and/or economic potential of inertial fusion reactors. Resolving these issues requires new knowledge through experiments, theory, and models. An attempt was made to identify the R&D required to resolve these issues. The R&D evaluation included a general description of required facilities, expected time duration, and costs.

The key issues are described in detail in Chapter 5. The description for each issue includes: potential impact, design specificity, level of concern, operating environment required in facilities to investigate the issue, the degree of relevance to MFE, and analysis to characterize the issue. As indicated earlier, the number of key issues is large, greater than one hundred. In order to provide a brief summary of the most important issues, a smaller number of issues (called critical issues) were identified. A critical issue is broader in score than a key issue; each critical issue may encompass several of the most important key issues for a number of components and technical disciplines.

Table 2.6-1 provides a list of the critical issues. These critical issues are presented in detail in Chapter 5. Following is a brief summary.

Table 2.6-1 List of Critical Issues

1. Demonstration of Moderate Gain at Low Driver Energy
2. Feasibility of Direct Drive Targets
3. Feasibility of Indirect Drive Targets for Heavy Ions
4. Feasibility of Indirect Drive Targets for Lasers
5. Cost Reduction Strategies for Heavy Ion Drivers
6. Demonstration of Higher Overall Laser Driver Efficiency
7. Tritium Self-Sufficiency in IFE Reactors
8. Cavity Clearing at IFE Pulse Repetition Rates
9. Performance, Reliability, and Lifetime of Final Laser Optics
10. Viability of Liquid Metal Film for First Wall Protection
11. Fabricability, Reliability, and Lifetime of SiC Composite Structures
12. Validation of Radiation Shielding Requirements, Design Tools, and Nuclear Data
13. Reliability and Lifetime of Laser and Heavy Ion Drivers
14. Demonstration of Large-Scale Non-Linear Optical Laser Driver Architecture
15. Demonstration of Cost Effective KrF Amplifiers
16. Demonstration of Low Cost, High Volume Target Production Techniques

(1) Demonstration of Moderate Gain at Low Driver Energy - The present U.S. national strategy envisions three major facilities for inertial fusion energy development at a cost of more than $1 billion per facility. Such a path makes the development of IFE very difficult in a constrained budget. Large capital expenditure requirements lead unavoidably to a long time scale. An alternative path that might potentially accelerate IFE development involves small to moderate size facilities with low fusion power. While such facilities may not be economically attractive they are most suitable for physics testing and engineering development. A key to the development of such small facilities is target designs that provide moderate gain (20-50) at low driver energy (1-2 MJ).

To help identify and quantify relevant target design goals, a system study was performed to define curves of required gain versus driver energy for a 100 MWe cost-limited demonstration power plant. Figure 2.6-1 shows the resulting gain requirement curves for a laser driver based on the Prometheus-L design at 10% and 15% efficiency for two different projected direct capital cost levels. Also shown is a comparison to possible pessimistic and optimistic physics limitations. The figure shows that target gains of 30-40 would provide a possible design window for 1-2 MJ driver energy. Such designs could likely be validated on Nova Upgrade. Figure 2.6-2 shows similar results for the Prometheus-H driver design. This figure shows that the higher heavy-ion driver efficiency leads to a possible design window with target gains of only 20-30 over the 1-2 MJ energy range. Thus, further design work on both heavy ion and laser targets appropriate for 1-2 MJ drive energy is clearly justified.

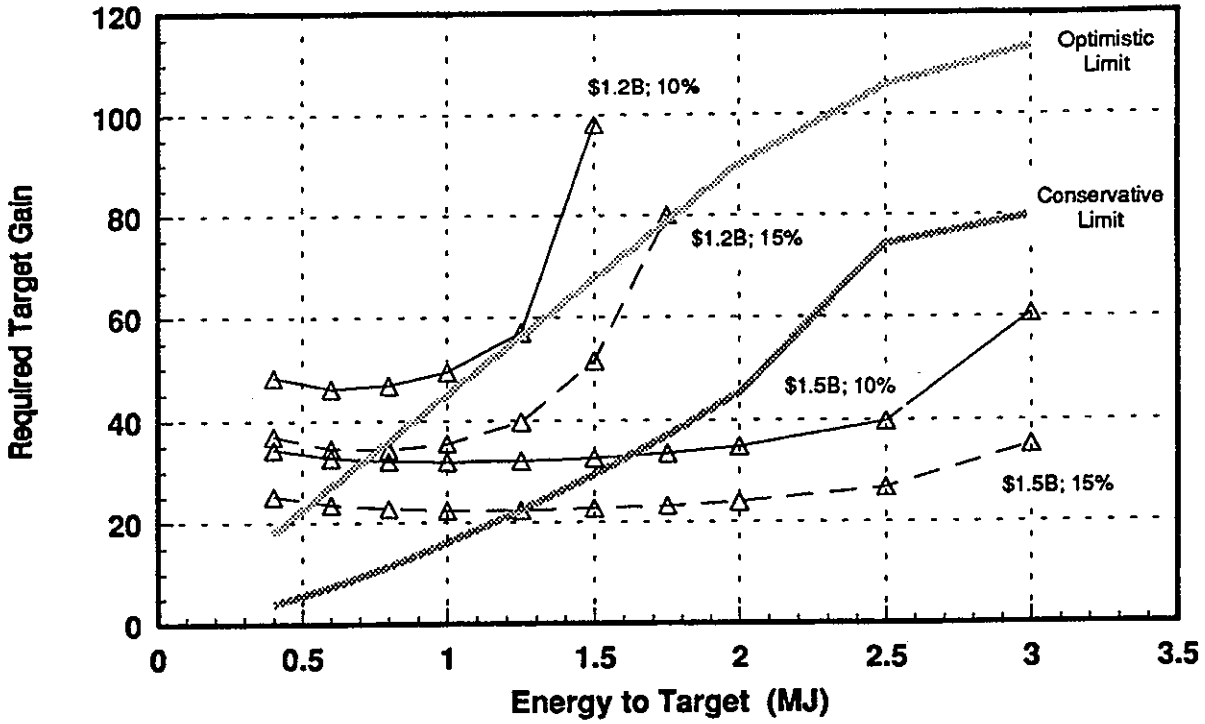

Figure 2.6-1. Projected 100 MWe Demonstration Power Plant Gain Space Windows for the Prometheus-L Driver Configuration. Values Indicated Only Include Direct Costs.

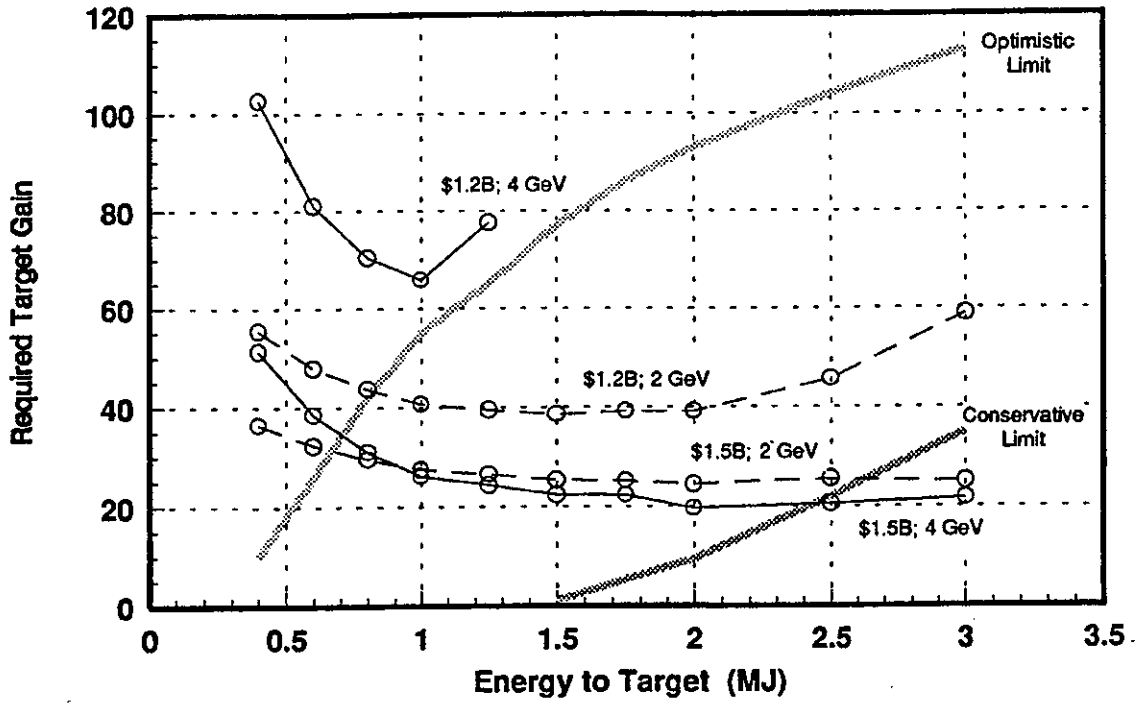

Figure 2.6-2. Projected 100 MWe Demonstration Power Plant Gain Space Windows for the Prometheus-H Driver Configuration. Values Indicated Only Include Direct Costs.

(2) Feasibility of Direct Drive Targets - There are strong incentives to consider direct-drive (DD) targets because of higher gains. However, the feasibility and performance characteristics of DD targets are presently uncertain. The fundamental Prometheus-L driver and cavity designs are strongly influenced by the direct-drive (DD) target illumination requirements given by the TWG. Unfortunately, the specified TWG requirements may contain some serious inconsistencies with published plasma physics requirements for efficient laser/target coupling. The laser driver spatial intensity profile in the target plane suggested by the TWG is not consistent with the Fresnel number of the beam at the location of the targets for the Prometheus-L design. In addition, the suggested long, 80 ns precursor pulse may produce significant deleterious effects, such as generation of non-linear scattering processes that may lead to target preheat, thereby preventing an efficient D/T implosion from occurring. TWG guidelines for DD targets appear to have been anchored on experiments conducted on miniature DD targets illuminated with only a few kJ of laser energy. Large reactor sized, multi-MJ DD targets will likely require different illumination scenarios. For reactor operation, the DD targets must also be accurately injected into the target chamber with an active tracking/alignment system capable of meeting the illumination uniformity requirements discussed in Chapter 5.

(3) Feasibility of Indirect Drive Targets for Heavy Ions - The feasibility of the indirect drive (ID) targets for the heavy ion (HI) driver is, in part, linked to the properties of the method used to transport the HI beam to the target, to the accuracy and reproducibility of the HI target launch system that repetitively propels the ID targets to the center of the target chamber, and to the ability of the high-Z hohlraum cavity to efficiently convert and smooth the radiation incident on the DT capsule. This study proposes innovative solutions to accomplish these tasks.

In the approach considered for the Prometheus-H IFE Reactor Design, seven heavy ion beamlets (six main and a prepulse) from two sides of the cavity are focused onto stripping gas jets at the back surface of the blanket. The beamlets are thereby highly stripped, yielding mega-ampere currents that trap the ions in a small diameter (5 mm) channel whose direction is (hopefully) accurately determined by the pre-pulse beam. This self-focused, small diameter beam subsequently strikes the energy converter regions at either end of the moving hohlraum target that has been accurately launched to arrive at the center of the reactor target chamber synchronously with the arrival of the HI beams.

Two types of ID heavy ion fusion targets were considered in this study:
(1) Lead and plastic targets designed for single-sided irradiation
(2) Similar targets designed for two-sided irradiation.

The feasibility of efficiently imploding both of these ID targets depends upon the successful resolution of a series of technical problems, including:

- Providing return paths for the MA beam currents incident on the target.
- Successful injection and self-pinching of the HI beams passing through the stripping jets into a self-focused, small diameter beam directed at the target.
- Accurate pointing of the transport channel(s) at the energy converter regions.
- Accurate launching of the targets to arrive at the center of the target chamber synchronously with the arrival of heavy ion beams.

(4) Feasibility of Indirect Drive Targets for Lasers - As was assumed in the indirect drive, heavy ion fusion target, the indirect drive laser fusion target considered in the Prometheus study is a similar lead, two-sided hohlraum. The feasibility of efficiently imploding this ID laser target involves concerns arising from three major sources:

- Closure of the two entrance apertures to the hohlraum by ablation plasma.
- Accurate target tracking and pointing of the required multiple laser beams to coincide with the two entrance apertures of the moving ID target.
- Accurate and reproducible launching of the indirect drive targets into the center of the target chamber.

Significant misalignment of the laser beams could damage the radiation casing of the target capsule and cause a target misfire.

(5) Cost Reduction Strategies for Heavy Ion Drivers - The attraction of the Heavy Ion (HI) approach to IFE has always been related to the fundamental technical feasibility of building a system with the required properties to drive a pellet to ignition. The basic accelerator technology is well developed, the beam physics is tractable, and existing accelerator systems have exhibited 25-year lifetimes with 95% availabilities. A system to provide the required average power could have been built ten years ago. The problem is cost. A 10 GeV linear accelerator built with today's technology would cost billions of dollars.

There are two key issues associated with the HI driver cost reduction strategies proposed by this study:

- Space charge limited transport of a bunched beam.
- High current storage rings for heavy ion beams.

Existing experiments and computer simulations indicate that transporting HI beams for several km at their space charge limit is feasible but this has not been demonstrated at the proposed beamlet current levels. More restrictive limits would increase the number of beamlets further complicating the LINAC design. The ILSE program will address many of these issues. The proposed use of high current storage rings results in significant cost savings for the LINAC but shifts technology risk to the storage rings. Issues of resonance losses and beam induced vacuum instability must be addressed.

(6) Demonstration of Higher Overall Laser Driver Efficiency - The excimer laser driver system has a number of components that can individually be optimized to improve efficiencies. The achievement of higher efficiency is now viewed as a crucial requirement for laser drivers to compete economically with heavy ion linacs for IFE. This, however, cannot be at the sacrifice of reliability. The laser driver consists of four major elements: (1) the excimer laser amplifiers, (2) the Raman accumulators, (3) the SBS pulse compressors, and (4) the computer controlled and self-aligning optical train which directs the laser beams through the various optical components and down into the target chamber.

The latter three elements require some additional development and testing before they can be judged adequate to be incorporated into a mature laser driver design. The major problem to be addressed here is the first element, the excimer laser amplifiers.

The key to an efficient, reliable Prometheus laser driver is the successful design, construction, and testing of modular excimer laser amplifiers.

During the past five years, relatively little work has been carried out in the U.S. with regard to improving the efficiency and the reliability of moderate-sized excimer laser amplifiers. Some analytical studies[1] have been carried out on both electron-beam excited excimer lasers (EBEELs) and electron-beam sustained electric discharge lasers (EBSEDLs) which offered (on paper) gross wall plug efficiencies as high as 17%. These efficiencies, however, are more likely to be reduced significantly if incorporated into a large laser system architecture. The main concern is that no experimental work in excimer amplifier development is either currently in progress or planned in the U.S. Work in the Soviet Union with sliding discharge cathodes in CO_2 discharge lasers has produced some promising results which may offer alternatives to the EBSEDLs.

(7) Tritium Self Sufficiency in IFE Reactors - Satisfying fuel self sufficiency conditions is necessary for a renewable energy source. A key condition is that the achievable tritium breeding ratio (TBR), Λ_a, must be equal to or exceed the required breeding ratio (Λ_r). Analysis shows considerable uncertainties in estimating Λ_a and Λ_r. The required TBR is a strong function of many reactor parameters as shown in Figure 2.6-3. Λ_r is particularly sensitive to the tritium fractional burnup in the target, the mean residence time of tritium in the target factory, the number of days of tritium reserve on site, and the reactor doubling time. For Prometheus, reference parameters Λ_r is ~1.05. However, Λ_r rises rapidly to ~1.2 or higher when significant changes are made in the reference parameter set, as shown in the figure.

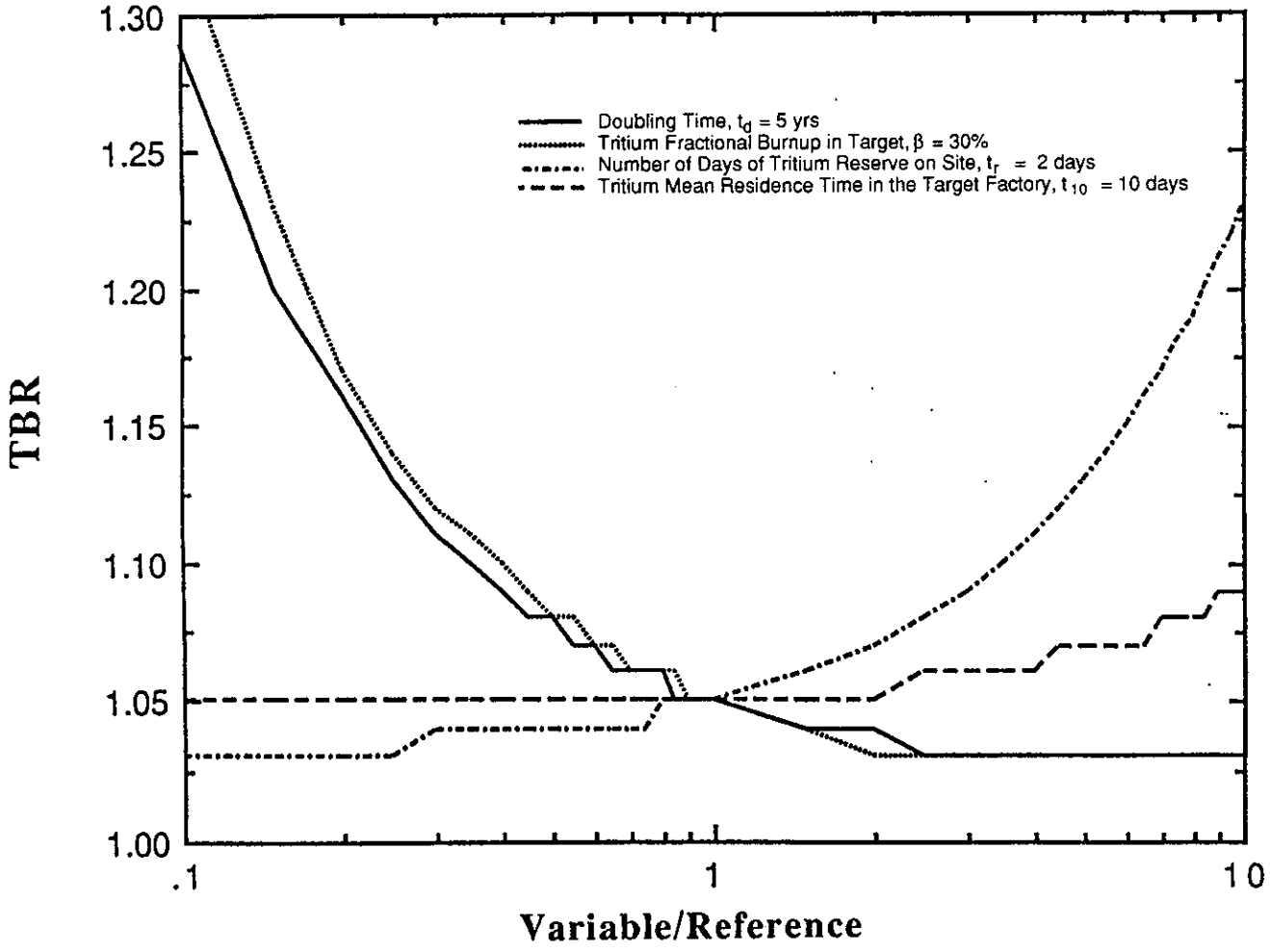

Figure 2.6-3. Variation of Required TBR with Reactor Parameters

The achievable TBR, Λ_a, is also a function of the reactor design with strong dependence on the first wall and blanket concepts. Accurate prediction of Λ_a suffers from uncertainties in the system definition and inaccuracies in prediction due to errors or approximations in basic nuclear data, calculational methods, and geometric representation.

For Prometheus, the reference Λ_a is ~1.2. Thus, the Prometheus design appears to satisfy the tritium self sufficiency conditions. However, in view of the large uncertainties in Λ_a and Λ_r, significant R&D is required. Furthermore, self sufficiency conditions impose clear requirements on the parameter space in which IFE reactors are allowed to operate. These are discussed in Chapter 5.

(8) Cavity Clearing at IFE Pulse Repetition Rates - IFE reactors must be pulsed several times per second. Following each pellet explosion, target debris and materials evaporated from the cavity surfaces must be removed before the next target is injected. The base pressure requirements are important for three reasons: (1) the time required to evacuate the chamber depends on the pressure, (2) the level of protection to the first wall (and final optics) afforded by the background gas depends strongly on pressure, and (3) propagation of targets and driver energy are strongly influenced by the base pressure. For the Prometheus designs, these issues are of greatest concern for the laser driver. However, heavy ion beam transport without transport channels involves comparable pressure requirements.

Calculations for Prometheus indicate the cavity pressure drops below 1 mtorr before the next shot, which is adequate for propagation of targets as well as laser and heavy ion beams. However, the actual physics of energy and mass transport and vapor recondensation is very complex under the extremely dynamic conditions following a target explosion. The cavity gas is partially ionized and subject to highly time-dependent processes such as hydrodynamic shock waves. Non-ideal effects such as liquid droplet formation and effects of penetration provide additional uncertainties.

(9) Performance, Reliability and Lifetime of Final Laser Optics - Previous IFE studies identified radiation protection of final optics as a serious issue in laser-driven reactors because of severe effects of radiation on the performance, reliability, and lifetime of the final optics. In this study, workable conceptual focal mirror designs were introduced. These designs involved both the dielectric turning mirror and the final optical component, the Grazing Incidence Metal Mirror (GIMM). Analyses indicate that, with proper selection of materials

and mechanical configuration, the GIMM lifetime may be very long—on the order of the plant lifetime. This approach, coupled with clever shielding designs and materials selection for the dielectric elements, will likely lead to great improvements in the overall laser reactor concept. All previous studies of laser fusion have concluded that the final mirror will need to be located in excess of 30-40 m away from the cavity center and that the lifetime and reliability will be small. An in-depth study of the performance, reliability, and lifetime of the final dielectric components for the GIMM geometry is necessary. Advances in this area will undoubtedly lead to significant improvements of the entire concept and will likely benefit other technological areas which rely on the reliable performance of large laser mirror systems.

(10) Viability of Liquid Metal Film for First Wall Protection - In the Prometheus designs, a thin liquid metal film wets the first wall in order to prevent the solid structures from rapidly degrading due to the extremely high instantaneous heat and particle loads. To prevent liquid from entering the cavity, the thickness of the film is maintained as small as possible. For this scheme to be successful, all structures exposed to the blast must be covered. Analysis of dry spots suggests that operation of the SiC wall can be operated at full power for 10 to 15 minutes without irreparable damage to the first wall.

While a great deal of research has been carried out on film flows, the materials, configuration, and environmental conditions for fusion are unique, and little effort has been expended in the IFE community to determine how films will behave under these conditions in a real engineering system. The major uncertainties include: film feeding and thickness control, blast effects, flow around geometric perturbations (such as beam penetrations), and protection of inverted surfaces.

The film thickness must be relatively uniform in Prometheus because the surface power conducts through the film. The local film thickness determines the local surface temperature, which strongly influences the condensation rate. Even for very thin films, the flow becomes turbulent and instabilities are likely to develop. Therefore, a better understanding of the nature of instabilities and possible remedies is critical. Good wetting between the solid surface and liquid film is very important.

Explosive effects resulting from the blast may lead to further problems. The problem of wall protection with films near inverted surfaces is particularly difficult.

(11) Fabricability, Reliability, and Lifetime of SiC Composite Structures - The viability of using SiC structures in the first wall and blanket is a key consideration of the laser and heavy ion designs. If these concepts are to be believable, efforts should be made to assess the factors involved in determination of acceptable lifetimes and to determine the appropriate manufacturing methods and their economics. Anticipated lifetimes for FW/B components are not well known. Without this knowledge, system reliability, maintenance, and economics would be seriously challenged. In order to perform this task, several investigations need to be considered. It is too simplistic, and perhaps misleading, to use the accumulated fluence, or displacements per atom, to make projections of lifetimes. The determination of such lifetimes would need knowledge of the various effects of radiation. The most prominent of those are neutron induced swelling, embrittlement, fiber shrinkage and/or detachment from the matrix, creep crack propagation at high temperatures, and crack bridging mechanisms during irradiation.

On the other hand, the technology to process and manufacture SiC composites is at its infancy. A detailed assessment of manufacturing methods, potential, and costs is needed. Manufacturing methods are classified into fiber production techniques and matrix processing technologies. A variety of possibilities exist, with potential consequences on both economics and design.

(12) Validation of Radiation Shielding Requirements, Design Tools, and Nuclear Data - Radiation shielding must protect both personnel and sensitive reactor components. Components with the most stringent protection requirements include the final optics in a laser-driven fusion reactor. Other components with important radiation protection requirements include magnets in the heavy ion driver and instrumentation and control. Two important requirements must be imposed on the radiation shield in order to enhance attractive environmental and safety features of IFE reactors. First, the bulk shield (immediately surrounding the blanket) must be designed so that the long-term activation in reactor components outside the cavity and inside the reactor building is minimum. Second, the IFE shield should be designed to permit some personnel access to the reactor building outside the bulk shield within days after shutdown.

These critical requirements on the shield combined with the fact that the shield is one of the largest (in volume and weight) and more expensive components in an IFE reactor necessitate careful shield design. Sophisticated capabilities for predicting the radiation field and associated radiation response in materials are required. Although advanced capabilities exist, uncertainties in

accuracy remain due to modeling complexities, nuclear data uncertainties, limitations of calculational methods in void regions and deep radiation penetration problems, and time dependent behavior of materials and components. Improvements in methods, data, and experimental verification of prediction capabilities are needed.

Establishing accurate radiation protection requirements is also necessary, particularly for components whose shielding is either physically difficult (e.g., final optics in laser driver) or results in substantial economic penalty.

(13) Reliability and Lifetime of Laser and Heavy Ion Drivers - The reliabilities and lifetimes of excimer laser and heavy ion driver systems profoundly affect the operating characteristics of an IFE reactor. The critical problems associated with the two drivers are discussed in Chapter 5. IFE can likely benefit from the decoupling of the driver from the cavity nuclear environment, but the drivers are complex, high technology pieces of equipment that require careful development to realize their potential.

(14) Demonstration of Large-Scale Non-Linear Optical Laser Driver Architecture - The fundament of the Non-Linear Optical subsystems proposed for the Prometheus-L driver is based upon a very strong experimental and theoretical basis of non-linear optics. Since both proposed subsystems are simply large optical cells filled with H_2 and SF_6 respectively, there are very few components present which can fail. The primary question is how well the system will function on the first pulse. If the electro-optical subsystems can be tailored to achieve first time operation, the overall architecture should prove to be as reliable as other state-of-the-art, high speed, high voltage electronics. A balance must be struck between the extremely high gains and concomitant high conversion efficiencies of which these systems are capable. Thus, the reliabilities and lifetimes of the two types of non-linear optical subsystems proposed for the Prometheus-L IFE reactor design hinge primarily on the support optical equipment that is associated with the non-linear optical (NLO) devices. The two NLO devices are: (1) the Raman accumulators, and (2) the SBS pulse compressors.

Numerous key non-linear optical (NLO) subscale experiments and analyses have been performed in the last 20 years that demonstrate the capabilities of these two types of NLO devices. In order to properly implement them, however, each needs to be supplied an appropriate Stokes seed beam, and therein lies most of the questions regarding successful implementation.

Subscale experiments have demonstrated efficiencies comparable to those proposed here for both Raman and Stimulated Brillouin conversion, but full aperture cells require technology development. This is also true for the large aperture Pockels cells proposed for converting the depleted SBS pump beams into a target prepulse. The SBS pulse compressor and attendant Pockels cell E/O switchyard represent the highest risk elements in the Prometheus-L design.

(15) Demonstration of Cost-Effective KrF Amplifiers - One of the key elements associated with developing a cost-effective KrF laser driver for the Prometheus study is the design of the output KrF laser amplifier module. These KrF amplifier modules represent the fundamental building blocks of the KrF driver, generate the output energy pulses for the KrF laser driver, and the nature of their design represents a major fundament of the laser driver reliability.

Previous Department of Energy (DOE) and Department of Defense (DOD) excimer laser research and development programs have identified two general excimer laser amplifier design configurations:

(1) Direct electron beam excitation of relatively large (V > 1000 liters) excimer laser amplifier volumes.
(2) Electric discharge excimer laser amplifiers with the excitation of the KrF excimer achieved along the neutral channel for geometries involving moderate volumes (<200 liters).

The first excimer laser amplifier design configuration, electron beam excited excimer lasers (EBEL), has received extensive development from both the DOE and the DOD with KrF amplifier modules as large as 2000 liters being constructed. The second configuration, electric discharge excimer lasers (EDEL), has been much less thoroughly investigated; some preliminary theoretical work was funded by DOE[1] several years ago, but little experimental verification of the predicted high EDEL efficiency was made.

The EBEL has received priority development over the EDEL because the EBEL scales to larger volumes (and hence larger output energies) much more readily than does the EDEL. For single-shot DOE applications and for some DOD applications, this scalability advantage of the EBEL has been important. For an IFE reactor application in which reliability for 10^9 cycles over long periods of time at repetition rates of 3-10 Hz is crucial, the potentially higher reliability of the EDEL enhances its attractiveness. Development issues confronting both approaches are summarized in Table 2.6-2.

Table 2.6-2 Summary of EBEL and EDEL Development Issues

No.	Description of Problem Area	Possible Solution
EBEL		
1	Foil Rupture	Homogenize E-Beam Current Density
2	Parasitic Oscillations	Lower Amplifier Reflectivities
3	Amplified Superfluorescence	Reduce Amplifier Solid Angle
4	High Cost of Large Windows	Segmented Optics
5	Radiation Damage from E-Beams	Lower Anode Voltage
6	Reduced Beam Quality	Phase Conjugation
7	Optics Damage	Reduce Radiation Fluence
8	Catastrophic Failure Mode	Redesign Foil Support Structure
EDEL		
1	Stabilization of Discharge	Discharge Uniformity; Control F_2 Burn
2	Uniformity of Discharge Excitation	Elimination of Cathode Fall Region
3	Reduced Excimer Beam Quality	Beam Combination in Raman Cell
4	Achieve 10^9 Shot Lifetime	Engineer Pulsed Power/Electrodes
5	Optics Damage	Reduce Radiation Fluence
6	Verify Excitation Efficiency	Conduct Full-Scale Experiments

(16) Demonstration of Low Cost, High Volume Target Production Techniques - Target production for IFE reactors will require technologies that are presently either non-existent or insufficiently developed for such an application. It is, therefore, very difficult to accurately estimate the production costs of such targets. These difficulties are further aggravated by the potential need for sabots to deliver the targets to the reactor chamber and, as in the indirect drive target, for an outer case which must meet stringent engineering requirements. Target cost is clearly a critical issue in light of the fact that IFE reactors will consume huge numbers of targets (on the order of 10^8 per year) and will be uneconomical and, therefore, impractical if these targets are too expensive.

Reference for 2.6

1. "New Techniques for KrF Laser Fusion Systems," Interim Report for Los Alamos National Laboratory, Mark Kuschner, et al., Spectra Technology, Inc,. Seattle, WA (1986).

2.7 Comparison of IFE Designs

There are several design and technology options for IFE reactors, e.g., laser and heavy-ion drivers, direct and indirect drive targets, and dry and wetted first wall. Comparison among options is necessary in order to select, or at least reduce, the number of options that are worthy of further R&D. This study developed a clear Evaluation Methodology that permits quantitative analysis and comparison of options. The insight gained from the process of applying the methodology is by itself as valuable as the quantitative results. The methodology was applied to compare the two Prometheus reactor designs developed in this study, one with laser and one with heavy ion-driver.

Design options for power plants that can be constructed today can generally be compared based on economics and safety and environmental attractiveness. However, fusion is in a relatively early stage of research and development. The data base is incomplete and success in developing particular design options for subsystems cannot be assured. Designers have to extrapolate present knowledge to predict performance in fusion power reactors, with the degree of extrapolation varying greatly from one design option to another. Furthermore, there are substantial differences among proposed design options in the probability of success and in the time and cost required to develop these options. Therefore, a prudent evaluation methodology for comparing fusion reactor conceptual designs must account for these differences.

Five major areas of evaluation were established. These are:

(1) Physics Feasibility
(2) Engineering Feasibility
(3) Economics
(4) Safety and Environment
(5) Research and Development Requirements

Each of the above areas is quantified through a system described in Chapter 5. In this system, a number of detailed criteria are developed for each area. For each criterion there is an attribute (index) that can be quantified. A weighting scale is devised for the attributes. The weighted sum of the attribute for each evaluation area represents a SCORE for this area.

The result of the evaluation process for a given reactor design concept is a numerical score for each of the five evaluation areas. No mixing of the scores for the five evaluation areas was attempted; i.e., the numerical scores for the five areas were not combined to derive one final composite score. Instead, the overall comparison is based on a qualitative judgment of the relative scores for the five areas. This process is highlighted in Figure 2.7-1. Ideally, a panel of knowledgeable experts would interpret the resulting scores in each of the five evaluation areas and collectively agree

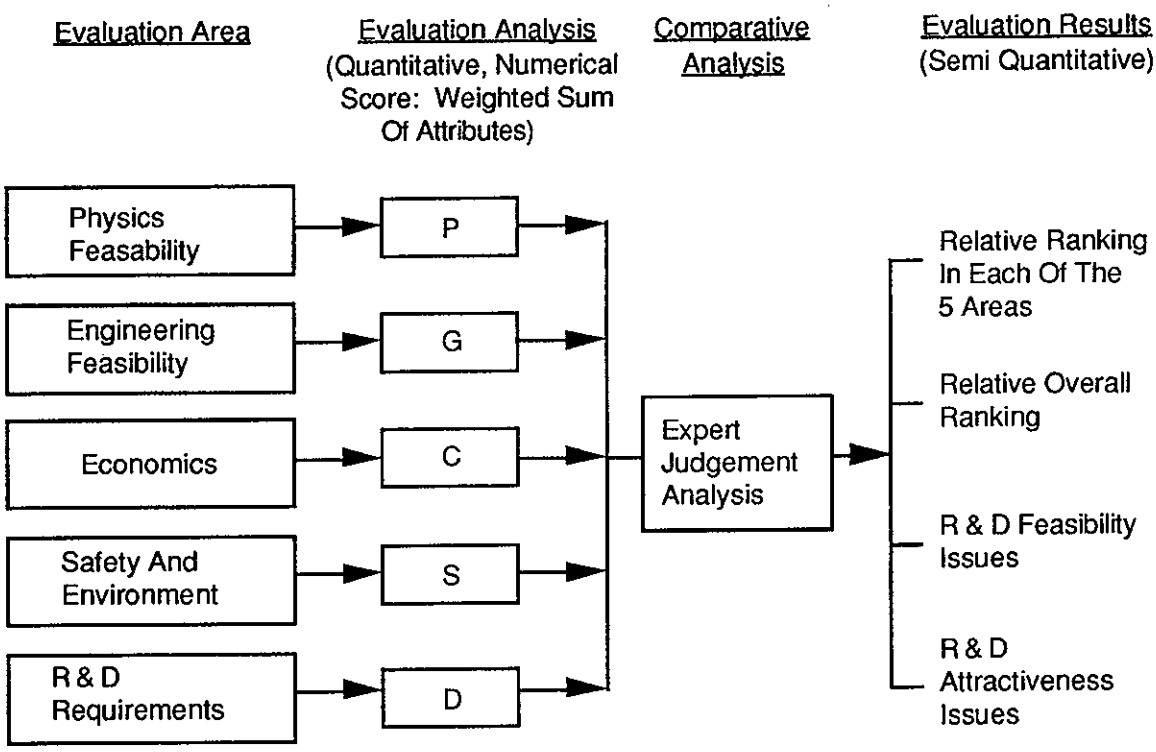

Figure 2.7-1. Evaluation Methodology Approach

on the relative merits/issues for both approaches. Time did not permit this part of the comparison to be completed.

This methodology was used to compare the laser- and heavy ion-driven reactor concepts developed in Prometheus. The details of the results for the five evaluation areas are given in Chapter 7. A summary of the final figures of merit for the five evaluation areas is given in Table 2.7-1. The scores were normalized so that higher numbers correspond to a more favorable assessment. Two key conclusions can be made based on the overall evaluation analysis and the scores in Table 2.7-1:

(1) Heavy ion-driven reactors appear to have an overall advantage over laser-driven reactors based on existing R&D data and performance projections.
(2) However, the differences in scores are not large and, given technology uncertainties, results of future R&D could change the overall ranking of the two IFE concepts.

Table 2.7-1. Summary of Scores for the Five Evaluation Areas

	Score*	
Evaluation Area	Laser-Driven	Heavy Ion-Driven
Physics Feasibility (P)	50	57
Engineering Feasibility (G)	85	93
Economics (C)	68	78
Safety and Environment (S)	95	93
R&D Requirements (D)	52	56

*Scores normalized so that higher numbers reflect better scores.

2.8 Study Conclusions

This study has contributed greatly to the advancement of the state-of-the-art for IFE conceptual reactor designs. The results show that self consistent designs can be developed for IFE commercial power plants that have excellent potential to be economically competitive with very attractive safety and environmental features while maintaining a high degree of technical credibility. The study has developed a number of innovative concepts that, if proven out, would resolve known problems and enhance the attractiveness of IFE power plants. Key issues have been identified and characterized and the R&D required to resolve them has been described and documented.

Targets - Both direct drive and indirect drive targets have been examined for use with the laser driver. From the data provided by the TWG, it is concluded that the direct drive target is more attractive for a commercial laser-driven power plant. The principal reasons are higher gain at the same driver energy and lower cost per target. However, significant uncertainties exist in the capability to realize this suggested performance advantage. For the heavy ion concept, the indirect drive target is chosen. The beam geometry for direct drive presents a very difficult engineering problem because of the stiffness of the high energy beams. Indirect drive targets mitigate these concerns because they are only illuminated from two sides. In addition, no gain data was provided for direct drive heavy ion targets.

The functions and processes necessary for a target factory have been identified and tested. It is concluded that both direct and indirect drive targets can be produced at 20 cents or less per target (fuel and O&M) assuming reactor-size shells can be mass produced using droplet generators combined with microencapsulation. Large, thick shells meeting the high requirements on surface finish and shell geometry required of reactor grade targets have not yet been produced using these methods. However, it is argued that no great technological leap of faith is necessary to assume they will be available. Few attempts have been made to create large, thick shells because there has been no demand for them. Available drivers require much smaller targets. If significant research and development resources are made available, it is considered very likely that the necessary technology will be developed. It is also concluded that the diffusion filling with beta layering techniques will make it possible to fill reactor targets with DT fuel and then deposit the fuel into a uniform ice layer as called for in the TWG guidelines. These techniques will make it possible to cheaply mass produce targets without surface holes or cracks and to dispense with fabrication steps such as joining and fitting shell hemispheres with fill plugs.

Two target injection systems have been developed—a pneumatic system for the heavy ion indirect target and an electromagnetic system with a sabot for the laser direct-drive

target. It is concluded that systems meeting the reliability and accuracy requirements of IFE reactors can be produced using presently available technology. Few conclusions can be drawn regarding the design and physical performance of IFE reactor targets in an unclassified report.

Laser Driver - During the course of this study, it has been demonstrated that the application of current excimer laser and non-linear optical technology will permit the construction of a laser driver capable of meeting the demanding performance requirements while maximizing safety and reliability. For direct-drive (DD) targets, the optimum Prometheus-L laser driver pulse was found to consist of a total energy of 4 MJ delivered in two temporal formats: a ramped precursor pulse containing 30% of the energy (or 1.2 MJ) and a main laser pulse with the remaining 70% (or 2.8 MJ). The 4 MJ is equally distributed among 60 beamlines (for DD targets) and delivered at a 5.65 pps repetition rate. Similar results were obtained for indirect-drive (ID) targets using a different beam configuration.

The Prometheus-L laser driver design achieves high levels of safety and reliability. This improved safety and reliability is accomplished through the use of numerous (~1,020) small, fail-safe electric discharge excimer lasers (EDELs), Raman accumulators, and SBS pulse compressors. Furthermore, it was found that gas pressures inside the excimer lasers, Raman accumulators, and stimulated Brillouin scattering (SBS) pulse compressors could be selected to lie near 1 amagat densities, thereby permitting the use of thinner windows and reducing gas overpressures. On the basis of currently available technology (together with projected future reliability development), an ultimate goal for mean firings between failure of ~10^9 amplifier pulses was projected. Past work suggests that moderate-sized electric discharge excimer lasers (EDELs) provide the most promising development pathway to this goal.

By reducing the required EDEL output energy to a moderate range lying between 4 and 6 kJ, it was found that the Prometheus-L laser design permits EDEL failures during normal operation to occur without forcing a corresponding shutdown of the IFE reactor. Since approximately 1,020 6-kJ EDELs are required in the 60-beam Prometheus-L laser driver, the failure of one amplifier would reduce the energy in a single beam by only 6%, an amount that could readily be overcome literally on the next firing of the laser driver by increasing the output energy of each remaining amplifier by 6%, a feat which could be automatically accomplished by the Prometheus-L computer control system.

It was found that the development of a comprehensive laser driver control system was a key element in meeting projected driver reliability requirements. In many cases, the analyses showed that the laser driver control system would be able to compensate for the loss of a particular driver component by employing redundant elements or by

increasing the output for similar elements working in parallel. These analyses indicated that it was feasible for each of the 60 Prometheus-L beamlines to deliver approximately 67 kJ to the target (for DD irradiation) following pulse compression.

It was also found that, by using the Prometheus-L driver design, the "depleted pump" pulse from the SBS pulse compressors could be used to generate the target precursor ramp pulse (required to contain ~30% of the laser energy). Because the short (SBS Stokes output) main pulse precedes the longer duration depleted pump pulse out of the SBS pulse compressor, an electro-optic switchyard is provided to invert temporarily the order of the pulses. In the Prometheus-L design, this is accomplished with a large aperture Pockels cell, a Brewster-angle polarizer, two mirrors, and several large aperture quarter-wave plates arranged in an optical delay line.

In this manner, the required complex, high power pulse shapes required for both DD and ID target irradiation can be generated at relatively high efficiency (~75% from the output of the discharge lasers to the target) and high reliability (10^9 firings) by the NLO beam combination and pulse compression subsystems of the Prometheus-L driver. Furthermore, a collimating mirror in each beamline, which focuses each of the 60 beams down through a radiation-limiting field stop located in the shielding, significantly reduces the amount of radiation escaping from the Prometheus-L target chamber.

Lastly, it was found that, by allowing the focusing mirror to image the field stop focus onto a plane located a few centimeters behind the DD target, it is feasible to apodize the laser beams. Thus, the incoming beams can be nested on the spherical surface of the target at relatively small angles of incidence ($\lambda_{max} < 23°$). Calculations indicate that this beam arrangement enhances inverse Bremsstrahlung target coupling compared to the conventional tangential focusing geometry. Supporting analyses suggest that the precise sensing of the target location required for such advanced illumination schemes can be accomplished holographically using laser beams reflected from a "shine shield" on either DD or ID targets.

Heavy Ion Driver - Performance optimization studies for the Prometheus-H design led to a HI driver energy of 7.8 MJ. This energy is provided in the form of 18 beamlets of 4 GeV lead ions at a pulse repetition rate of 3.54 pps. Six of these 18 beamlets (three per side) are used to form a single, larger prepulse for each side of the target. The remaining 12 beamlets (six per side) form the main target compression pulse.

For the indirect drive HI target, the optimized pulse consists of a ramped precursor of approximately 30 ns duration containing ~30% of the energy and a main driver pulse of 7.3 ns duration having the remainder of the driver energy. The six main beamlet focusing magnets are bundled around the single precursor magnet on an 8.5° cone.

In the Prometheus-H focal geometry, the precursor beams enter the target chamber on axis of a self-pinching transport channel.

During the study, it was concluded that a single-beam LINAC consisting of a ramp-gradient and constant-gradient section operated in a 30-kHz burst mode could generate the 18 HI beamlets serially at significantly lower cost than was projected to accelerate the beamlets in parallel. Since the energy must be delivered to the HI target simultaneously, the LINAC output is transferred into 14 superconducting storage rings to hold the beamlets until the total energy is generated (<1 ms). The Prometheus-H control system then initiates appropriate switching magnets that eject the 12 main pulse beamlets into one multiple beam buncher accelerator (designed to create 7.3 ns pulses) and eject the remaining two precursor beamlets into a second buncher accelerator (designed to create 30 ns pulses).

It was observed that the application of current superconducting accelerator and particle beam technology permitted the construction of a HI driver capable of meeting the derived HI driver performance requirements. An important element in the Prometheus-H control system was the capability to sense driver component failure modes before failure occurs.

A key feature of the Prometheus-H driver beam transport is a pair of pre-formed channels combined with self-pinched beam propagation to the target through two small (2-cm diameter) openings in the target chamber blanket (for two-sided ID targets). Although review of previous work has shown that this HI beam self-pinched channelling approach requires additional technological development, the resulting focusing geometry has significant shielding advantages over conventional ballistic focusing, which would require focusing through 14 relatively large openings in the HI target chamber blanket.

Lastly, it was determined that the six superconducting main pulse beamlet focusing magnets can be configured with an allowance for radiation shielding on a cone subtending a small angle (8.5°). By passing the beams through a lead vapor neutralizing cell, the beams form small waists (<6-mm diameter) at the rear surface of the blanket that intersect at a common point. Further calculations showed that a lead vapor jet at each HI focus could then serve to strip the 4 GeV lead beams to a high charge state thereby boosting the beam current above 1 MA. The resulting high solenoidal magnetic field of the combined stripped beams is capable of collapsing all six main HI beamlets on each side of the target chamber to self-pinch within the channel and re-image the 6-mm diameter focal spot on the target.

Reactor Cavity - Design work on the reactor cavity shows that the cylindrical configuration is more favorable than other geometries. It is consistent with

conventional plant layout and, at the same time, allows for better control over the flow of the thin liquid film on the surface of the first wall.

The unique physical separation of first wall and blanket functions resulted in a number of important consequences. First, the lifetime of the FW system, which is shown to be governed mainly by radiation-induced swelling, will be shorter than that of blanket modules. Thus FW modules can be separately changed on a more frequent basis. The overall reliability of the cavity is thus enhanced and the downtime minimized. The first wall system handles over 40% of the total power in a relatively small volume. In fact, the average power density in the FW system is about a factor of 20 higher than that of the blanket/reflector system. We conclude that the separation between the functions of the first wall and the blanket adds a desirable flexibility to IFE reactor designs.

The wetted wall concept adopted in our study offers several advantages over other wall protection schemes. The concept allows for good accommodation of beam lines, low liquid metal inventory with the associated safety benefits, and shorter time between successive pulses.

With a ^{6}Li enrichment of 25%, a tritium breeding ratio of 1.2 is achieved in the cavity design. The current nuclear design of the blanket results in a power multiplication factor of 1.14. The thermal-hydraulic design approach uses low-pressure helium coolant with an inlet pressure of 1.5 MPa to enhance the system safety and component reliability.

Structural materials are selected to achieve the following design goals:

(1) High-temperature operation or improved thermodynamic cycle efficiency.
(2) Low-activation for shallow land burial waste disposal.
(3) Low afterheat for mitigation of operational accidents.

An optimum choice, which satisfies all these conditions, was concluded to be the SiC/SiC composite material.

For the laser optical system, a unique design was achieved for the last optical component: the Grazing Incidence Metal Mirror (GIMM). It was concluded that a long lifetime for the GIMM can be achieved if the optical function of the surface is separated from the structural function. This is realized by depositing a thin layer of aluminum on top of a rigidly clamped structural composite. When the thickness of the aluminum layer is graded, such that the leading edge of the mirror is thinner than the trailing edge, plant lifetime can possibly be achieved for this sensitive component.

A high degree of safety and environmental attractiveness was achieved in this design. The choice of materials leads to low long-term radioactivity, and short-term radioactivity is so low that decay heat can be accommodated through entirely passive means. The reactor building was designed to allow personnel access after only one day following shut down. The design has a high degree of tolerance to failures. None of the accident scenarios that were considered could lead to public exposure.

Balance-of-Plant and Safety - The fuel processing system necessary to support the IFE reactor power plant is available with the state-of-the-art technology. Current development in tritium processing and handling technology will further improve the safety and environmental performance of the tritium systems.

The balance-of-plant system appears to be a mature technology. Further developments to improve the thermal conversion efficiency and BOP availability can provide significant improvement in the economic competitiveness of IFE power plants.

The Prometheus configuration and engineering features were carefully selected to maximize reliability and enhance maintainability. Fully remote maintenance operations are provided for. High overall availability for the power plant, approximately 80%, is estimated.

The Prometheus study has identified applicable safety and environmental regulations that must be factored into the design of a commercially viable IFE power plant and demonstrated before they can be met. The ESECOM level of safety assurance methodology[1] was applied to Prometheus in assessing off-site doses due to releases of key radionuclides present in the plant. With the exception of W^{185} and Pb^{203}, the Prometheus Inventories allow the plant to be classified as totally passively safe (LSA=1). The tungsten isotope was also identified in the ESECOM study,[1] but not seen as a problem due to its immobility. The lead isotope, however, is unique to Prometheus with its lead coolant, and design features to remove lead afterheat in the event of loss of cooling have been incorporated to address this issue. The careful selection of materials in Prometheus, particularly the structural material (SiC) has minimized the long-term activation. Practically all materials in Prometheus meet Class C or better for waste disposal.

Critical Issues - Although the Prometheus reactor power plants look attractive, many technical issues must be resolved and a substantial program of R&D must be undertaken on the path to commercialization. Detailed technical issues were identified and characterized. The critical issues are:

1. Demonstration of Moderate Gain at Low Driver Energy
2. Feasibility of Direct Drive Targets

3. Feasibility of Indirect Drive Targets for Heavy Ions
4. Feasibility of Indirect Drive Targets for Lasers
5. Cost Reduction Strategies for Heavy Ion Drivers
6. Demonstration of Higher Overall Laser Driver Efficiency
7. Tritium Self-Sufficiency in IFE Reactors
8. Cavity Clearing at IFE Pulse Repetition Rates
9. Performance, Reliability, and Lifetime of Final Laser Optics
10. Viability of Liquid Metal Film for First Wall Protection
11. Fabricability, Reliability, and Lifetime of SiC Composite Structures
12. Validation of Radiation Shielding Design Tools and Nuclear Data
13. Reliability and Lifetime of Laser and Heavy Ion Drivers
14. Demonstration of Large-Scale Non-Linear Optics Laser Driver Architecture
15. Demonstration of Cost Effective KrF Amplifiers
16. Demonstration of Low Cost, High Volume Target Production Techniques

The R&D program required to develop the data base for the design and construction of an IFE Experimental Power Reactor (IEPR) is roughly $2B for either the laser-driven or heavy-ion-driven reactors. The most extensive and relatively expensive parts of the R&D program relate to the driver-target development and coupling.

The study has demonstrated that quantitative evaluation methodology can be developed and applied successfully in comparing design and technology options. The evaluation methodology developed in this study includes five areas: physics, feasibility, engineering feasibility, economics, safety and environment, and R&D requirements. The methodology can be applied in the future for other applications. Comparative evaluation of Prometheus-L and H leads to two conclusions:

(1) The heavy-ion driven reactors appear to have an overall advantage over laser-driven reactors based on existing R&D data and performance projections.
(2) The differences in scores are not large and future R&D results could change the overall ranking of the two IFE concepts.

Reference for 2.8

1. J. P. Holdren et al., "Report of the Senior Committee on Environmental, Safety, and Economic Aspects of Magnetic Fusion Energy," LLNL Report URL-53766, 25 September 1989.

This page intentionally left blank.

McDonnell Douglas Aerospace
P O Box 516, St Louis, Missouri 63166-0516 (314) 232-0232

MCDONNELL DOUGLAS